




2013

## Turning stealth liposomes into cationic liposomes for anticancer drug delivery

Vijay Gyanani  
*University of the Pacific*

Follow this and additional works at: [https://scholarlycommons.pacific.edu/uop\\_etds](https://scholarlycommons.pacific.edu/uop_etds)

 Part of the [Medical Pharmacology Commons](#), [Medicinal-Pharmaceutical Chemistry Commons](#), [Pharmaceutical Preparations Commons](#), and the [Pharmacy and Pharmaceutical Sciences Commons](#)

---

### Recommended Citation

Gyanani, Vijay. (2013). *Turning stealth liposomes into cationic liposomes for anticancer drug delivery*. University of the Pacific, Dissertation. [https://scholarlycommons.pacific.edu/uop\\_etds/147](https://scholarlycommons.pacific.edu/uop_etds/147)

This Dissertation is brought to you for free and open access by the Graduate School at Scholarly Commons. It has been accepted for inclusion in University of the Pacific Theses and Dissertations by an authorized administrator of Scholarly Commons. For more information, please contact [mgibney@pacific.edu](mailto:mgibney@pacific.edu).

**TURNING STEALTH LIPOSOMES INTO CATIONIC LIPOSOMES FOR  
ANTICANCER DRUG DELIVERY**

by

**Vijay Gyanani**

**A Dissertation Submitted to  
Office of Research and Graduate Studies  
In Partial Fulfillment of the  
Requirements for the Degree of  
DOCTOR OF PHILOSOPHY**

**Thomas J. Long School of Pharmacy and Health Sciences  
Pharmaceutical and Chemical Sciences**

**University of the Pacific  
Stockton, California  
2013**

**TURNING STEALTH LIPOSOMES INTO CATIONIC LIPOSOMES FOR  
ANTICANCER DRUG DELIVERY**

by

**Vijay Gyanani**

**APPROVED BY:**

**Dissertation Advisor: Xin Guo, Ph.D.**

**Committee Member: Bhaskara R. Jasti, Ph.D.**

**Committee Member: Xiaoling Li, Ph.D.**

**Committee Member: Dongxiao Zhang, Ph.D.**

**Committee Member: Timothy Smith, Ph.D.**

**Interim Dean of Graduate Studies: Bhaskara R. Jasti, Ph.D.**

**TURNING STEALTH LIPOSOMES INTO CATIONIC LIPOSOMES FOR  
ANTICANCER DRUG DELIVERY**

**Copyright 2013**

**by**

**Vijay Gyanani**

## ACKNOWLEDGEMENTS

I would like to pay my earnest gratitude to Dr. Guo for his guidance, constant support and mentorship that had made this work possible. I have enjoyed intellectual discussions with him both within the purview of my research and outside. I would like to thank Dr. Li, Dr. Jasti, Dr. Smith and Dr. Zhang for serving on my dissertation committee.

I appreciate Dr. Franz and Dr. Samoshin and Dr. Curtis for characterizing my compounds. I am grateful to Dr. Eggers for teaching me and allowing me to use his Microcal DSC instrument at SJSU.

I want to thank graduate school at UOP for granting me teaching assistantship that has made my stay possible here in Stockton. My appreciation goes to Dr. Samoshina for her elderly advice and support all these years. I want to thank Lynda for taking care of all the chemical purchases and Kathy for all my paperwork at UOP.

I want to thank Holly and Shen for creating a lively and cooperative atmosphere in the lab. My sincere appreciations go to Poonam, Shila and Pompeya for valuable discussions, friendship and moral support.

I wish to express my special thanks to my parents and siblings for their unconditional love, support and encouragement all my life.

## Turning Stealth Liposomes into Cationic Liposomes for Anticancer Drug Delivery

### Abstract

by Vijay Gyanani

University of the Pacific  
2013

Targeting the anticancer agents selectively to cancer cells is desirable to improve the efficacy and to reduce the side effects of anticancer therapy. Previously reported passive tumor targeting by PEGylated liposomes (stealth liposomes) have resulted in their higher tumor accumulation. However their interaction with cancer cells has been minimal due to the steric hindrance of the PEG coating.

This dissertation reports two approaches to enhance the interaction of stealth liposomes with cancer cells. First, we designed a lipid-hydrazone-PEG conjugate that removes the PEG coating at acidic pH as in the tumor interstitium. However, such a conjugate was highly unstable on shelf.

Second we developed lipids with imidazole headgroups. Such lipids can protonate to provide positive charges on liposome surface at lowered pH. Additionally, negatively charged PEGylated phospholipids can cluster with the protonated imidazole lipids to display excess positive charges on the surface of the liposomes, thus enhancing their interaction with negatively charged cancer cells.

We prepared convertible liposome formulations I, II and III consisting of one of the three imidazole-based lipids DHI, DHMI and DHDMI with estimated pKa values of 5.53, 6.2 and 6.75, respectively. Zeta potential measurement confirmed the increase of positive surface charge of such liposomes at lowered pHs. DSC studies showed that at pH 6.0 formulation I formed two lipid phases, whereas the control liposome IV remained a one-phase system at pHs 7.4 and 6.0. The interaction of such convertible liposomes with negatively charged model liposomes mimicking biomembranes at lowered pH was substantiated by 3-4 times increase in average sizes of the mixture of the convertible liposomes and the model liposomes at pH 6.0 compared to pH 7.4.

The doxorubicin-loaded convertible liposomes show increased cytotoxicity in B16F10 (murine melanoma) and HeLa cells at pH 6.0 as compared to pH 7.4. Liposome III shows the highest cell kill at pH 6.0 for both the cells. The control formulation IV showed no difference in cytotoxicity at pH 7.4 and 6.0. Uptake of convertible liposome II by B16F10 cells increased by 57 % as the pH was lowered from 7.4 to 6.0.

## Table of Contents

LIST OF TABLES.....	9
LIST OF FIGURES.....	10
LIST OF SCHEMES.....	14
<b>CHAPTER</b>	
1 Introduction.....	15
Cancer Epidemiology.....	15
Cancer Nomenclature and Pathology.....	15
Challenges and Limitations of Current Anticancer Therapies.....	17
Tumor Targeting and its Challenges.....	23
Strategies of Triggered Release from Liposomes.....	31
Conclusion.....	41
2 Acid Labile Linkers for the Design of pH-Sensitive Lipids and Liposomes.....	42
Acetal Linker.....	43
Vinyl Ether Linker.....	47
Ortho Ester.....	52
Hydrazone Linker.....	55
Shedding of PEG Coating by Hydrolysis of Hydrazone Linker.....	58
pH-sensitivity of DHG-Hz-PEG.....	71
Separation of DHG-Hz-PEG.....	72
3 Design, Preparation and Characteriation of pH-Sensitive Convertible Liposomes for Anticancer Drug Delivery.....	74



Introduction.....	74
Tumor pH.....	78
Materials and Methods.....	81
Results and Discussion.....	104
4 Summary and Conclusion.....	128
REFERENCES.....	131

## LIST OF TABLES

Table	Page
2.1 pH Dependence of 50% Release Time of Calcein.....	50
3.1 Lipid composition of Convertible (I, II, III) and Control (IV) Liposomes.....	98
3.2 Adjustment of pH of the media with glacial acetic acid .....	103
3.3 Calculated pKa of Imidazole based Lipids.....	106

## LIST OF FIGURES

Figure	Page
1.1 Overexpression of Pgp transporter proteins leading to efflux of drug from the cells.....	21
1.2 'Enhanced Permeation and Retention' effect showing the extravasation of liposomes in tumor tissue.....	27
1.3 Doxil coated with Polyethylene Glycol.....	30
1.4 (a) Drug release from liposomes by photoisomerization of lipids.....	32
1.4 (b) Drug release from liposomes by photocleavage of lipids.....	33
1.4 (c) Drug release from liposomes by photopolymerization of lipids .....	35
1.5 A) enhanced accumulation of liposomes by EPR B) increased pore size of tumor vasculature C) increased drug release from the liposomes.....	36
1.6 Traditional and lysolipid containing liposomes.....	38
1.7 Iron oxide nanoparticles incorporated in lipid membrane.....	40
2.1 Acetal linker.....	43
2.2 pH-sensitive acetal based glycolipid.....	45
2.3 Chemical Structure of BD2 lipid.....	46
2.4 Vinyl Ether Linkage.....	47
2.5 Vinyl Ether lipids prepared by Thomson and Associates.....	49
2.6 Structure of the 'POD' lipid.....	53
2.7 Ortho ester lipids designed by Masson et al.....	55
2.8 Chemical structure of hydrazone linker.....	56

2.9	Chemical structures of guanidinium-based cationic lipids.....	57
2.10	Extracellular matrix over cells.....	59
2.11	Concept of design of hydrazone based pH-sensitive liposome.....	60
2.12	NMR Spectrum of DHG Ester.....	65
2.13	NMR Spectrum of DHG Hydrazone.....	67
2.14	NMR Spectrum of mPEG <sub>2000</sub> Acetaldehyde.....	69
2.15	TLC showing the formation of DHG-Hz-PEG lipid.....	70
2.16	Acidified hydrolysis of the reaction mixture shows the formation of DHG-hydrazone.....	71
2.17	TLC of the eluent showing the DHG-Hz-PEG eluting out of the column.....	72
3.1	Concept of design of convertible liposomes: protonation and clustering of PEG coating on liposome surface in response to lowered pH.....	76
3.2	Formation of lipid domains on the liposome surface at mildly acidic tumor microenvironment.....	77
3.3	Three types of lipids (DPPE-PEG, Imidazole lipid and DSPC) comprising the convertible liposome, Negatively charged DPPE-PEG and protonable Imidazole lipids interact at low pH.....	77
3.4	Picture of solid tumor showing heterogeneous and leaky vasculature and hypoxic region.....	79
3.5	Structure of pH-protonable imidazole lipids.....	80
3.6	DART mass spectral analysis of DPI.....	84
3.7	NMR spectrum of DPI.....	85
3.8	DART mass spectral analysis of DHI.....	89
3.9	NMR spectrum of DHI.....	90
3.10	DART mass spectral analysis of DHMI.....	92
3.11	NMR spectrum of DHMI.....	93

3.12 DART mass spectral analysis of DHDMI.....	95
3.13 NMR spectrum of DHDMI.....	96
3.14 (a) Change of zeta potential values of liposome formulations (I-IV) with pH.....	107
3.14 (b) Change of zeta potential values of liposome formulations (I-IV) with percent (%) Ionization of imidazole lipid incorporated in convertible liposomes. *Percent Ionization was calculated by Henderson–Hasselbalch equation using estimated average pKa values of imidazole lipids.....	108
3.15 DSC thermogram of control liposome IV and convertible liposome formulation I.....	109
3.16 Change of average sizes of equimolar mixture of model liposome and either I, II, III or IV with pH.....	110
3.17 Loading of DOX into liposomes by ammonium sulfate gradient.....	111
3.18 DOX retention in convertible liposome formulation I at pH 7.4 prepared by ammonium sulfate gradient method.....	112
3.19 DOX retention in liposome formulation I prepared by manganese sulfate method.....	113
3.20 Cytotoxicity of free DOX, liposome formulations of DOX and empty liposome (formulation I without DOX) against B16-F10 murine melanoma cells in serum-free medium after three hours of incubation. Mean and SD of cell viability (%) are presented (n = 4) (* p < 0.05, student t-test).....	116
3.21 Cytotoxicity of free DOX, liposome formulations of DOX and empty liposome (formulation I without DOX) against B16-F10 murine melanoma cells in serum-free medium after twelve hours of incubation. Mean and SD of cell viability (%) are presented (n = 4) (* p < 0.05, student t-test).....	117
3.22 Cytotoxicity of free DOX, liposome formulations of DOX and empty liposome (formulation I without DOX) against B16-F10 murine melanoma cells in complete medium after three hours of incubation. Mean and SD of cell viability (%) are presented (n = 4).....	118
3.23 Cytotoxicity of free DOX, liposome formulations of DOX and empty liposome (formulation I without DOX) against B16-F10 murine melanoma cells in complete medium after twelve hours of incubation. Mean and SD of cell viability (%) are presented (n = 4) (* p < 0.05, student t-test).....	119

24 Cytotoxicity of free DOX, liposome formulations of DOX and empty liposome (formulation I without DOX) against Hela cells in serum-free medium after three hours of incubation. Mean and SD of cell viability (%) are presented (n = 4) (* p < 0.05, student t-test).....	120
25 Cytotoxicity of free DOX, liposome formulations of DOX and empty liposome (formulation I without DOX) against Hela cells in serum-free medium after twelve hours of incubation. Mean and SD of cell viability (%) are presented (n = 4) (* p < 0.05, student t-test).....	121
26 Cytotoxicity of free DOX, liposome formulations of DOX and empty liposome (formulation I without DOX) against Hela cells in complete medium after three hours of incubation. Mean and SD of cell viability (%) are presented (n = 4).....	122
27 Cytotoxicity of free DOX, liposome formulations of DOX and empty liposome (formulation I without DOX) against Hela cells in complete medium after twelve hours of incubation. Mean and SD of cell viability (%) are presented (n = 4) (* p < 0.05, student t-test).....	123
3.28 Cytotoxicity of free DOX and liposome formulations of DOX against DOX concentrations (0.1, 1, 10 µg/mL) in B16F10 cells at pH 6.0 in serum free media after 12 hours of incubation. *Average values of percent cell viability were taken.....	124
3.29 Cytotoxicity of free DOX and liposome formulations of DOX against DOX concentrations (0.1, 1, 10 µg/mL) in Hela cells at pH 6.0 in serum free media after 12 hours of incubation. *Average values of percent cell viability were taken.....	124
3.30 Flow Cytometry of DOX uptake by B16F10 cells.....	126
3.31 Mean fluorescent intensity of B16F10 cells treated with free DOX or liposomal DOX by flow cytometry.....	127

## LIST OF SCHEMES

Scheme	Page
2.1 Acidic hydrolysis of Acetal.....	44
2.2 Mechanism of acid catalyzed hydrolysis BD2 lipid.....	46
2.3 Hydrolysis mechanism of Vinyl Ether under acidic conditions.....	48
2.4 Acid catalyzed hydrolysis of DPPIsC.....	50
2.5 Acid Hydrolysis of DHCho-MPEG5000.....	51
2.6 Hydrolysis mechanism of Orthoester.....	52
2.7 Acidic hydrolysis of orthoester based lipid.....	53
2.8 Acid Hydrolysis of Hydrazone.....	61
2.9 Synthesis of DHG-Hz-PEG conjugate.....	64
2.10 Synthesis of mPEG <sub>2000</sub> Acetaldehyde.....	68
3.1 Synthesis of DPI.....	83
3.2 Synthesis of DHI, DHMI and DHDMI.....	88

## **Chapter 1: Introduction**

### **Cancer Epidemiology**

Cancer is a group of diseases characterized by uncontrolled growth of abnormal cells that have a potential to invade other tissues (1,2). Cancer is a foremost cause of death worldwide which lead to 7.6 million deaths worldwide (around 13 % of all deaths) in 2008 (3). The total number of deaths due to cancer will continue to rise to an estimated 3.1 million in 2030 (3). In United States cancer is the most common cause of death preceded by only heart disease, American cancer society estimates that in 2013 about 80,350 Americans are expected to die of cancer, which accounts for 1600 deaths a day and nearly one of every 4 deaths. About 1,660,290 new cancer cases are expected to be diagnosed in 2013 (1). From 1991 to 2006, the death rate from heart diseases (most common cause of death) declined to two thirds but that from cancer declined much more slowly to 83% despite technological advances in medical and allied health fields (4). This highlights the importance of anticancer research and warrants the time, money and effort to discover novel ways to treat cancer.

### **Cancer Nomenclature and Pathology**

The term 'Cancer' is derived from the Greek word 'Karkinos' meaning crab (5). Early observers saw spread and persistence of cancer as crab-like and hence the term (6). An abnormal growth of cells forming a lesion or lump is called a 'Neoplasm' or 'Tumor'. A



widely accepted definition of Neoplasm by Sir Rupert Willis (Willis, 1952) states "an abnormal mass of tissue, the growth of which exceeds and is uncoordinated with that of normal tissue and persists in the same excessive manner after cessation of stimulus which evoked the change". Neoplasm is characterized by its irreversible nature. Tumors can be cancerous or non cancerous. Non cancerous tumors, also called benign tumors, are limited to certain part of body and are not ominous to the host. While cancerous tumors or malignant tumors de-differentiate from the tissue of origin and invade to other parts of the body causing significant damage to the host owing to its uncontrolled growth and spread. The development of malignant tumor is a multistep process comprising of initiation, promotion and propagation stages. Initiation of tumor involves genetic alteration in a single cell leading to abnormal growth (8). During the cell promotion stage actively proliferating cell population is generated by the division of the mutated cell. Tumor progression continues as the further mutations of the proliferative cell population takes place and some of these mutations result in a clone of cells with higher growth potential. This clone of cells outnumbers other cells in the tumor in a process called 'clonal selection'. The clone of cells may undergo frequent genetic alterations to produce a new clone of cells with higher mutation potential as a result of their increasing genetic instability. The progression stage is thus a multi step process in that a series of clone of cells with ever increased proliferative capacity and metastatic potential are produced (8).

It is very important for a pathologist to identify the tumor and classify a tumor as benign or malignant. The criteria for the diagnosis of a malignant tumor include size of primary tumor, the depth of tissue invasion at primary tumor site, the extent of spread to local

ymph nodes and presence or absence of distant metastasis (7). The deliverance of anticancer therapy depends on the diagnosis of a malignant tumor.

Tumor nomenclature describes tumor by the tissue of their origin – epithelial, connective, muscular or nervous (5). As a general rule, a suffix ‘oma’ is applied to nearly all tumor types whether benign or malignant and irrespective of the histological origin (5) except for tumors of hematopoietic and lymphopoietic systems where a suffix ‘emia’ is used.

### **Challenges and Limitations of Current Anticancer Therapies**

Current most commonly employed anticancer strategies include surgery, radiotherapy and chemotherapy. Although these anticancer strategies have their own advantages, there are certain limitations associated with them.

**1.1 Cancer surgery.** Surgery, for instance, may seem to be a convenient option for removing solid tumors; but it should be noted that not all tumors can be surgically removed. If the tumor is sufficiently big so as to impose serious damage on the surrounding normal tissue or regular functioning of the organ e.g. normal functioning of brain including thinking, speaking etc. surgery is not considered as an antitumor strategy. Prostate, ovarian and uterine surgery may cause permanent damage to fertility, while lung cancer surgery may cause breathing problems and breathlessness. Lung surgery, in some instances, has also been known to affect voice and vocal cord tissues. Oral cancer surgery procedures such as Glossectomy although may not eliminate the ability to speak but speech is not as clear and swallowing may be difficult. On the other hand laryngectomy completely eliminates regular speaking. Regardless of the above

mentioned complications associated with tumor removal at various sites, surgery itself has inherent issues such as infection and local nerve damage.

**1.2 Chemotherapy.** For treatments such as chemotherapy either free drug or most likely a combination of drugs is administered in the body. Although chemotherapy is one of the few treatment options for metastasized cancer the major drawback of chemotherapy is its poor selectivity. Since cancer cells originate from normal cells that grow out of control, anticancer drugs that suppress growth of cancer cells also affect the growth of normal cells. The poor selectivity of common chemotherapeutic drugs is due to the proliferative nature of cancer cells. Not only that the anticancer drugs have toxic effects on cancer cells, they also have potential to impose serious damage to bone marrow, gastrointestinal tract and hair follicle (9). To cite a few examples: the dose-limiting hematotoxicity including thrombocytopenia and neutropenia are prevalent in carboplatin and/or carboplatin in combination with other chemotherapeutic agents. Skin effects especially keratitis are common side effects of chlorambucil. Cisplatin has been known to accumulate in the kidney by a transport mediated process after continuous and prolonged exposure and cause severe dose dependent tubular and glomerular dysfunction, mitochondrial swelling and nuclear pallor in distal nephron (11). Cumulative toxicity due to Anthracyclines, doxorubicin being a most common example, may cause cardiomyocyte damage and apoptosis due to production of free radicals and acute cardiotoxicity that may include arrhythmias, pericarditis, myocarditis and acute heart failure. Additionally, chronic cardiotoxicity associated with anthracyclines include conditions such as left ventricular dysfunction. For breast cancer treatment in particular, the cyclophosphamide, methotrexate and 5-fluorouracil (CMF) regimen has been known

cause neutropenia, alopecia and emesis (14). In case of 5-fluorouracil containing regimens e.g. cyclophosphamide, doxorubicin (Adriamycin), and 5-fluorouracil (CAF) or 5-fluorouracil, doxorubicin, and cyclophosphamide (FAC), mucositis appears to be common than non fluorouracil regimens like doxorubicin and cyclophosphamide (AC) (14). It is interesting to note that paclitaxel when administered in higher dose (i.e. 225 mg/m<sup>2</sup>) in sequential regimen has shown severe and recurrent neuromuscular toxicity as compared to lower dose (i.e., 175 mg/m<sup>2</sup>).

Besides aforementioned notable examples of severe side effects of chemotherapeutic agents, there are cases where patients are beleaguered with side effects that are not malignant but do have a significant effect on the quality of life and may result in discontinuation or undue disruption of chemotherapy. Skin diseases are the prominent amongst them (16). Common side effects on skin i.e. skin rash, skin dryness, hyperpigmentation and on mucosal membrane include Steven Johnson Syndrome and toxic epidermic necrolysis are caused by commonly used drugs such as Cyclophosphamide, Chlorambucil, Busulfan and Procarbazine. Novel anticancer agents such as EGFR inhibitors markedly cause skin dryness and follicular rash which can then result in pruritis or other infections (16). The most common of the follicular rash is the papulo-pustular rash. Other common skin effects such as Erythma and swelling are associated with administration of antimetabolites such as 5-Fluorouracil and capecitabine (16).

In addition to the poor selectivity of chemotherapy mentioned hitherto, the other major limitation is the development of multidrug resistance (MDR) (Fig. 1.1). Cancer cells may develop resistance that might begin against a single drug or a group of drugs with

similar mechanism of action but may transform into cross resistance against other drugs with different targets or mechanism of actions in a process called multidrug resistance (MDR) (27). MDR leads to growth of heterogeneous cancer cells due to mutator phenotype as a result of selection of cells that are able to grow in the presence of chemotherapeutic drug/s (27). Drug resistance in cancer cells is developed either by modification in drug target or by enhancement of the repair mechanisms of the cells such as DNA repair and induction of cytochrome oxidases (27). Additionally, one of the most prominent mechanisms of multi-drug resistance is the over-expression of ABC binding cassette transporters based efflux transporters. The increased efflux transporters reduce the amount of drug to suboptimal levels in the cells (27). MDR can also develop from reduced intracellular uptake of hydrophilic drugs e.g folate analogues, cisplatin etc. (89). Examples for the later are ciaplatin, methotrexate, 5 fluorouracil etc. Furthermore inefficiency in apoptotic cycles may lead to MDR, precisely due to ineffective p53 or alterations in ceramide levels.

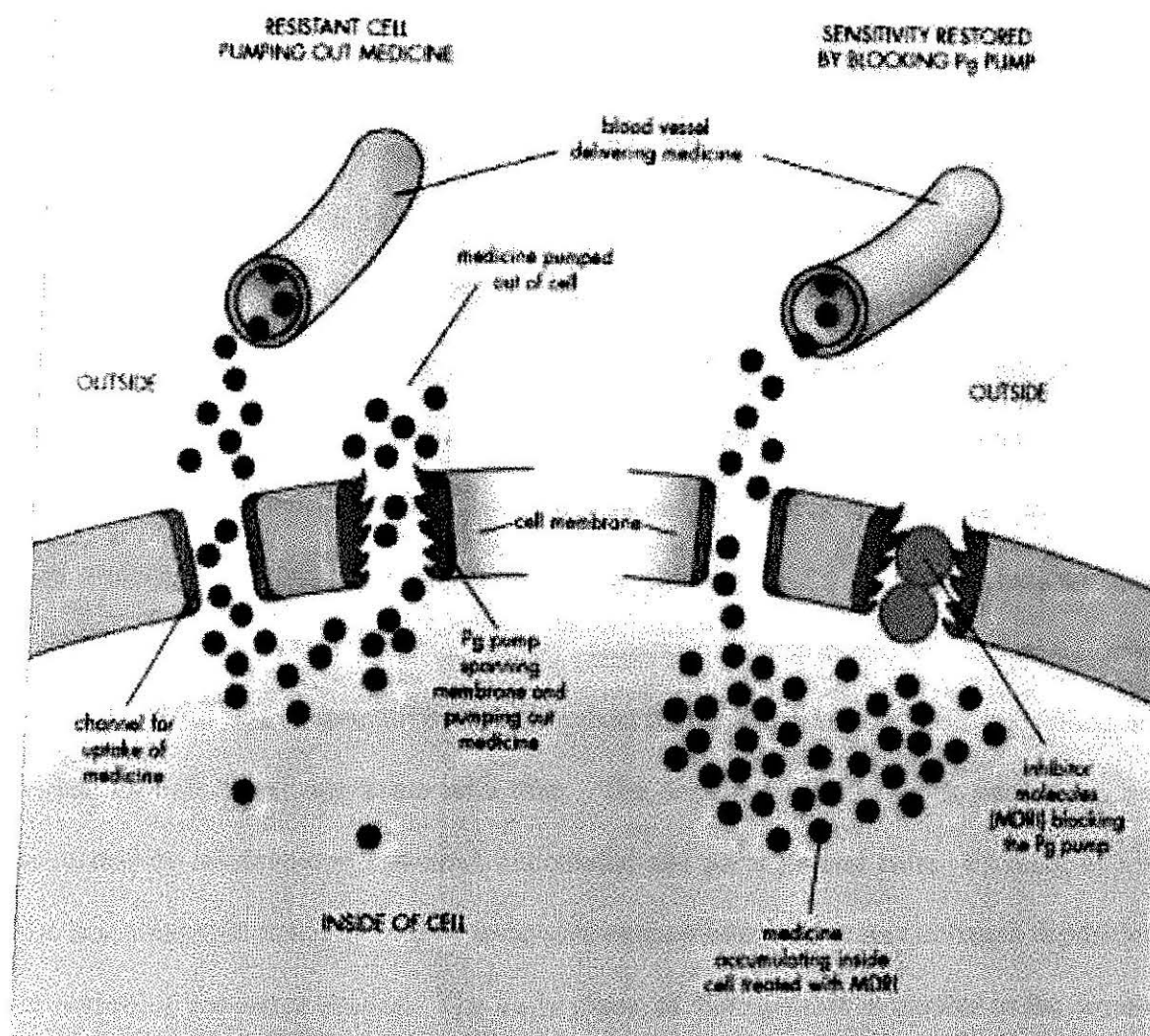


Fig. 1.1 Overexpression of Pgp transporter proteins leading to efflux of drug from the cells. (Reproduced from (92))

Of the reasons mentioned above and the fact that chemotherapeutic agents have narrow therapeutic index in that there is a small difference in the dose required for an anticancer effect and the dose causing significant toxicity, limits the therapeutic implication of chemotherapy. Furthermore, the damage to normal cells entails reduction in the dose of

the anticancer drug which eventually leads to inefficient disease control, drug resistance and metastasis.

**1.3 Radiotherapy.** Radiotherapy, another commonly practiced anticancer therapy, employs the use of high energy X rays for the treatment of cancer. The applications of radiotherapy vary from tumor kill to tumor shrinkage to pain relief. While the side effects of an anticancer drug or a combination of drugs are systemic, the side effects of radiation therapy are more of the local nature (in the proximity of the tumor). Radiation side effects on patients are manifested either as early effects or late effects. Early effects are mainly skin related effects which include skin erythema and desquamation. Late radiation effects include fibrosis, atrophy, radiation induced blood vessel and neuronal damage. While it is important to note that short term effects are reversible, late effects are either irreversible or aggravate with time. The response manifested as late effects are mediated by inflammatory, stromal, endothelial and parenchymal cells. Fibrosis, one of the late effects, is characterized by excessive extracellular matrix and collagen deposition in region of irradiated tissues. The early phase of fibrogenesis is similar to the wound healing process characterized by initiation of cytokine cascades essentially marked by release of tumour-necrosis factor- $\alpha$  (TNF $\alpha$ ), interleukins 1 and 6 (IL1 and IL6) and other growth factor in the irradiated tissue (17). While in a regular wound healing process TNF $\alpha$  and connective tissue growth factor (CTGF) downregulate TNF  $\beta$  which is a strong fibrotic factor; the wound healing in irradiated tissues continue for years, which leads to fibrosis of tissues (17). Another aspect of radiation side effects is the known to be affected by the reduced oxygen content (hypoxia) in the tumor environment. It is reported that radiosensitivity of cells is diminished due to hypoxic environment which

nduces high levels of heat shock protein in tumor cells and also stimulate increase in number of cells with high proliferative capabilities (13). Specifically the increased expression and stabilization of hypoxia inducing factor HIF 1  $\alpha$  is responsible for the increase in radioresistance of cells. The HIF1 $\alpha$  expression is increased by activation of phosphatidylinositol 3-kinase (PI3K)/Akt/mammalian target of rapamycin (mTOR) pathway and increased stability of HIF 1  $\alpha$  by its interaction with Heat shock protein 90 (Hsp 90) (18).

### **Tumor Targeting and its Challenges**

As mentioned earlier chemotherapy and radiotherapy have many side effects and the most common reason for chemotherapeutic side effects is the non specific, indiscriminate effect on normal and tumor cells. The anticancer drug effect has its basis in fast multiplying cancer cell lines, which therefore can affect rapidly dividing normal cells. It is interesting to note that only 5-10% of the drug administered reaches tumor tissue (25). Paul Ehrlich introduced the term 'magic bullets' to selectively target a drug to disease-causing organisms. Since then a number of targeted drug delivery systems have been developed. Most of the novel drug delivery systems developed in the past few decades include liposomes, prodrugs, polymer conjugates, micelles and dendritic systems. Tumor targeting approaches can be broadly divided into two categories: Active and passive targeting.

**1.4 Active targeting.** Active targeting exploits phenotypic, biochemical and morphological differences between normal and cancer cells (26). Most common tumor targeting strategy employ biologically specific interactions such as antigen-antibody or



ligand-receptor binding for delivering cytotoxic agents locally in the tumor tissue and may involve drug uptake by receptor mediated endocytosis through association of the drug or drug carrier molecule with the antigen or ligand (26). Precisely, tumor targeting incorporates tumor specific ligands on nanocarriers/drug conjugates that can bind and deliver anticancer drugs to tumor cells, thereby sparing normal cells. Conversely, antigen heterogeneity in cancer cells presents a major limitation to active targeting; different types of cancer or even same type of cancer at different developmental stages express different pathological and biochemical profiles. Receptor density is also an important parameter in active targeting. It is crucial that the number of receptors/targets is over-expressed in the tumor cells compared to normal cells. For example, a receptor density of  $10^5$  per cell (29) of ErbB2 is required for improved breast cancer therapeutic efficacy. Similarly B cell targeting by liposomes grafted with anti-CD19 antibody requires a CD19 density in the range of  $10^4$  -  $10^5$  per cell (28). At any stage of cancer development down-regulation or shedding of antigen from cancer cell surface might severely affect therapeutic outcome. Shed antigens circulating around cancer cells may compete for binding of the ligand and therefore reduce the binding and internalization of the therapeutic agent (29). Furthermore, if the binding affinity between the targeting ligand and its receptor is too high it will hinder the quantitative uptake of anticancer agent in the tumor due to high affinity binding with the first few target cells - a phenomenon known as binding-site barrier (29). As an example, Adams et al (30) showed that bio-distribution of single chain Fv molecules (SCFv) in SK-OV-3 tumors is regulated by the binding affinity of the SCFv molecules to the her2neu receptor overexpressed by the

cancer cells. The excessively high binding affinity of mutant scFv beyond  $10^{-9}$  M plateaued the quantity of scFv distributed in the tumor (30).

**1.4.1 Antibody and antibody fragments.** As targeting agents, whole antibodies are stable in solution but are usually immunogenic and can bind to macrophages via the Fc domain, thus increasing their clearance and shortening their circulation half lives (29). To reduce the immunogenicity of antibodies, chimeric or humanized antibodies were developed but their production is very expensive. Additionally, large antibodies when used as targeting moieties for nanoparticles thwart attempts of multivalent decoration on the nanoparticle surface due to the steric hindrance. Antibody fragments, on the other hand, such as the Fab or scFv domains are more specific to their targets but have stability issues and carry less avidity due to their monovalent binding domain. When non-antibody small molecules such as RGD, folate and transferrin are used as the homing moiety, the targeting is not exclusive to tumor tissues and affect normal tissues. Also, free folate molecules present in the body can compete with the folate target ligand for its receptor on cancer cell surface (29).

**1.4.2 Immunotoxins and immunoconjugates.** Immunotoxins and Immunoconjugates although have been recently clinically approved but find limitations for anticancer therapies due to their moderate to severe side effects. Immunotoxins are either antibodies or antibody derived proteins that are linked to toxins. Patients on immunotoxins as anticancer agents have expressed high levels of hepatic transaminase levels, indicating localization of toxin in liver. Additionally flu-like symptoms and vascular leak syndrome have been observed in patients on immunotoxins. Anti B4 blocked ricin have demonstrated Human antimouse antibody responses and anti-ricin responses (29).

immunconjugates are similar to immunotoxins except for the cytotoxic drug is linked to the antibody or protein instead of the toxin. Immunconjugates works on the principal of antigen-antibody binding as mentioned earlier. The major limitation these systems is the number of drugs linked to antibody. On an average 3-10 molecules of drug have been known to be attached to an antibody molecule without affecting the antibody binding affinity (29), e.g. approximately 8 molecules of doxorubicin are coupled with BR96 antibody (31). Immunconjugates have shown limited success due to: 1) large number of antibodies needed to deliver therapeutic amount of drug 2) reduced internalization of drugs 3) suboptimal drug release from the conjugate (29) 4) toxicities induced by the treatment, e.g. severe gastrointestinal toxicities induced by BR96-Dox. immunconjugate (31).

**1.4.3 Immunoliposomes.** Liposomes are nanometer lipid bilayer vesicles with aqueous interiors that can encapsulate hundreds of thousands of drug molecules and thus address the issue of limited number of drug molecules bound to the antibody or any other ligand, thereby reducing the high amount of immunconjugates required to be administered to have sufficient drug at the tumor site. Immunoliposomes, are liposomes with targeting antibodies attached to their surface. The high payload ensures very high drug to antibody ratio. However, the challenges with immunoliposomes are similar to other active targeting approaches viz. the decoration of large number of antibody molecules on liposome surface increases their clearance, development and production. The receptor/antigen density and the avidity of ligand for the receptor/antigen may pose internalization issues or the binding-site barrier phenomenon leading to limited tumor penetration and reduced cytotoxic effect on antigen negative cancer cells.

**1.5 Passive tumor targeting.** Passive targeting of nanocarriers does not employ any targeting ligand but relies only on the 'Enhanced Permeation and Retention' effect (Fig. 1.2) for their accumulation in the tumor tissue and retention in the tumor cells. The enhanced permeation of nanocarriers in the tumor occurs due to leaky tumor vasculature while the retention of the nanocarrier at the tumor site is due to the dysfunctional lymphatic drainage (28). Although the challenges imposed by active targeting e.g. antigen heterogeneity, ligand avidity etc are not associated with passive targeting, it has certain limitations. The major limitations associated with only liposomal systems will be discussed here.

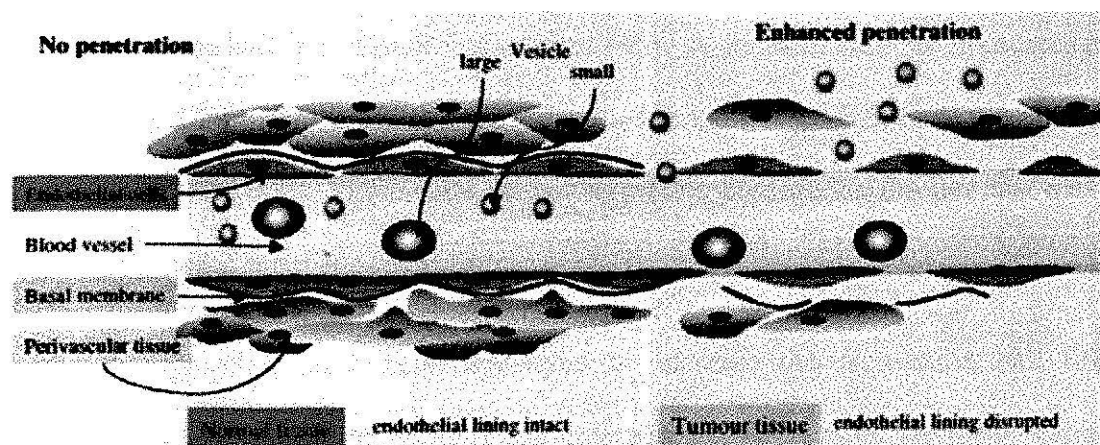


Fig. 1.2 'Enhanced Permeation and Retention' effect showing the extravasation of liposomes in tumor tissue (reproduced from <http://www.regulon.org/profile.html>)

**1.5.1 Conventional liposomes.** The first generation liposomal introduced were the conventional liposomes (90). Upon intravenous administration conventional liposomes are recognized and captured by the reticuloendothelial system (RES). This approach has

been exploited in treating parasitic and microbial infections of the RES. A classic example is Ambisome (AmB) which delivers amphotericin B to fungus-infected macrophages. However, conventional liposomes have minimal effect beyond cells of RES due to extensive blood clearance and short circulation half life (35, 36). Semple et al (40) reported that cationic liposomes made of 1,2-dioleoyl-3-N,N,N-trimethylaminopropane chloride (DOTMA):DOPC (1:1 mol mol<sup>-1</sup>) and DOTMA:DOPE (1:1 mol mol<sup>-1</sup>) have a protein binding (PB) value in excess of 500g protein /mol and are cleared rapidly from circulation in mice (40). Inclusion of 50% of the cationic lipid DOTMA in the liposome composition results in strong interactions with serum protein to the extent that they together form clots in plasma (41). A similar formulation employing DODAC instead of DOTMA with DOPE acquired a PB value of 800 g protein /mol and had a circulation half life of only few minutes (40). A series of cationic liposomes made by oku et al, 1996 (42) have displayed PB values ranging from 400-1100 g proteins/mol of total lipid (40), (42). The results are not surprising considering the fact that majority of plasma proteins carry negative charges at physiological pH (40).

Different approaches have been employed to increase the circulation half life of liposomes in vivo. Papahadjopoulos and coworkers (39) prepared sterically stabilized liposomes with hydrogenated phosphatidyl inositol/ phosphatidyl choline/ cholesterol (HPI/HPC/chol) which showed a liposome-associated doxorubicin half life of 15.5 hrs while conventional liposomes based on egg-derived phosphatidyl glycerol, phosphatidyl choline and cholesterol showed a liposome associated drug half life of only 1 hr.

**1.5.2 Stealth Liposomes.** Another strategy to improve liposome blood circulation time is to coat a hydrophilic polymer such as Polyethylene Glycol (PEG) on the liposome surface. The main feature of having PEG grafted on the liposome surface is the flexibility which permits a small percentage of PEG-lipids on the liposome to impart a sterically stabilized hydrophilic shell around the liposome. The hydrophilic, sterically stabilized PEG coating reduces adsorption of serum proteins on liposomes and their subsequent clearance by the RES. As the PEG hides the surface of liposome from being recognized these liposomes are called 'stealth liposomes'. The drug epirubicin has a half life of only 14 min. However, when encapsulated in Stealth liposomes (SL) the half life increased dramatically to 18 hrs. Also, the free epirubicin and its SL encapsulated-epirubicin showed more than 200-fold difference in both AUC and in clearance (39).

An example of stealth liposome, which is now commercially available is 'Doxil' manufactured by Janssen Pharmaceuticals (Fig. 1.3).

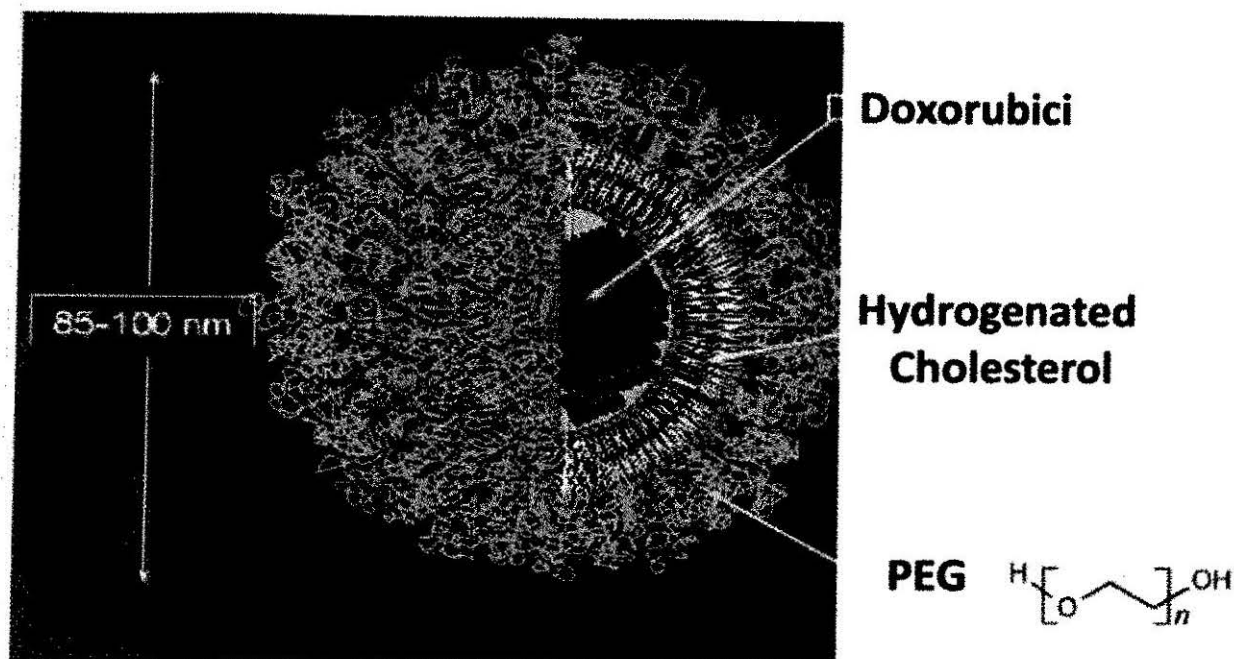


Fig. 1.3 Doxil coated with Polyethylene Glycol (adapted from (94))

The protein binding values of PEGylated liposomes are reported to be much lower compared to the conventional liposomes. Semple et al (40) reported that liposomes made of DSPC:CH and EPC:CH:DOPA in a lipid mol ratio 55:45 and 35:45:20 had PB values of 19 and 46 respectively. When 5% DSPE-PEG were included in above compositions the PB values dropped to 7 and 25 respectively (40). Du et al (46) showed that adhesion of erythrocytes, lymphocytes and macrophages onto glass surface coated with DPPE/DSPE-PEG liposomes drastically decreased as the DSPE-PEG mol% in such liposomes increased from 0 to 1%. However, the rate of decrease slows down as the PEG mol% increases further from 1 to 5 %.

Despite the increase in the accumulation of sterically stabilized liposomes in the tumor vicinity, the steric hindrance of the polymer chains on the liposome surface has posed a challenge in the interaction of liposome with tumor cells. Hong et al 1999, (43) reported

that the  $T_e$  ( $AUC_{tumor}/AUC_{plasma}$ ) ratio of DSPC/Cholesterol liposomes were 0.87 compared to 0.31 in the PEGylated liposome with 6 % DSPE-PEG in mice bearing C26 tumor. Similar findings were reported by Parr et al 1997; (44), where DSPC/Cholesterol and DSPC/Cholesterol/PEG-PE liposomes in Lewis lung model suggested a  $T_e$  value of 0.76 and 0.4 respectively.

The reduced interaction and binding of sterically stabilized liposomes with tumor cells reduces intracellular uptake of these carriers which causes the therapy to completely rely on the slow release of encapsulated drug from the liposome which might be suboptimal for tumor elimination.

### **Strategies of Triggered Release from Liposomes**

To increase the release of drug from the liposomes various strategies have been introduced including external stimuli (ultrasound, light and temperature change) but each one of them have their own challenges.

**1.6 Triggered release by ultrasound.** Ultrasound is a non invasive technique which can be focused to target tissues, can alter the permeability of cell membranes and can be controlled (47) (48). Acoustically active liposomes (ACL), liposomes that have air pockets and are responsive to reduced pressure or ultrasound, prepared by Huang et al (47) used ultrasound as the triggering mechanism for calcein release from EggPC/DPPE/DPPG/CH liposomes at a molar ratio of 69:8:8:15. Although the calcein release was carefully controlled, the encapsulation efficiency of calcein during liposome preparation was very low ( $\leq 20\%$ ) and the encapsulation and triggered release of hydrophobic drugs remained untested.



**1.7 Triggered release by light.** The light-sensitive liposomes exploit photoisomerization, photocleavage or photopolymerization of photoresponsive lipids in liposome membrane. The majority of photoisomerizable liposomes incorporate azobenzene lipids that isomerizes to cis form upon illuminated by ultraviolet light and switches back to the trans- form upon exposure to blue light (49) (Fig. 1.4 (a)).

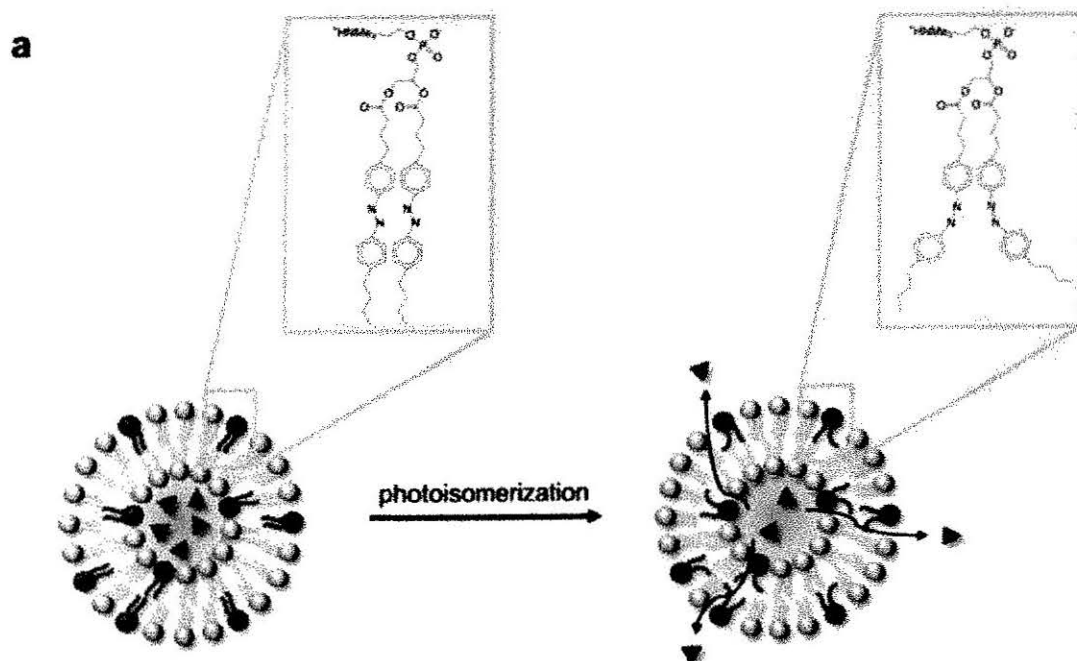


Fig. 1.4 (a) Drug release from liposomes by photoisomerization of lipids (Reproduced with permission from (49))

Conversion to the cis- form can destabilize the membrane and release drug contents. Although azobenzene derivatives have been extensively studied, retinoyl-phospholipids (50) and spiropyran, which converts to merocyanine at low wavelength of 365 nm have also been reported (51). The major drawback of photo-isomerization is that the

wavelength required to photo-isomerize the photosensitive lipids is in the lower range (lower visible or UV) which has limited penetration in the body.

The second major strategy of triggering liposomes by light is to incorporate photocleavable lipids in the liposomal membrane (Fig. 1.4 (b)). Thompson et al (52) reported the use of photocleavable lipids derived from plasmalogen. Photocleavage is enhanced by incorporating photosensitizers such as zinc phthalocyanine, tin octabutoxyphthalocyanine, or bacteriochlorophyll a. into the hydrophobic region of the liposomal bilayer (42).

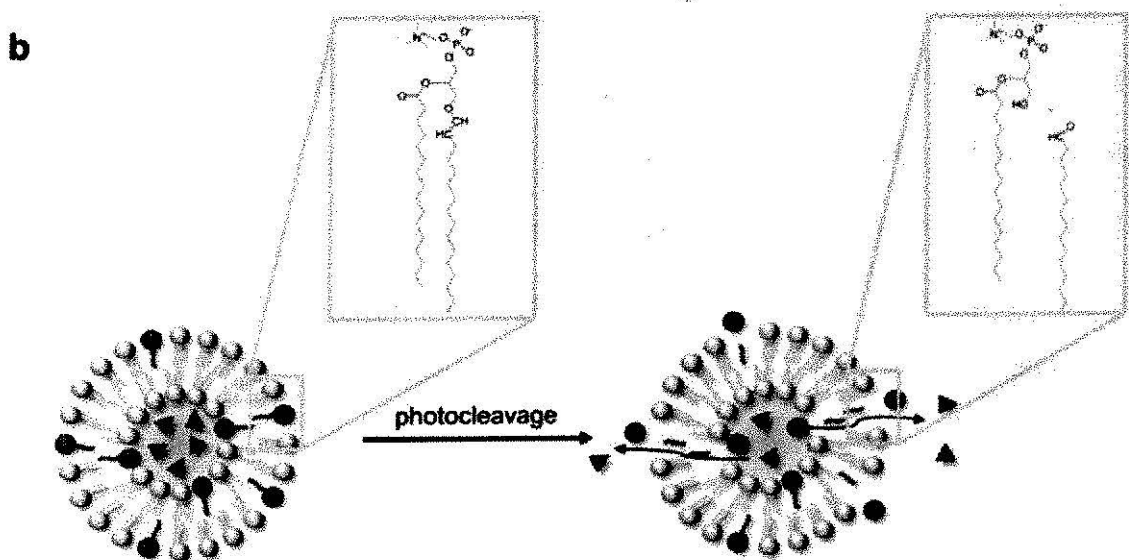


Fig. 1.4 (b) Drug release from liposomes by photocleavage of lipids (Reproduced with permission from (49))

Apart from naturally occurring plasmalogen lipids, synthetic photocleavable dithiane-based lipids have been reported (53) (54) to increase the drug release from liposomes. Interestingly Zhang and coworkers synthesized a DOPE-based photocleavable lipid called NVOC-DOPE which upon illumination by xenon lamp yielded free DOPE and subsequent membrane destabilization.

To date, the most successful of all the photo-induced triggering mechanisms is the plasmalogen based photosensitive liposomes although the sensitization of photocleavage of plasmalogen by sensitizers have resulted in production of reactive oxygen species which compromises the safety in patients.

A third light-induced drug releasing mechanism is the photo-polymerization (Fig. 1.4 (c)). The polymerization of cross a linking lipid 1,2-bis[10-(2',4'-hexadienoyloxy)-decanoyl]-*sn*-phosphatidylcholine in liposomes upon UV illumination yielded more than 100-fold increase in the release of fluorescent agent (56). The wavelength of the UV light can be adjusted by encapsulating photosensitizer dyes that can trigger the polymerization of lipids at higher wavelengths of light that are considered biologically safe. The incorporation of 1,1'-dioctadecyl-3,3,3',3'- tetramethylindocarbocyanine iodide (DiI) dye is one such example (49).

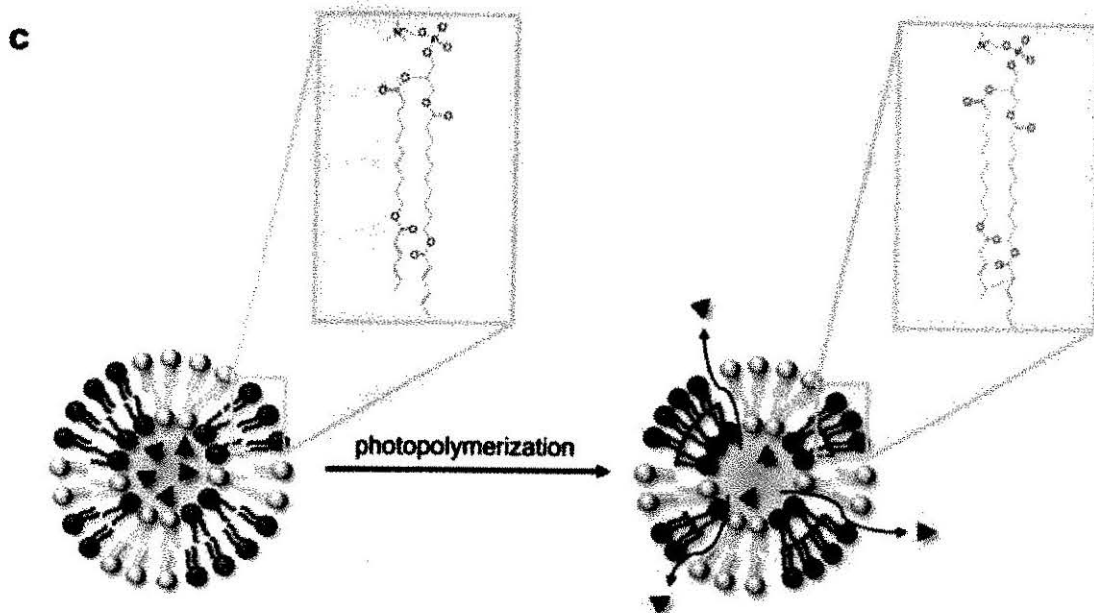


Fig. 1.4 (c) Drug release from liposomes by photopolymerization of lipids  
(Reproduced with permission from (49))

Although similar to photocleavable triggering strategy in terms of safe wavelength range, the stability of polymerizable lipids have not been tested yet (49).

In a photochemical triggering approach, O.V. Gerasimov et al, who explored photo-oxidative triggering in Bchl:DPPIsC liposomes, suggested that the photo-oxidative triggering method is severely limited by the low  $P_{O_2}$  level in the tumor environment. The ineffective photo-oxidation leads to creation of physiologically conducive atmosphere for growth of non apoptotic cells due to faulty photo-oxidation of tumor tissues (57).

**1.8 Triggered release by hyperthermia.** Yatvin et al (58) in 1978 reported heat-triggered release of neomycin from thermosensitive liposomes. An array of thermosensitive liposomal systems have since then been developed to increase the drug release at the tumor site. The thermo-triggered release approach is multifaceted in that

the application of heat 1) enhances vascular permeability and therefore accumulation at the tumor site, 2) enhances the release of drug from thermosensitive liposome at the tumor site, 3) probably increases localized blood supply and alter the intracellular uptake of drugs. Fig. 1.5 aptly illustrates the first two points.

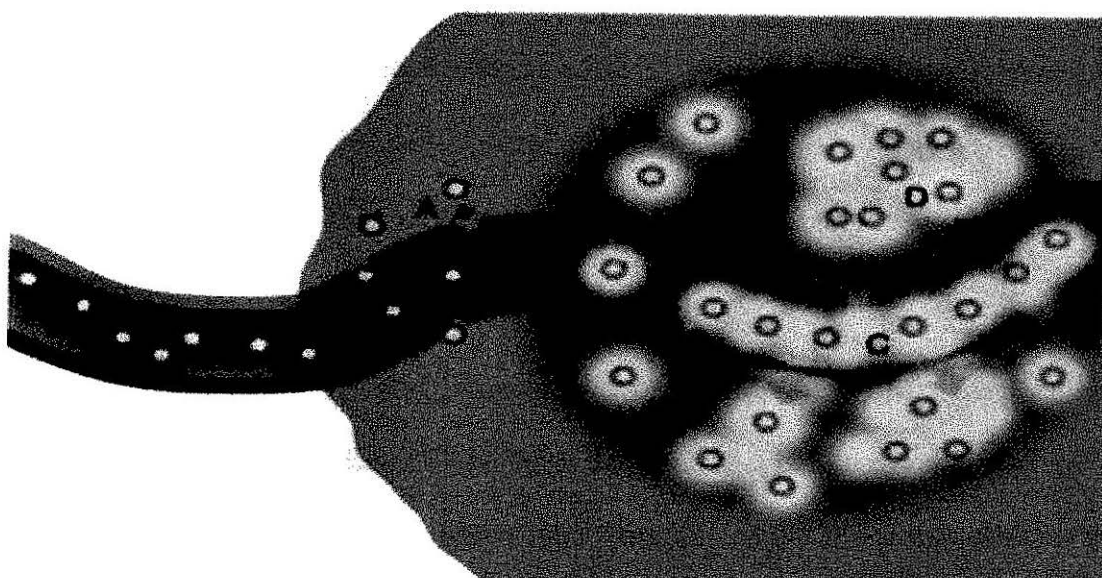


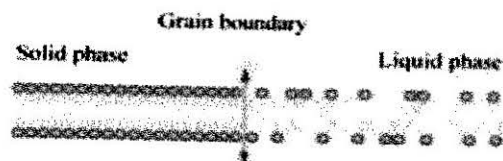
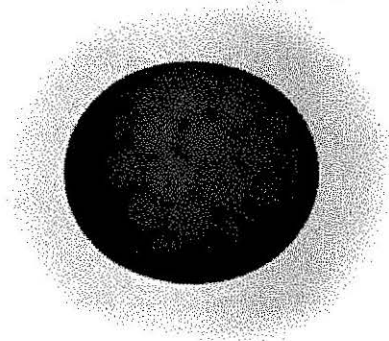
Fig. 1.5 A) enhanced accumulation of liposomes by EPR B) increased pore size of tumor vasculature C) increased drug release from the liposomes. (reproduced with permission from (59))

Traditionally thermosensitive liposomes have employed lipids that undergo conformational change from the *trans*- form to the *gauche*- form (59) at the lipid transition temperature, which converts the lipid membrane from the gel phase to the liquid crystalline phase of higher fluidity, which in turn enhances the drug leakage from the liposome. However the incorporation of purely lipid of lower melting temperature

such as DPPC (MP = 41°C) has shown slow and less amount of drug release. Also, the retention of drug molecules during circulation has been challenging. Incorporation of lipids of higher melting temperature such as DSPC (MP = 54°C) to increase packing incompatibility and therefore enhance drug release yielded broad peaks in Differential Scanning Calorimetry and necessitated higher triggering temperature (higher than 43°C) which can cause necrosis to normal tissues surrounding the tumor tissue. An estimate by Mosherer and coworkers (62) showed that the initiation of necrosis on porcine muscle begins after 30 min. of heat application at 40-43°C. Fine tuning the drug release at mild hyperthermia conditions (39-41°C) while maintaining the sharp melting peak so as to ensure efficient drug release in lethal doses remains a challenge for thermo-sensitive liposome research.

Another approach of preparing thermosensitive liposomes is the incorporation of lysolipids in the lipid membrane. Lysolipids are lipids that have bulkier head group with single acyl chain. These lipids typically form micelles and the lateral movement of these lipids as the temperature approaches transition, results in the accumulation of these lipids at pockets which start melting first, thus creating a micelle like curved structure at these pockets (Fig. 1.6).

Traditional thermosensitive liposome



Lysolipid-containing thermosensitive liposome

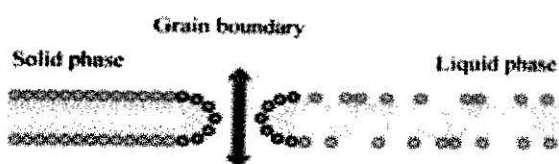
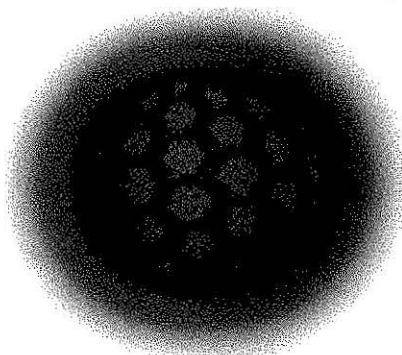


Fig 1.6 Traditional and lysolipid containing liposomes.  
(reproduced with permission from (59))

The formation of curved structures releases drug through the pores thus formed. Needham and coworkers (63) incorporated 10 % of the lysolipid MPPC in liposomes which resulted in reduction in phase transition temperature from 43°C to 39-40 °C and rapid drug release (approx. 50% released in 20s heating at 42°C). In general induction of lysolipids in liposomes drastically reduces the heating time which in turn reduces the possibility of onset of necrosis in surrounding tissues (59). However, the in vivo stability of the lysolipid containing liposomes remains a challenge. Banno and coworkers (65) reported that 70 % of the lysolipids were desorped from the liposome surface in vivo after one hour of injection and the amount of drug released from the liposomes recovered

from mice plasma after and 4 hrs of injection was 20 % and 50 % less. This suggests decrease in thermo sensitivity of liposomes after desorption of lysolipids. Sandstrom et al (66) demonstrated release of 50 % drug from lysolipid liposomes after 1 hour of injection in vivo.

The application of heat has been thus far, limited to superficially located tumors with regional heating. For localized hyperthermia microwave and radiowave applicator have been used (64) but the therapeutic depth of the external temperature stimuli is limited to 3 cm. For deep seated tumors microwave and radiofrequency electrodes with expandable prongs can be used but this approach remains invasive and is limited to the body area where insertion is practical (59).

Focused ultrasound although has been developed that can control the temperature remotely in deeply seated tissues with restricted focal zone but the monitoring of temperature still is done by invasion of temperature probe (59).

**1.9 Triggered release by magnetic field from magnetic liposomes.** Another strategy to triggered drug release is the application of magnetic field. Amstad et al, incorporated lipid coated iron oxide nanoparticles in the liposome membrane (Fig. 1.7) and showed the enhanced release of contents upon application of alternating magnetic field (AMF) due to local heating by iron oxide nanoparticles and thereby increase in membrane permeability. (68).



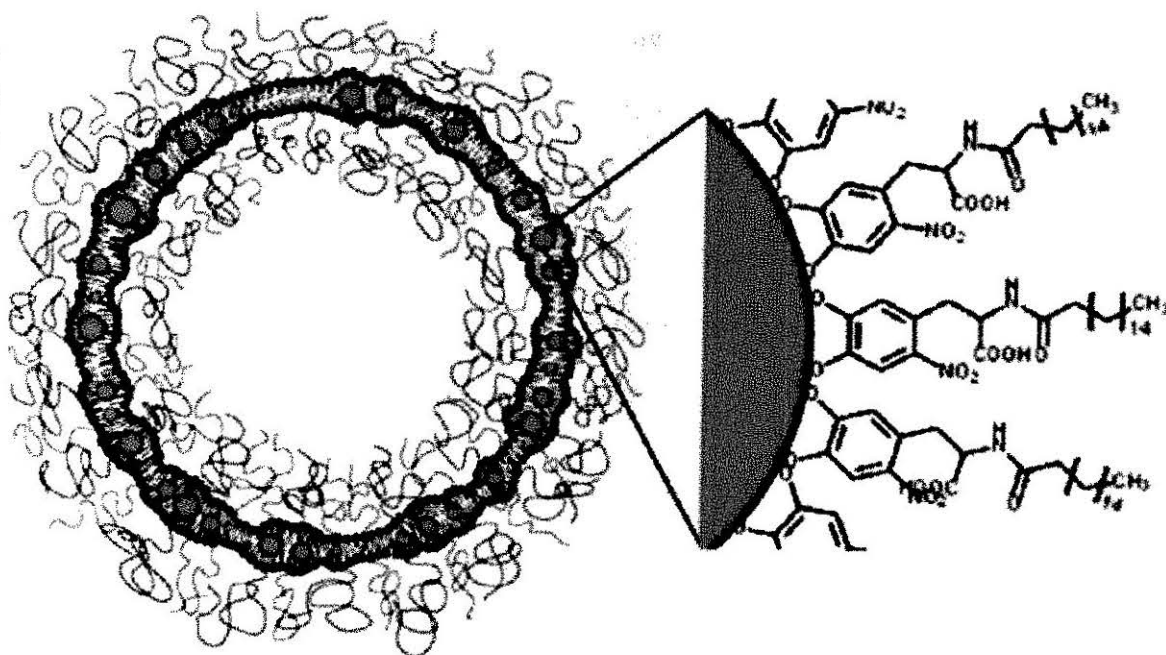


Fig 1.7 Iron oxide nanoparticles incorporated in lipid membrane.  
(reproduced with permission from (68))

Similar work was done by Babincova et al (69) where increasing concentration of ferromagnetic material in the membrane showed increased membrane permeability viz. as much as 70 % release of adriamycin at a ferocolloid concentration of 1.2 mg Fe/mL.

Another approach to prepare magnetic liposomes is to encapsulate magnetite particles in the liposomes which can then be directed to the tumor site by placing a magnet in the tumor vicinity externally. Nobuto et al (70), showed that the application of steady magnetic field of 0.4 tesla around tumor implanted limb of Syrian male hamsters increased the dox. concentration in tumor by 3 to 4 fold after intravenous administration of the magnetic liposomes. In the similar limb tumor model design, (71) instead of externally placing a magnet, magnet or non magnetic alloy was placed in the center of the tumor. Intravenously administered, adriamycin-loaded magnetic liposomes showed

significant antitumor activity and greater accumulation in tumor vasculature under magnetic force compared to magnetic liposomes without magnetic force (non magnetic alloy).

In one example, liposomes loaded with Tc 99 albumin resulted 25-fold increase in radioactivity in the left kidney of the rats under study where SmCo magnet was implanted compared to the right kidney without the magnet (72).

In an interesting study (73) RGD coated magnetic liposomes were first uptaken by monocytes and neutrophils and then magnetically directed to brain for the delivery of the model drug diclofenac sodium.

Furthermore, Magnetoliposomes prepared with bacterial magnetic particles containing cis-diamminedichloroplatinum (II) (CDDP) have been observed (74) to have 1.7 fold concentration at tumor site than the one ones prepared by artificial magnetic material.

## **Conclusion**

Commonly employed anticancer therapies and common tumor targeting strategies were reviewed and their limitations and challenges were discussed. Although active targeting employs specific ligand to enhance the drug delivery, antigen heterogeneity, high cost of production, immunogenicity and insufficient stability remain as its pressing challenges. Passive targeting by liposomes is an attractive approach to bypass these issues but the release of the cargo drug needs to be optimized. Because the drop of pH is involved in the interstitial space of many solid tumors, it serves as an attractive approach to trigger the release of anticancer drugs from liposome. Liposomes that respond to low pH (pH-sensitive liposomes) will be discussed in the following chapters.

## **Chapter 2: Acid Labile Linkers for the Design of pH-Sensitive Lipids and Liposomes**

The pH gradients in the tumor tissues present an interesting trigger. The pH in the tumor interstitium is 6.5 to 7.0 while the pH of the tumor core may be as low as 6.0. Once the formulation is endocytosed it meets even lower pH environment in the endosomal/lysosomal pathways where the pH is 2-3 units lower than in the blood circulation. Such lower pH can be exploited for either increased intracellular uptake of liposomes in the tumor tissue or destabilization of the liposome membrane for drug release intracellularly.

One attractive approach of designing pH-sensitive liposomes is to incorporate pH-cleavable lipids in the liposomes. pH-cleavable lipids can be constructed by incorporating an acid labile linker between the hydrophilic head and lipophilic tail of the lipid. The acidic environment catalyzes the hydrolysis of the lipid. An ideal liposomal formulation made of pH-cleavable lipids will be relatively stable at physiological pH and will destabilize upon cleavage of pH sensitive lipid either in the tumor environment or in the endosome/lysosome compartment of the cancer cells to release drug contents. Cordes and bull (76) have described the mechanism and catalysis of acetals, ketals and orthoesters. A number of acid-labile lipid structures have been designed to study their enhanced cytotoxic effects. The hydrolysis mechanism and pH sensitivity of such lipids are discussed in this section according to their acid-labile linkers.

### Acetal Linker

Acetal linker (Fig. 2.1) is an acid-labile linker where one carbon is attached to an alkyl group, a hydrogen atom and two alkoxy groups. The acidic hydrolysis of the acetal linker is shown in Scheme 2.1

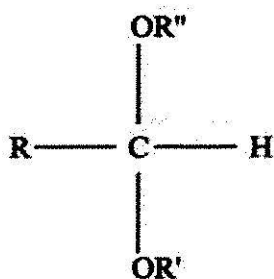
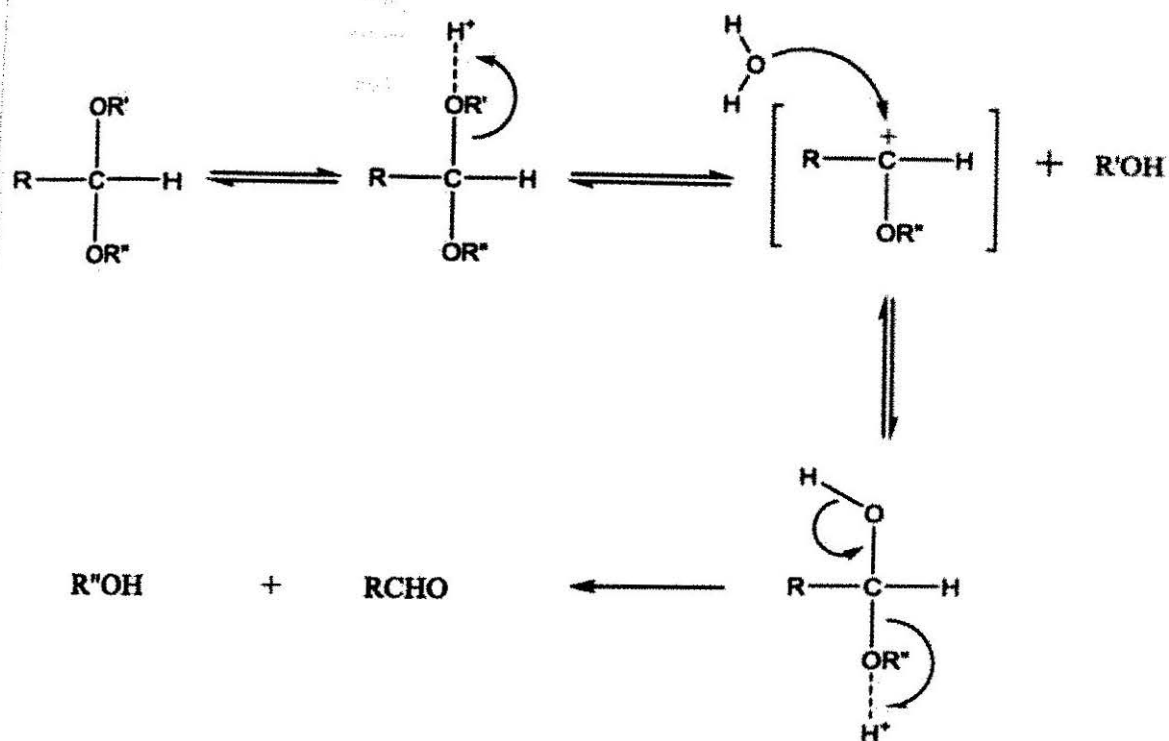


Fig. 2.1 Acetal linker



Scheme 2.1 Acidic hydrolysis of Acetal

Song and Hollingsworth (77) designed pH-sensitive acetal-based glycolipid (Fig. 2.2) and measured its pH sensitivity in ethanol. While 0.01 % addition of DCl started acetal cleavage which completed in 5 hours, addition of acetic acid from 1 to 20% did not show any significant acetal cleavage after 14 hours of observation under NMR. The pH sensitivity of the acetal based glycolipid remains to be tested in vivo.

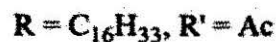
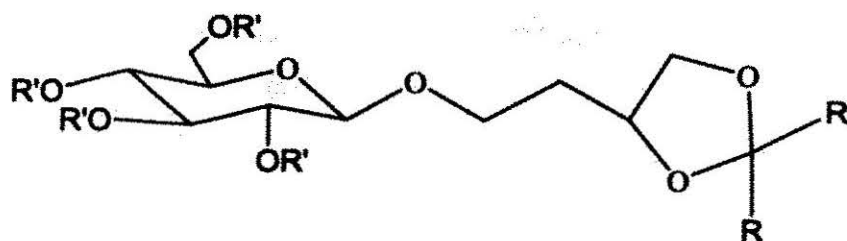


Fig. 2.2 pH-sensitive acetal based glycolipid

Asokan et al in 2004 (78) designed a 'bis-detergent' BD2 (Fig. 2.3) by cross linking two single chain tertiary amine detergents through an acetal linker. The pKa of headgroup was determined to be  $6.37 \pm 0.36$ . Liposomes prepared by 75 mol% of BD2 and 25 mol% of phosphatidyl choline demonstrated a hydrolysis half life of 3 hrs at pH 5.0 and showed complete hydrolysis at pH 4.0 after 6 hrs. The design of 'bis-detergent' irreversibly cleaves two single chain lipids which results in disruption of liposomes and release of drug content (Scheme 2.2).

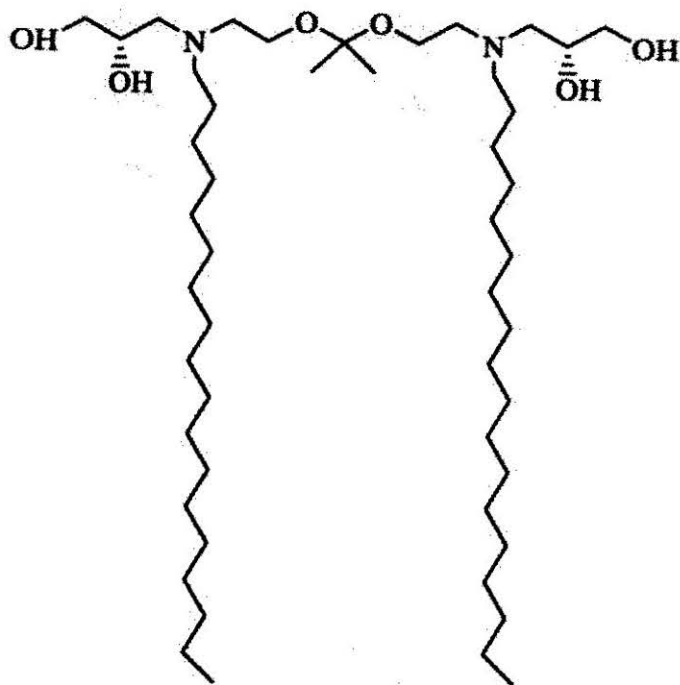
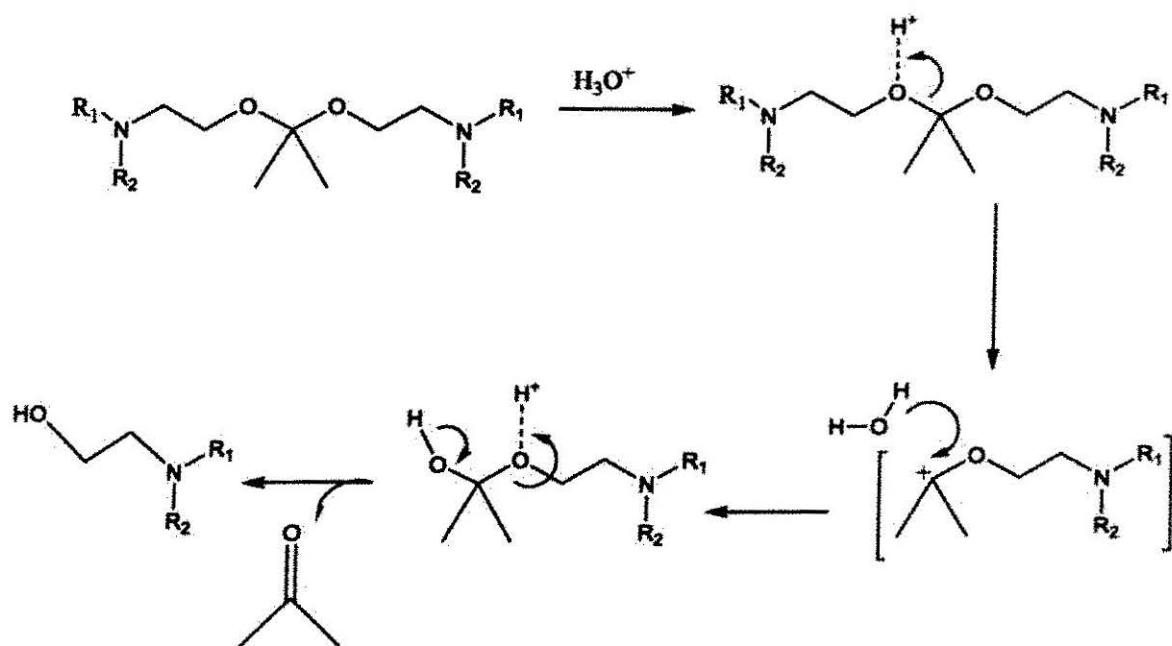


Fig. 2.3 Chemical Structure of BD2 lipid



Scheme 2.2 Mechanism of acid catalyzed hydrolysis BD2 lipid.

The liposomes made of BD2 were shown to enhance the intracellular delivery of Texas red-labeled oligonucleotides (TR-ON) and ON-705 compared to liposome with BD1 lipids (bis-detergent without pH labile linker).

### Vinyl Ether Linker

Vinyl ether (Fig. 2.4) is another linker which is relatively stable at neutral pH and hydrolyzes in acidic environment (Scheme 2.3).

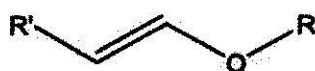
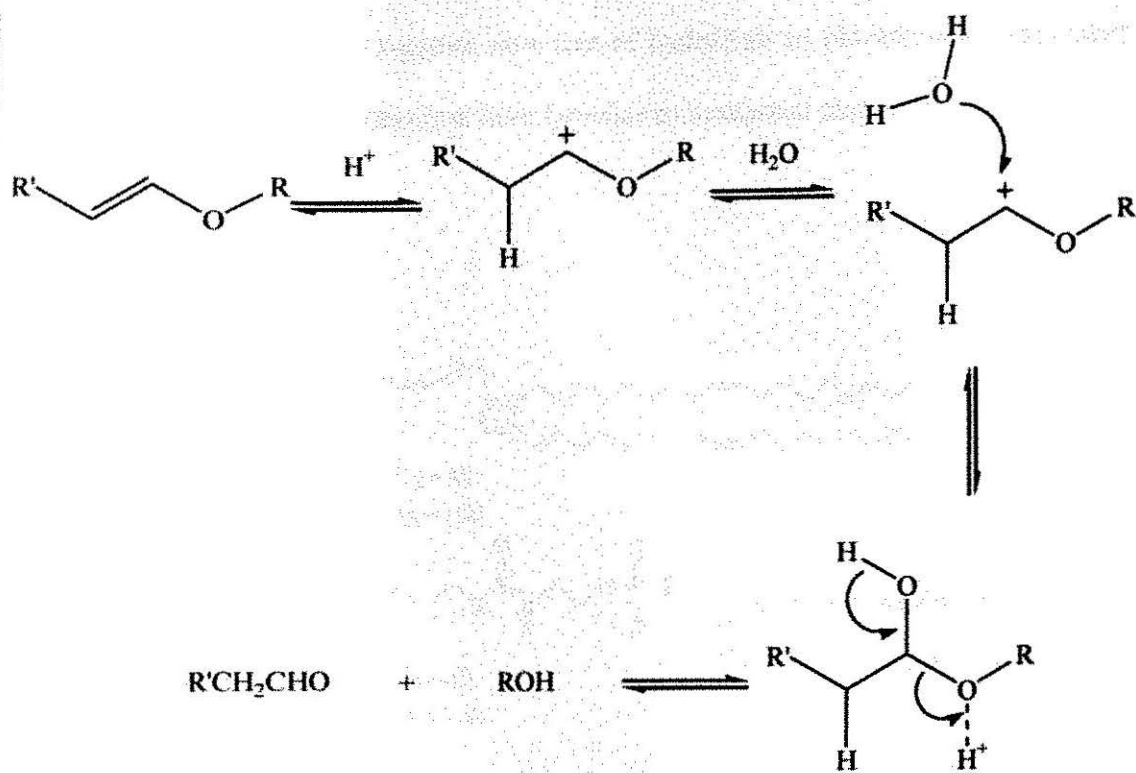


Fig. 2.4 Vinyl Ether Linkage





Scheme 2.3 Hydrolysis mechanism of Vinyl Ether under acidic conditions

Thompson and associates (79) have designed a series of lipids (Fig. 2.5) with vinyl ether linkages between the lipid tail and polar head group. They prepared liposomes with DOPE and pH-sensitive vinyl ether lipids. The mol % of DOPE was 90 % or higher, the high percentage of DOPE helps the transition of liposome from lamellar to hexagonal phase as the head group of vinyl ether pH-sensitive lipid cleaves from the lipid. The conversion of the liposome from lamellar to the hexagonal phase is dependent upon the kinetics of acidic hydrolysis of vinyl ether group. The best formulation that could achieve content release as much as 60% when calcein was used as a model dye was ST 352/DOPE in the molar ratio 5/95 after  $\approx 45$  hours at pH 4.5. The slow release of

contents from the liposome suggests slow rate of hydrolysis of pH-sensitive vinyl ether lipids and therefore slower transition from lamellar to hexagonal phase.

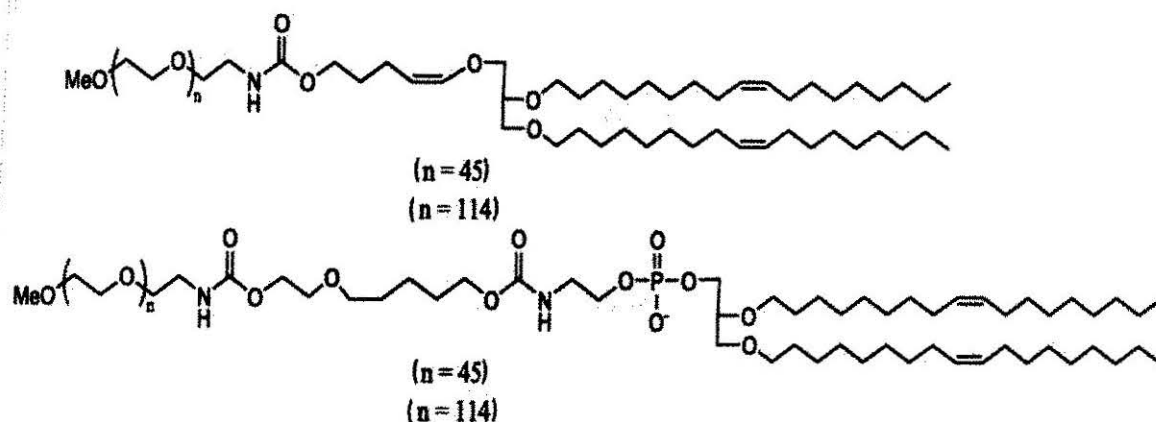
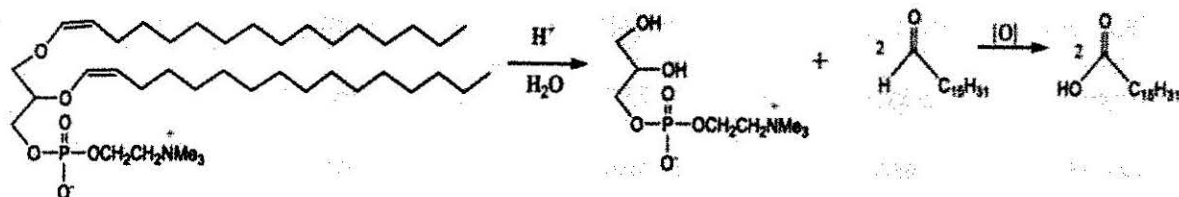


Fig. 2.5 Vinyl Ether lipids prepared by Thomson and Associates

Thompson and associates (80) in 1998, synthesized vinyl ether based pH-sensitive lipids (DPPIsC) (Scheme 2.4) where vinyl ether was linked between each of the two hydrophobic tails and the rest of the lipid molecule. Although the liposomes made of DPPIsC were very stable at pH 7.4 the calcein release kinetics of these liposomes suggested less pH sensitivity (see Table 2.1).



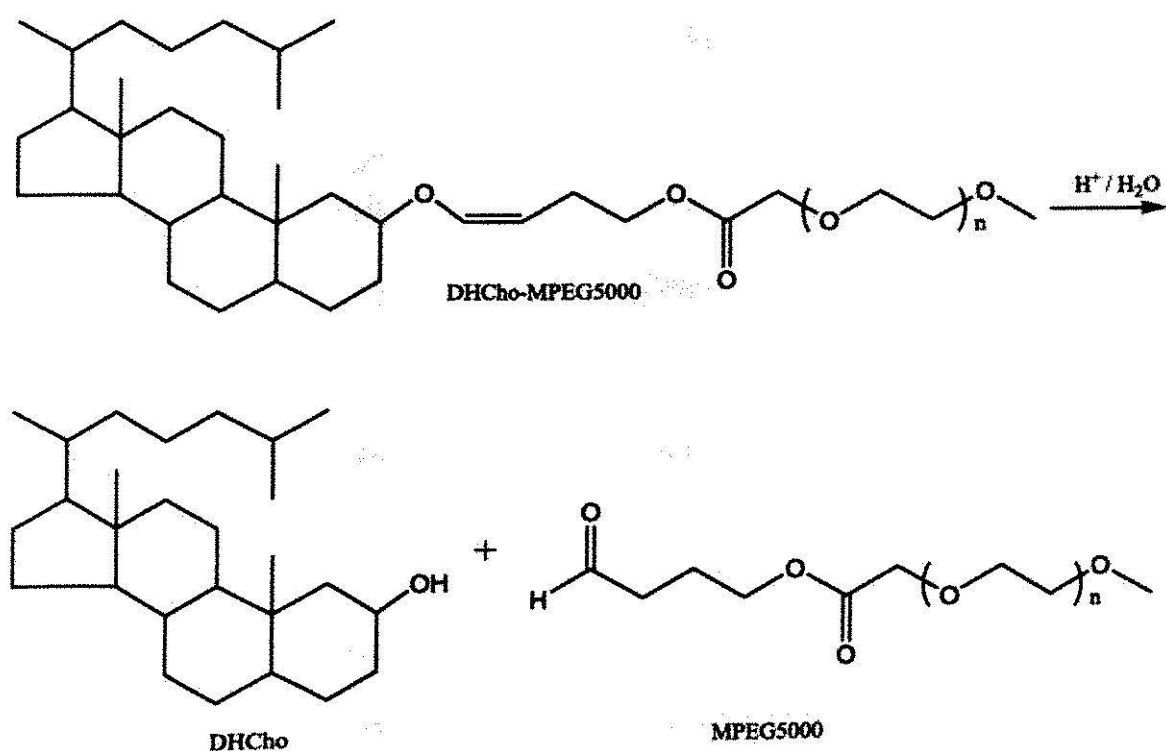
Scheme 2.4 Acid catalyzed hydrolysis of DPPIC

**Table 2.1** pH Dependence of 50% Release Time of Calcein

pH	$t_{50\% \text{ release (min)}}$
2.3	1.5
3.2	3.6
4.5	76
5.3	230
6.3	1740

The calcein release studies from liposomes made of pure DPPIC at  $37^\circ\text{C}$  indicate that the time required to release 50 % of calcein was  $\approx 4$  h at pH 5.3 while it took  $\approx 29$  h for 50 % calcein release at pH 6.3. Slow calcein release at lowered pH coupled with the fact that no calcein release was detected after 48 hrs of incubation at pH 7.4 suggest high stability of liposomes and less pH sensitivity of the vinyl ether lipids. However, less pH

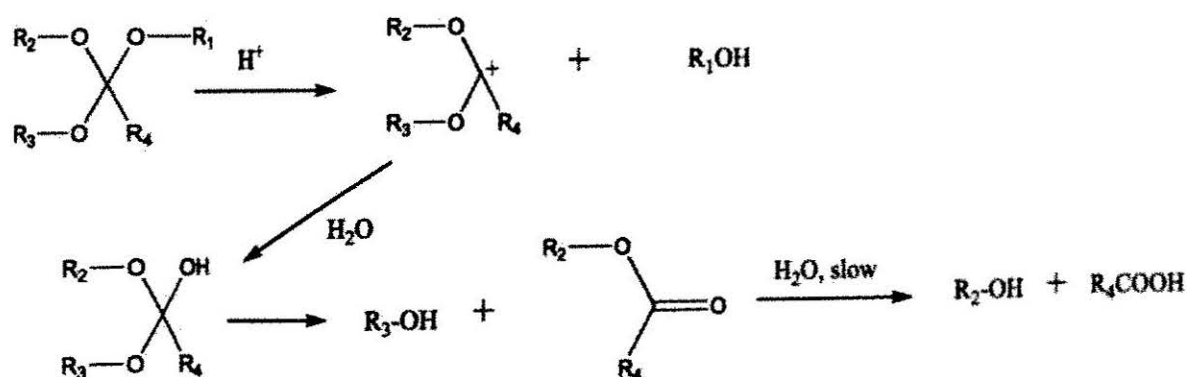
sensitivity at lower pH's reduce the release of encapsulated contents from the liposomes. Another study by bergstrand et al, (82) employed DHCh-MPEG 5000 (Scheme 2.5) lipids where vinyl ether was linked between PEG 5000 and hydrogenated cholesterol. The leakage percent of DHCh-MPEG 5000/DOPE liposomes at a molar ratio of 1:99 was about 22 % after 20 hrs of incubation at pH 4.5. Also, even 5 days of incubation of the conjugate at that pH could not completely hydrolyze the conjugate.



Scheme. 2.5 Acid Hydrolysis of DHCh-MPEG5000

## Ortho Ester

Orthoester is a more pH-sensitive linker than vinyl ether and is also found to be relatively stable at physiological pH. The acid-triggered hydrolysis of orthoester involves a stabilized dialkoxy carbonium ion (Scheme 2.6) that further degrades to an alcohol and an ester compound (81).



Scheme 2.6 Hydrolysis mechanism of Orthoester

Guo and Szoka synthesized a pH sensitive 'POD' lipid with a diorthoester linker (Fig 2.6) and incorporated it into liposomes. (Hydrolysis Scheme 2.7)

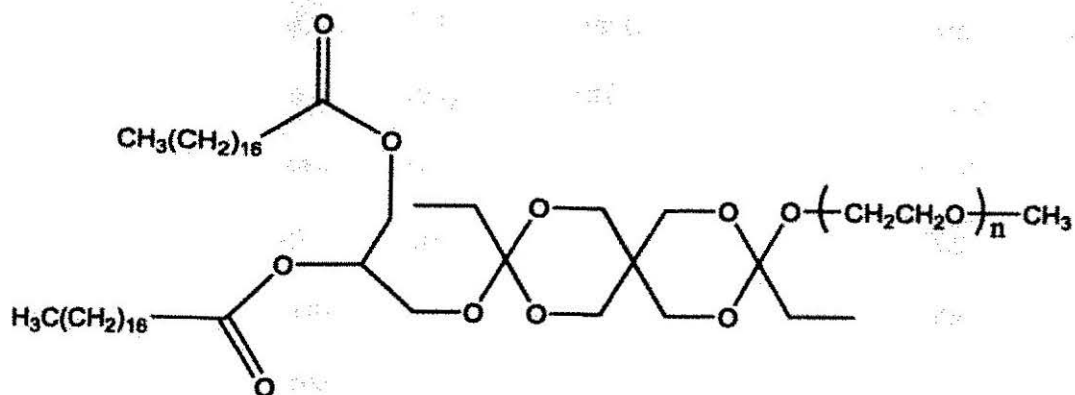
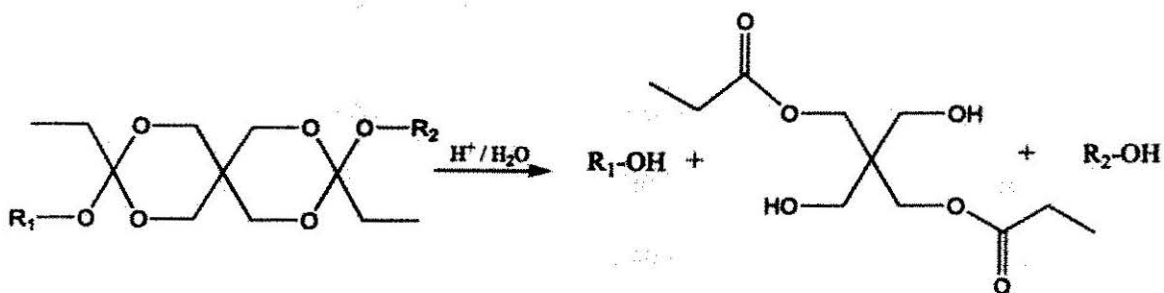


Fig. 2.6 Structure of the 'POD' lipid



Scheme. 2.7 Acidic hydrolysis of orthoester based lipid

The incorporation of POD and DOPE in a ratio of 1/9 in liposome membrane stabilizes the liposome at physiological pH but at low-pH POD hydrolyzes to shed off the PEG coating to convert the DOPE-rich liposome membrane to a hexagonal phase.

The stability of 10 mol % of POD incorporated into liposomes at alkaline pH 8.5 was about 2 weeks. In vivo studies on POD/DOPE liposomes suggested a half life of 200 min (83) while the half life of DSPE-PEG/DOPE liposomes was  $\approx$  295 min. Stability studies of POD conjugate suggested that it remained intact for 3 hours at 37°C while complete

hydrolysis was observed at pH 5 within 1 hour (81). The POD liposomes resulted in extensive content release and aggregation at pH 5-6 (81). The release of contents from the liposomes contains two phases: a lag phase when the contents slowly leaks through the liposome membranes followed by a burst phase when sufficient POD hydrolysis triggers the lamellar-to-inverted hexagonal phase change of the liposomes to quickly release most of the contents.

The POD has also been exploited in intracellular delivery of plasmid DNA (81). Stabilized plasmid-lipid particles (SPLP) composed of DOTAP, DOPE and plasmid DNA and 13 mol % POD resulted in liposome collapse within 110 min. at pH 5.3 whereas the pH-insensitive liposomes without POD remained stable at lowered pH.

Instead of diorthoester, masson et al (84) designed five and six membered ring orthoester based lipids (Fig. 2.7) and incorporated them into lipoplexes. The conjugates were stable for several days at pH 7.5 but the long term stability of lipoplexes composed of the pH sensitive orthoester lipids was not determined.

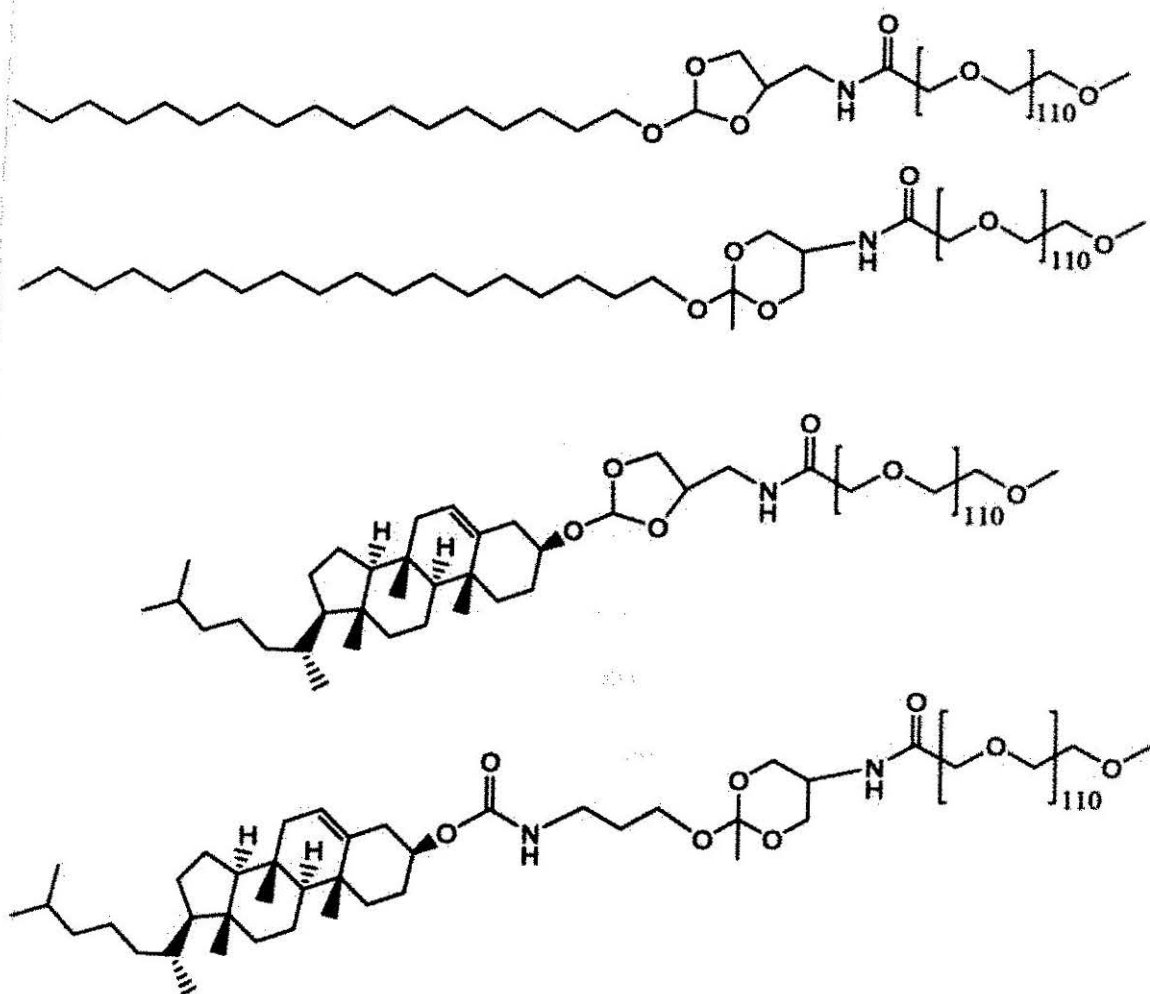


Fig. 2.7 Ortho ester lipids designed by Masson et al.

### Hydrazone Linker

Hydrazone presents another linker (Fig. 2.8) that has been exploited by researchers for pH-triggered drug/gene delivery.



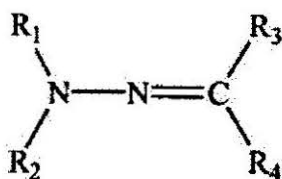


Fig. 2.8 Chemical structure of hydrazone linker.

Aissaoui et al (95) synthesized a series of cationic guanidinium based lipids (Fig. 2.9) where acylhydrazone linker was used to link head group with a steroid lipid tail. All the lipids were demonstrated to undergo acid-catalyzed hydrolysis. It was observed that unsaturated compounds BGBH-cholest-4-enone and BGTH-cholest-4-enone showed slower hydrolysis kinetics with half lives 1.9 and 2.3 days at pH 4.8 than the saturated BGBH-cholestanone and BGTH-cholestanone compounds with half lives of 1.2 and 1.3 days respectively. The lipoplexes composed of bis-guanidinium bis-(2-aminoethyl)amine hydrazone (BGBH)-cholest-4-enone/DNA mediated efficient gene transfection in mammalian cells and in mouse airways.

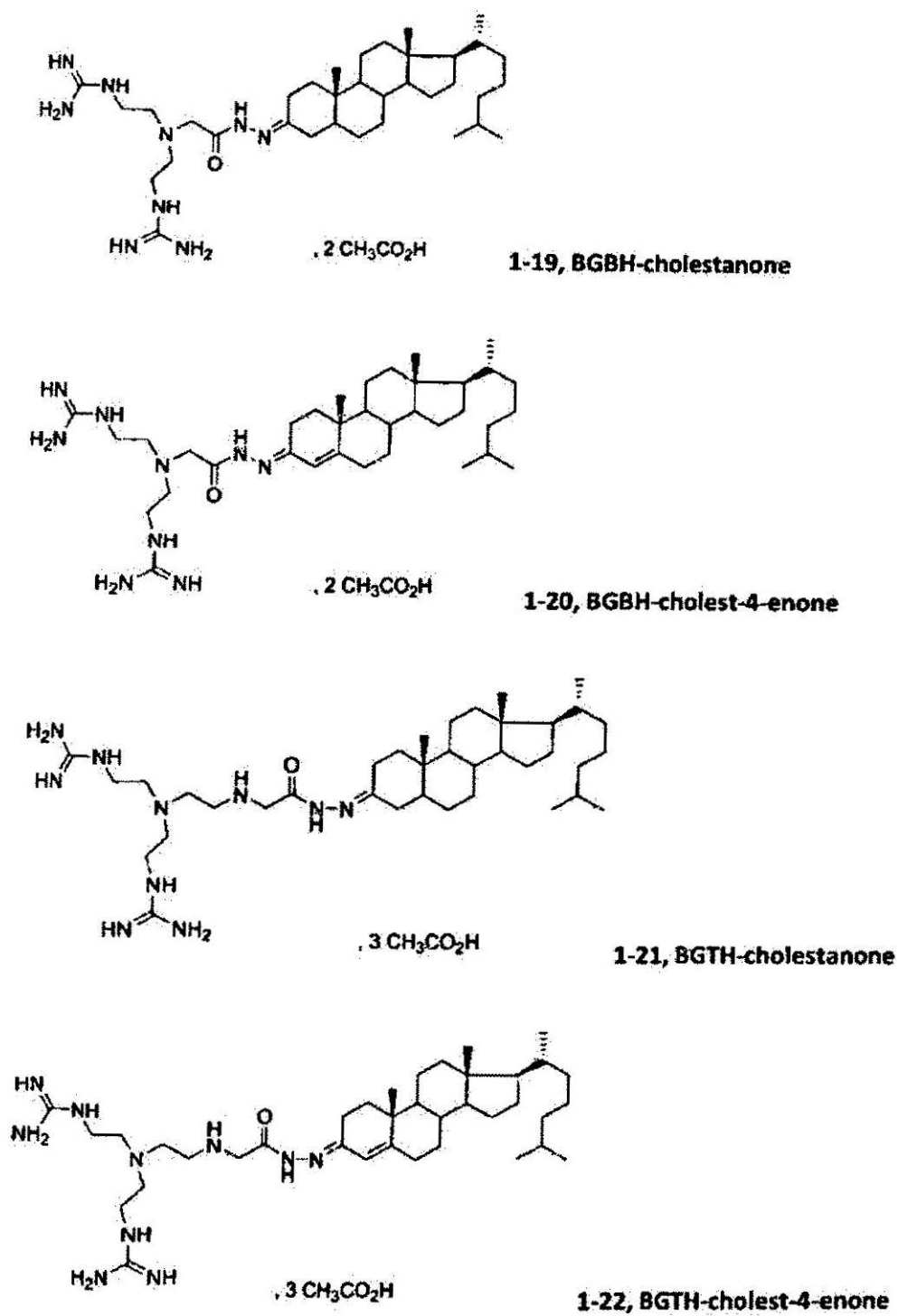


Figure 2.9 Chemical structures of guanidinium-based cationic lipids.

### **Shedding of PEG Coating by Hydrolysis of Hydrazone Linker**

Based on the review of pH-sensitive linkers we propose a strategy to improve intracellular uptake of liposomes by shedding the PEG coating that hinders the interaction of liposomes with the cell surface in the vicinity of tumor. The PEG coating can be removed by placing a hydrozone linker between lipid tails and polar head group. While hydrated PEG coating around the liposome surface hinders the hydrophobic interactions with serum proteins and immune cells in blood circulation, the removal of the PEG coating will lead to increased interaction of the liposomes with cancer cells at the acidic tumor interstitium.

One common feature of all cells is negatively charged cell surface. The presence of negatively charged lipids such as phosphatidylserine (PS) and phosphatidyl inositol (PI) impart negative charge on the cell surface. Vance and Steenbergen in 2005 (85), determined that approximately 15 % of PS and PI were found in rat liver cell membrane. Additionally the cell surface has an abundance of extracellular matrix (ECM) that contains proteoglycans and glycosaminoglycans which provide a majority of negative charges at the cell surface (Fig. 2.10). Additionally, tumor surface charge was found to be even more negative than normal cells (88). The glycosaminoglycans in the ECM include heparan sulfate, chondroitin sulfate and hyaluronic acid.

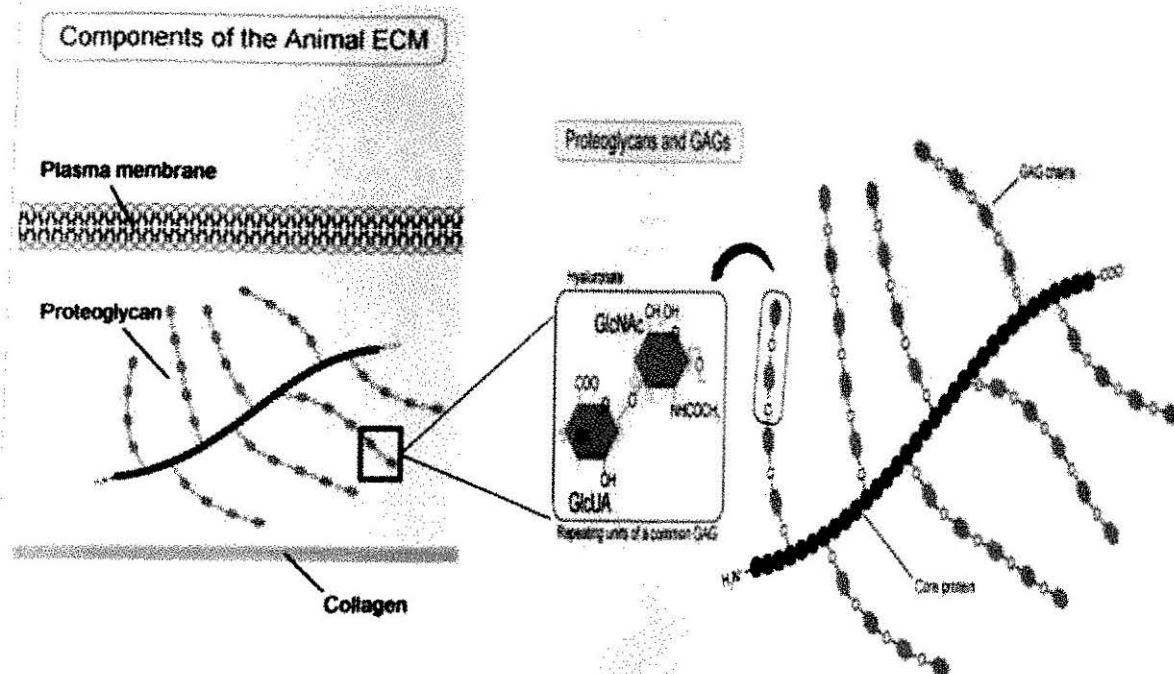


Fig. 2.10 Extracellular matrix over cells

Work of Mounkes et al (86) and Mislick et al (87) established that heparin/heparan sulfate and chondroitin sulfate play a crucial role in intracellular uptake of cationic lipoplexes.

Based on the aforementioned, we propose a pH-sensitive liposomal system that will act as a stealth liposome at physiological pH and convert to cationic liposome at lowered pH in the tumor environment for increased intracellular uptake (Fig. 2.11).

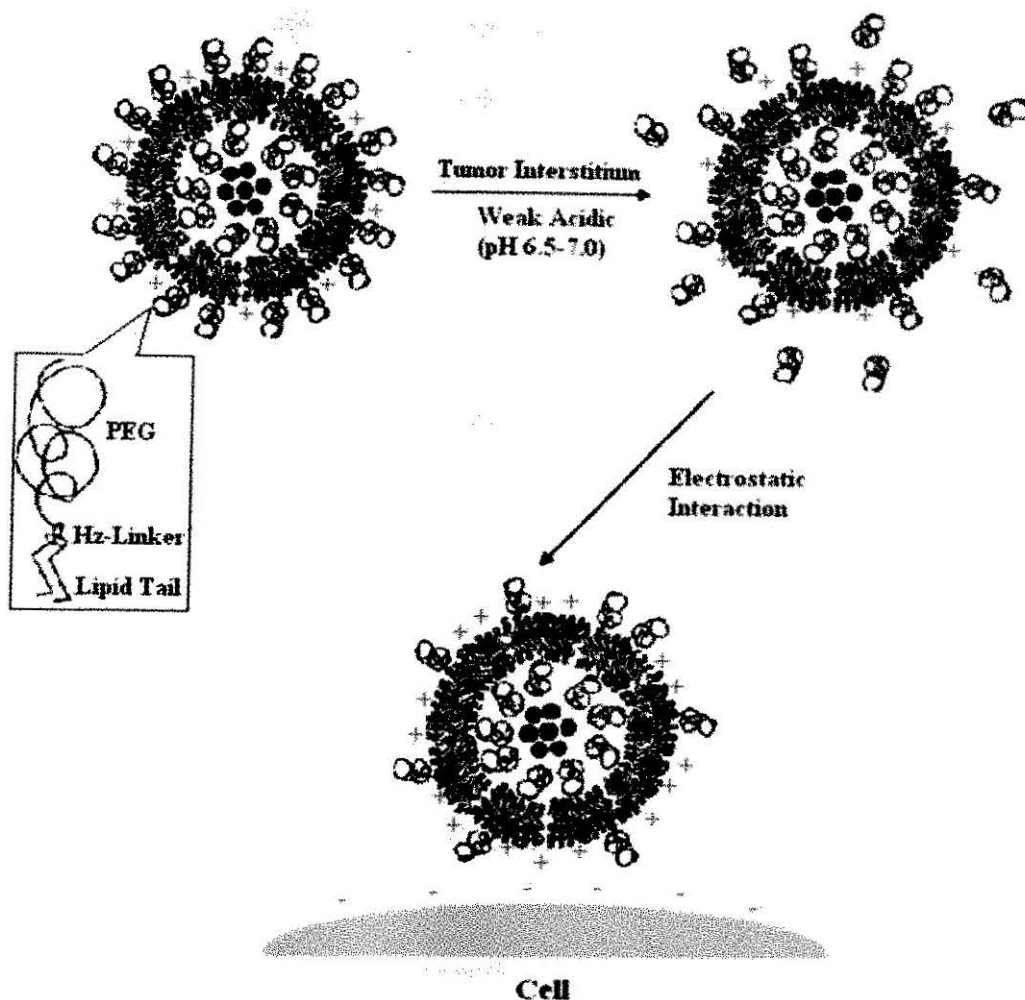
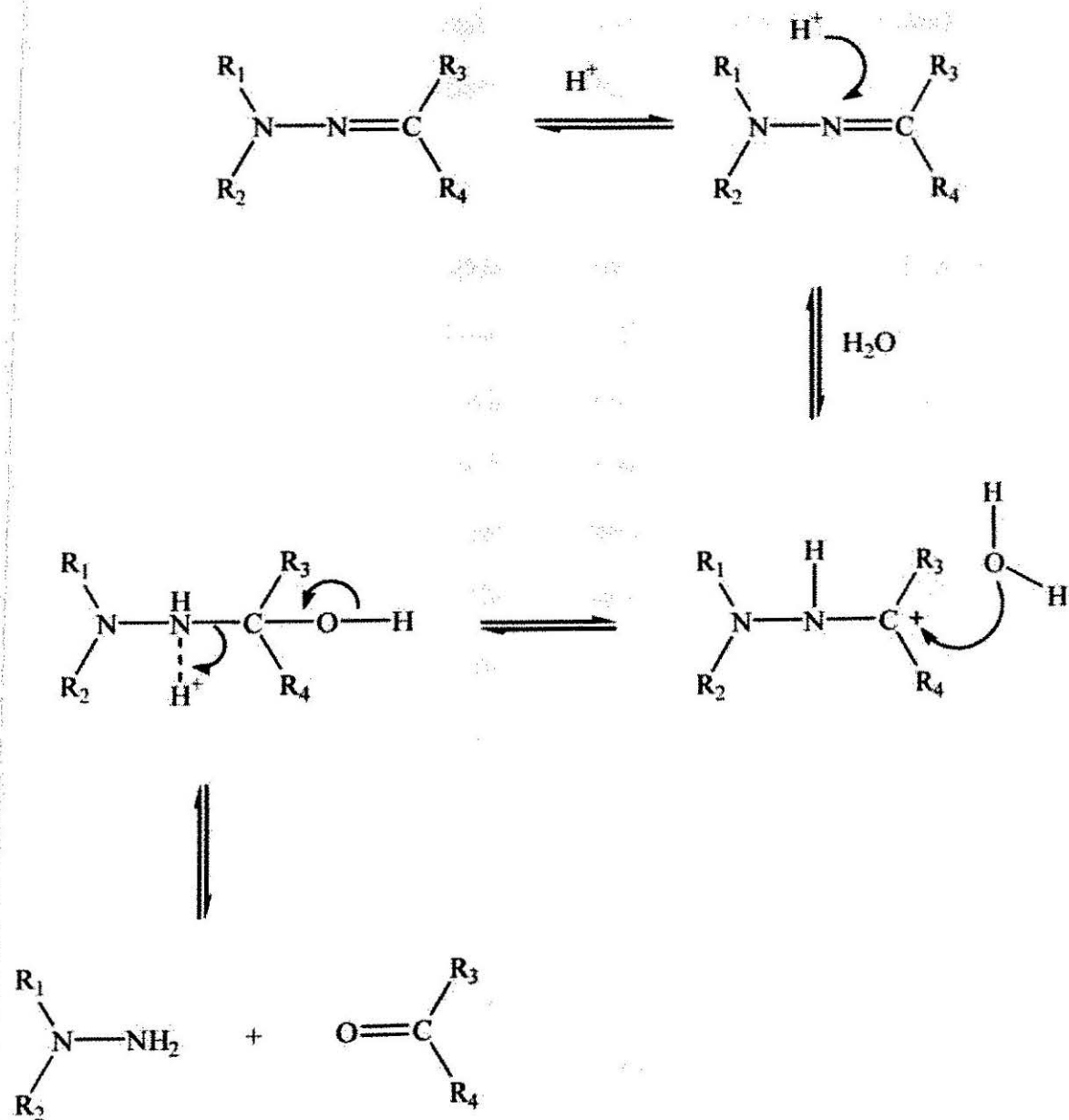


Fig. 2.11 Concept of design of hydrazone based pH-sensitive liposome

To achieve the pH triggering a novel PEG-lipid conjugate containing hydrazone linker can be introduced in the liposome membrane as mentioned earlier. The hydrazone linker is expected to hydrolyze at low-pH environment to shed off the PEG coating and leave a hydrazide lipid which can acquire positive charges on liposome surface in the weakly acidic tumor interstitium (**Scheme 2.8**). The formulation design can also contain

excessive positively charged lipid (e.g DOTAP) to overcome the limited mol% of PEG-lipid conjugates that can be incorporated into the liposome membrane.



Scheme 2.8 Acid Hydrolysis of Hydrazone

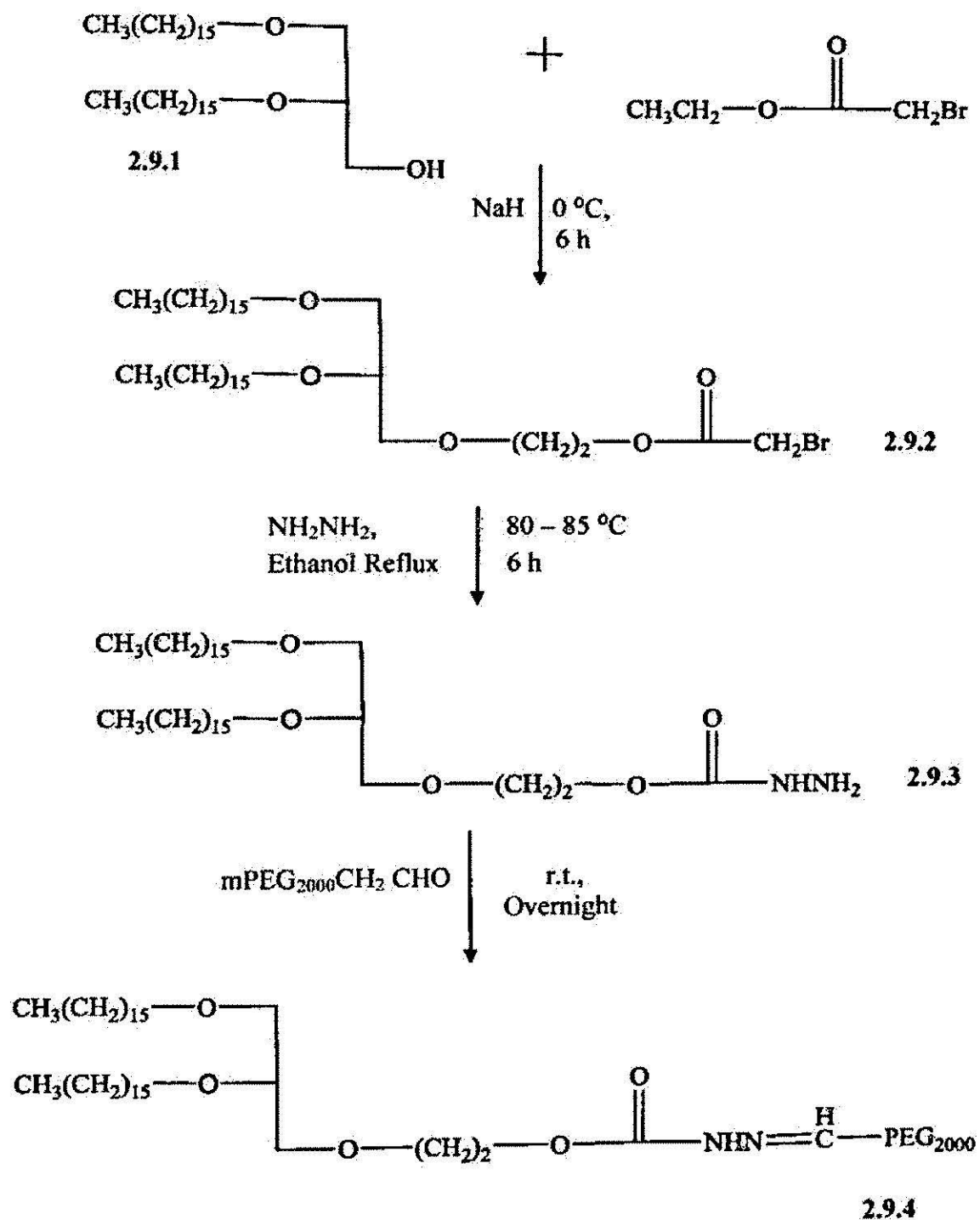
**2.1 Materials and methods.** 1,2-Di-O-hexadecyl-*rac*-glycerol (DHG) was purchased from Bachem. Ethyl Bromoacetate, sodium hydride (60% dispersion in mineral oil), hydrazine hydrate (80%), Iodobenzene diacetate (BAIB), 2,2,6,6-Tetramethylpiperidine-1-oxyl-4-amino-4-carboxylic acid (TEMPO) were acquired from Fisher Scientific. Polyethylene glycol 2000 monomethyl ether was obtained from Sigma Aldrich. All other organic solvents were purchased either from Sigma, Fisher or VWR.

## 2.2 Synthesis

**2.2.1 Synthesis of ethyl-2-(2,3-bis(hexadecyloxy)propoxy)acetate (DHG Ester)(2.9.2, Scheme 2.9).** 1,2-Di-O-hexadecyl-*rac*-glycerol (DHG) (1.5 g, 2.77 mmol, 1 equiv.), (2.9.1, Scheme 2.9) was dissolved in 20 mL of tetrahydrofuran. Sodium hydride (60% in mineral oil) (0.44 g, 11.08 mmol, 4 equiv.) was washed with hexane in a separate round bottom flask. Hexane was removed and DHG solution was added to sodium hydride at the bottom of the flask. The reaction was allowed to run for 30 min. under argon at room temperature. Temperature was lowered to 0°C and Ethyl Bromoacetate (1.85 g, 11.08 mmol, 4 equiv.) was added to the reaction mixture. The reaction mixture was stirred under argon for 6 hours and monitored by TLC (silica gel 60 F254, EMD chemicals, Germany) developed with ethyl acetate/hexane = 1/10. Then H<sub>2</sub>O was added and the mixture was washed with diethyl ether. The combined organic layers were dried over sodium sulfate, filtered, concentrated in vacuum and purified by silica gel chromatography with a gradient mobile phase of Ethyl acetate/Hexane (1/20 to 1/10, v/v). (Yield 51%) (MALDI +ve ion mode: 650.6 (M+Na)<sup>+</sup>, <sup>1</sup>HNMR (600 MHz, CDCl<sub>3</sub>) (Fig. 2.12): δ 0.83-0.87 (t, 6H, 2 CH<sub>3</sub>(CH<sub>2</sub>)<sub>15</sub>-), 1.18-1.32 (m, 52H, 2 -OCH<sub>2</sub>CH<sub>2</sub>(CH<sub>2</sub>)<sub>13</sub>CH<sub>3</sub>),

1.53 (m, 4H, 2 -OCH<sub>2</sub>CH<sub>2</sub>(CH<sub>2</sub>)<sub>13</sub>CH<sub>3</sub>), 3.38-3.68 (m, 7H, CH<sub>3</sub>(CH<sub>2</sub>)<sub>14</sub>CH<sub>2</sub>OCH<sub>2</sub>CHO-  
,CH<sub>2</sub>), 4.1-4.26 (m, 4H, CH<sub>2</sub>COOCH<sub>2</sub>).





Scheme 2.9 Synthesis of DHG-Hz-PEG conjugate

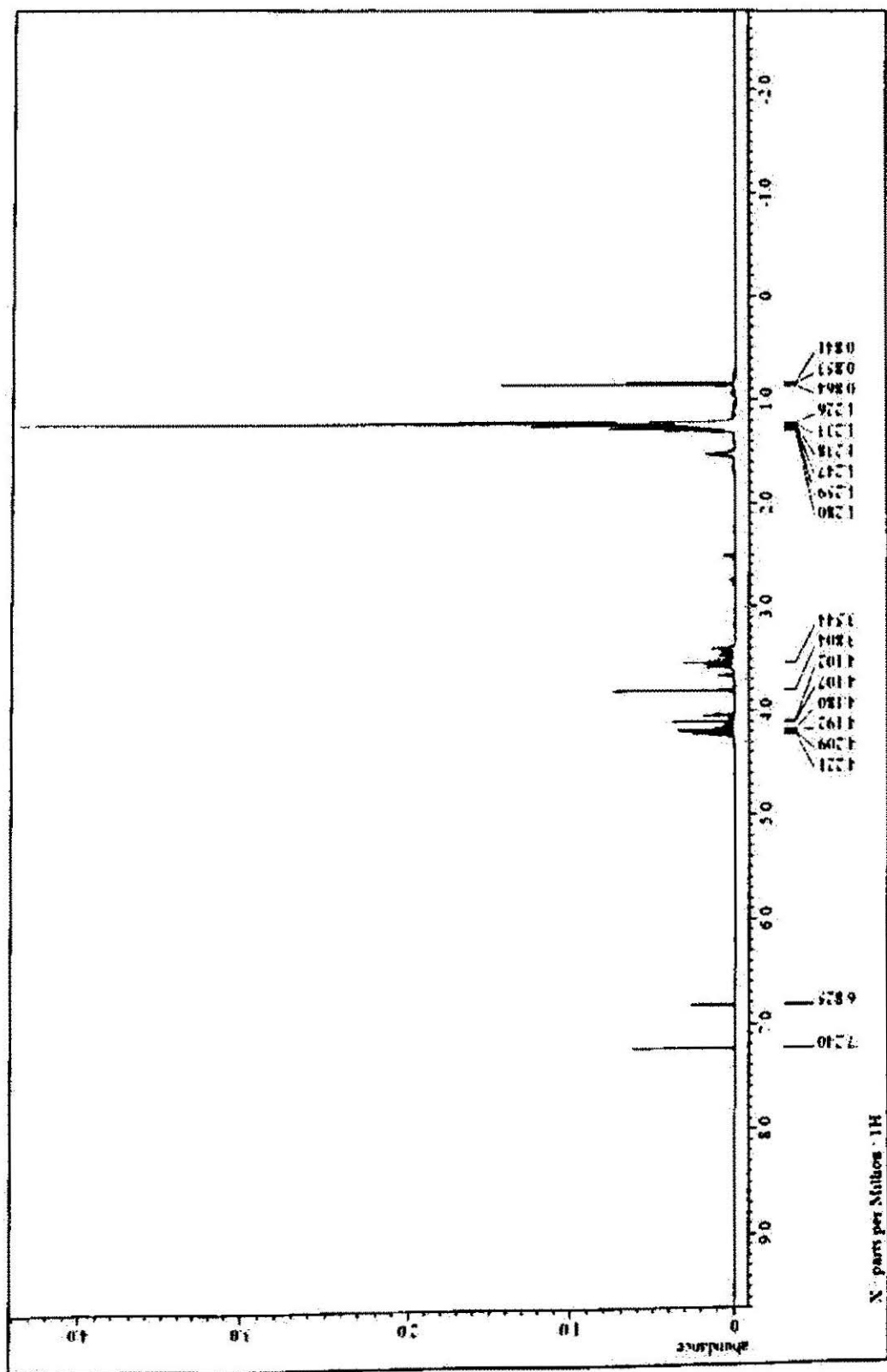


Fig. 2.12 NMR Spectrum of DiG Ester

**2.2.2 Synthesis of 2-(2,3-bis(hexadecyloxy)propoxy)ethyl Hydrazinecarboxylate (DHG Hydrazide) (2.9.3, Scheme 2.9).** Ethyl-2-(2,3-bis(hexadecyloxy)propoxy)acetate (2.9.2, 0.48 g, 0.765 mmol, 1 equiv.) was dissolved in ethanol at 50°C under argon followed by addition of hydrazine hydrate (2.3 mmol, 3 equiv.). The temperature was raised to 80-85°C and ethanol was allowed to reflux for 6 hours under argon. The reaction mixture was monitored by TLC developed with ethanol / 2% NH<sub>4</sub>OH. The reaction was cooled to 0°C, the separated precipitate was filtered off and washed with ethanol. (Yield 100 %), AccuTOF (M + H)<sup>+</sup> 613.5 <sup>1</sup>HNMR (600 MHz, CDCl<sub>3</sub>) (Fig. 2.13): δ 0.84-0.89 (t, 6H, 2 - (CH<sub>2</sub>)<sub>15</sub>CH<sub>3</sub>), 1.2-1.35 (m, 52H, 2 -OCH<sub>2</sub>CH<sub>2</sub>(CH<sub>2</sub>)<sub>13</sub>CH<sub>3</sub>), 1.56 (m, 4H, 2 -OCH<sub>2</sub>CH<sub>2</sub>(CH<sub>2</sub>)<sub>13</sub>CH<sub>3</sub>), 3.38-3.72 (m, 7H, CH<sub>3</sub>(CH<sub>2</sub>)<sub>14</sub>CH<sub>2</sub>OCH<sub>2</sub>CH<sub>2</sub>O-, CH<sub>2</sub>), 4.4 (s, 2H, -NH-NH<sub>2</sub>), 9.04 (s, 1H, -NH-NH<sub>2</sub>)

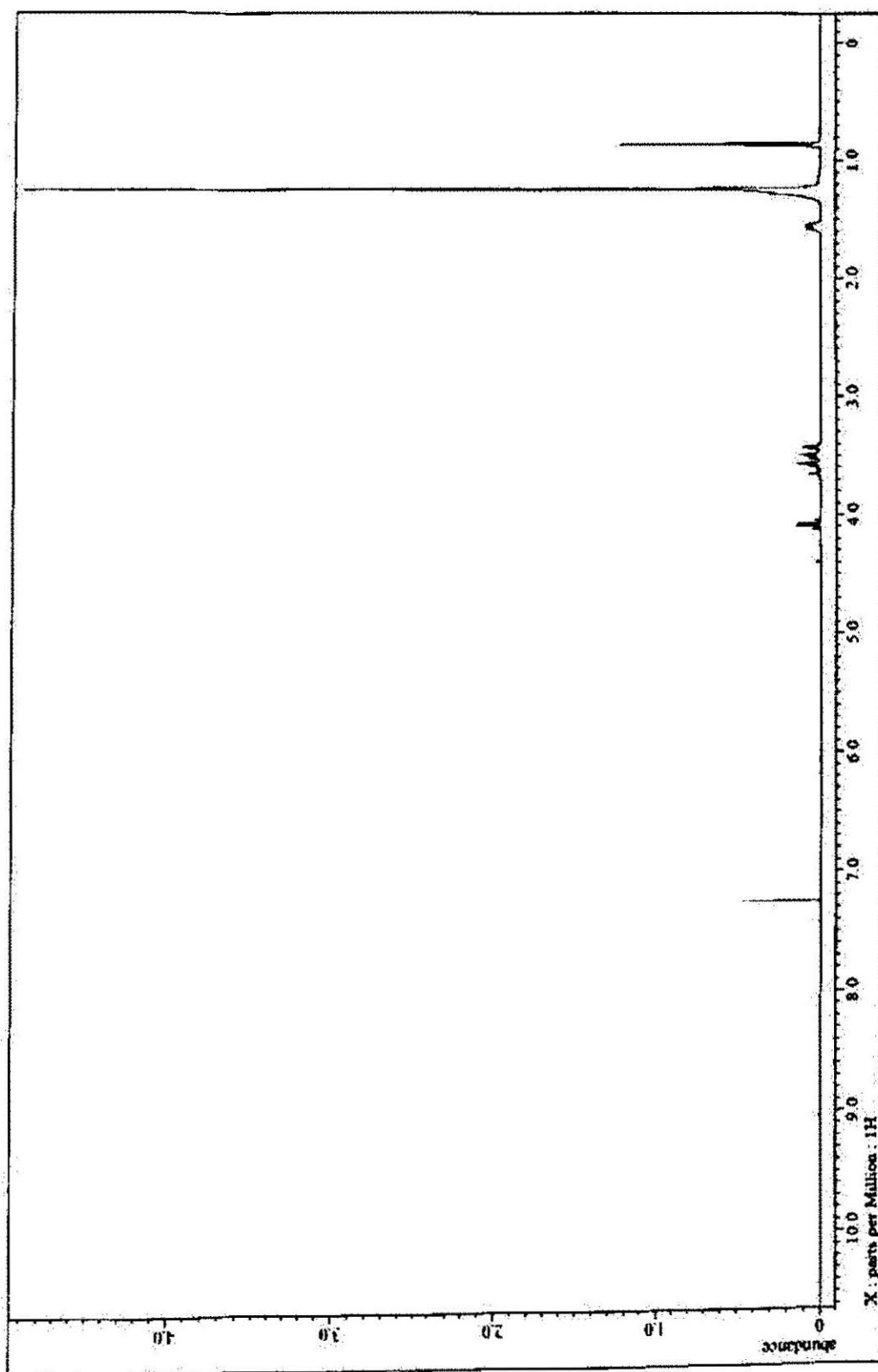
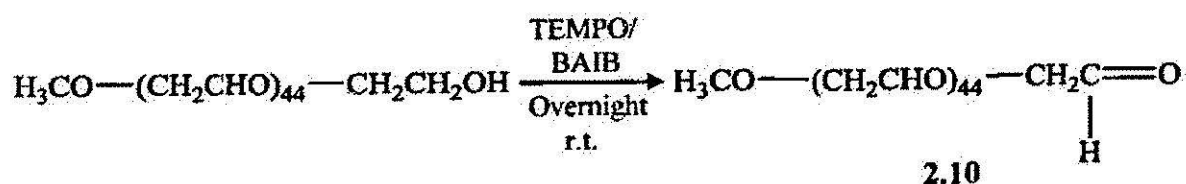
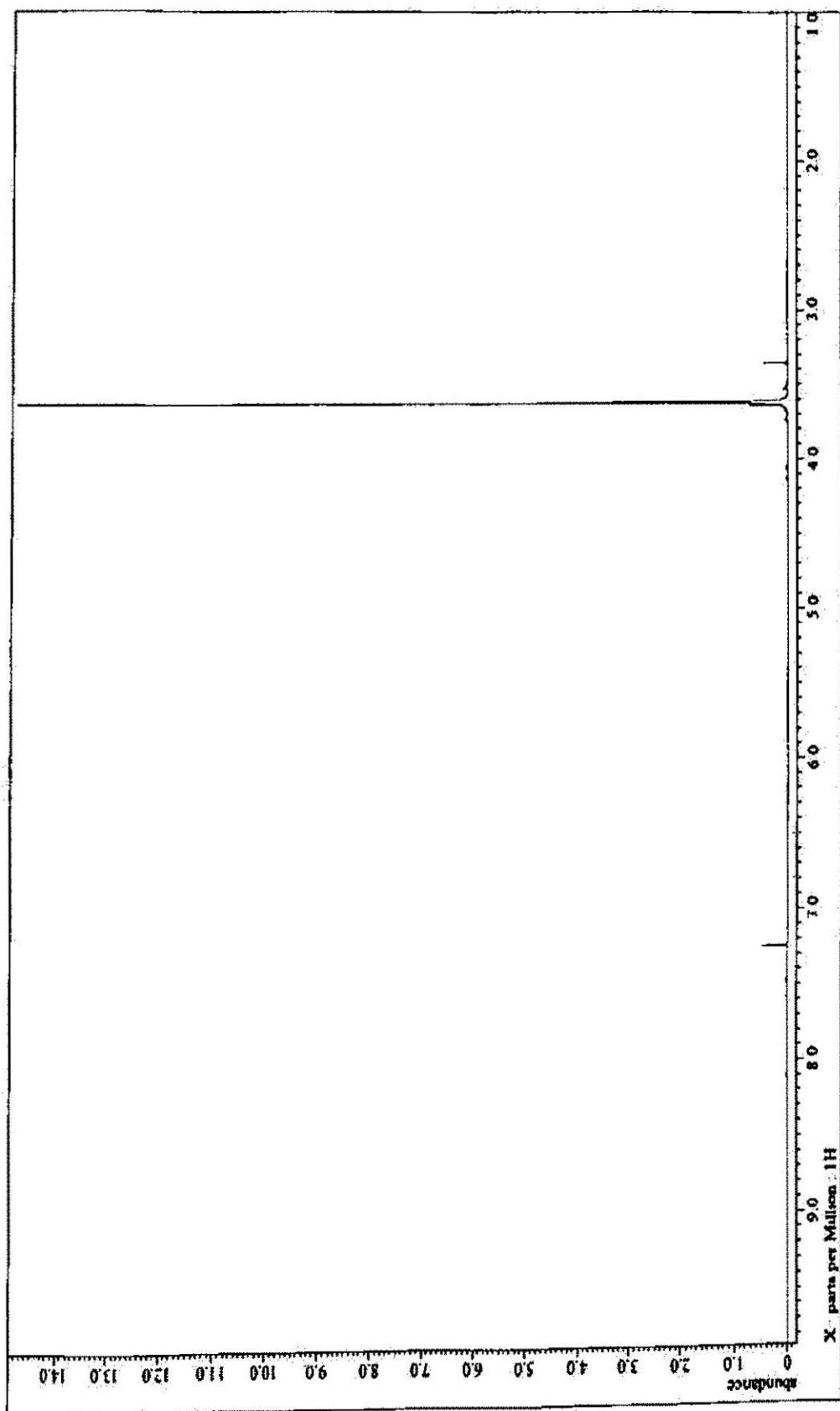


Fig. 2.13 NMR Spectrum of DHG Hydrazide

**2.2.3 Synthesis of mPEG-2000 Acetaldehyde (2.10, Scheme 2.10).** Polyethylene glycol 2000 monomethyl ether (mPEG) (2g) was dissolved in 20 mL of anhydrous toluene and dried under vacuum. 15 mL of dichloromethane was added to previously dried mPEG. TEMPO (0.035g, 0.224 mmol) was added followed by addition of BAIB (1g, 3.1 mmol). The reaction was stirred at room temperature overnight under argon. The mixture was then precipitated by adding 150 mL of anhydrous diethyl ether, filtered and dried. (Yield 56 %)  $^1\text{H NMR}$  (600 MHz,  $\text{CDCl}_3$ ) (Fig. 2.14):  $\delta$  3.35 (s, 3H), 3.50 – 3.70 (m, 176H), 4.13 (s, 2H), 9.71 (s, 1H)



Scheme 2.10 Synthesis of mPEG<sub>2000</sub> Acetaldehyde

Fig. 2.14 NMR Spectrum of mPEG<sub>1000</sub> Acetaldehyde

**2.2.4 Synthesis of DHG-Hz-PEG (2.9.4, Scheme 2.9).** Hydrazide activated DHG (0.1g, 0.172 mmol) was dissolved in chloroform followed by addition of mPEG-Aldehyde (0.86g, 0.43 mmol). The reaction mixture was stirred overnight under argon at room temperature and monitored by TLC developed with  $\text{CH}_3\text{OH}/\text{CH}_2\text{Cl}_2$  1/9 with 2% ammonium hydroxide (Fig 2.15).

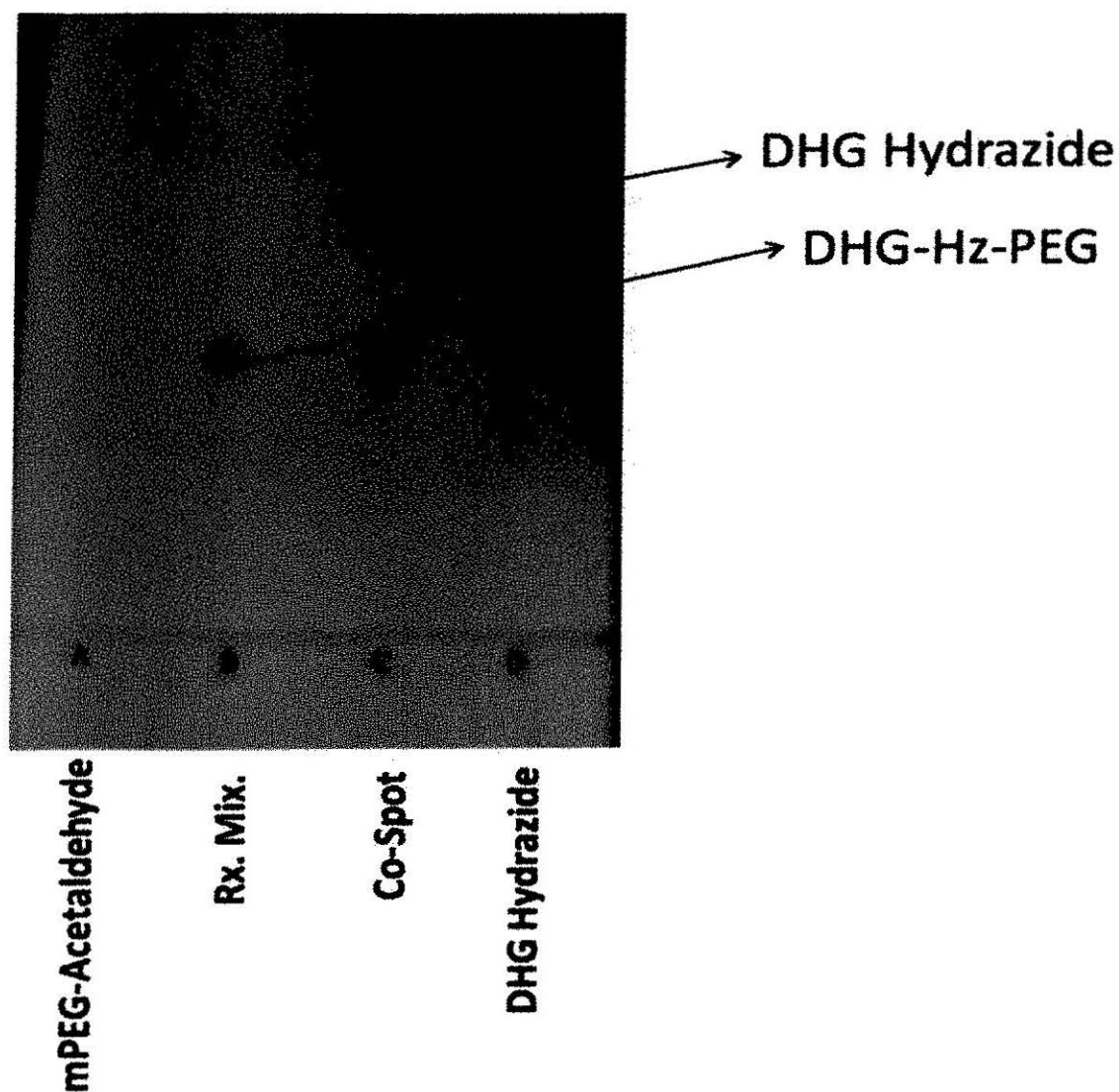


Fig. 2.15 TLC showing the formation of DHG-Hz-PEG lipid

### pH-sensitivity of DHG-Hz-PEG

The pH sensitivity of DHG-Hz-PEG was tested by adding 2% acetic acid in the ethanolic solution of the reaction mixture. The acidified reaction mixture immediately shows the spot characteristic of DHG hydrazide (Fig. 2.16) suggesting hydrolysis of the DHG-Hz-PEG conjugate (Scheme 2.8).

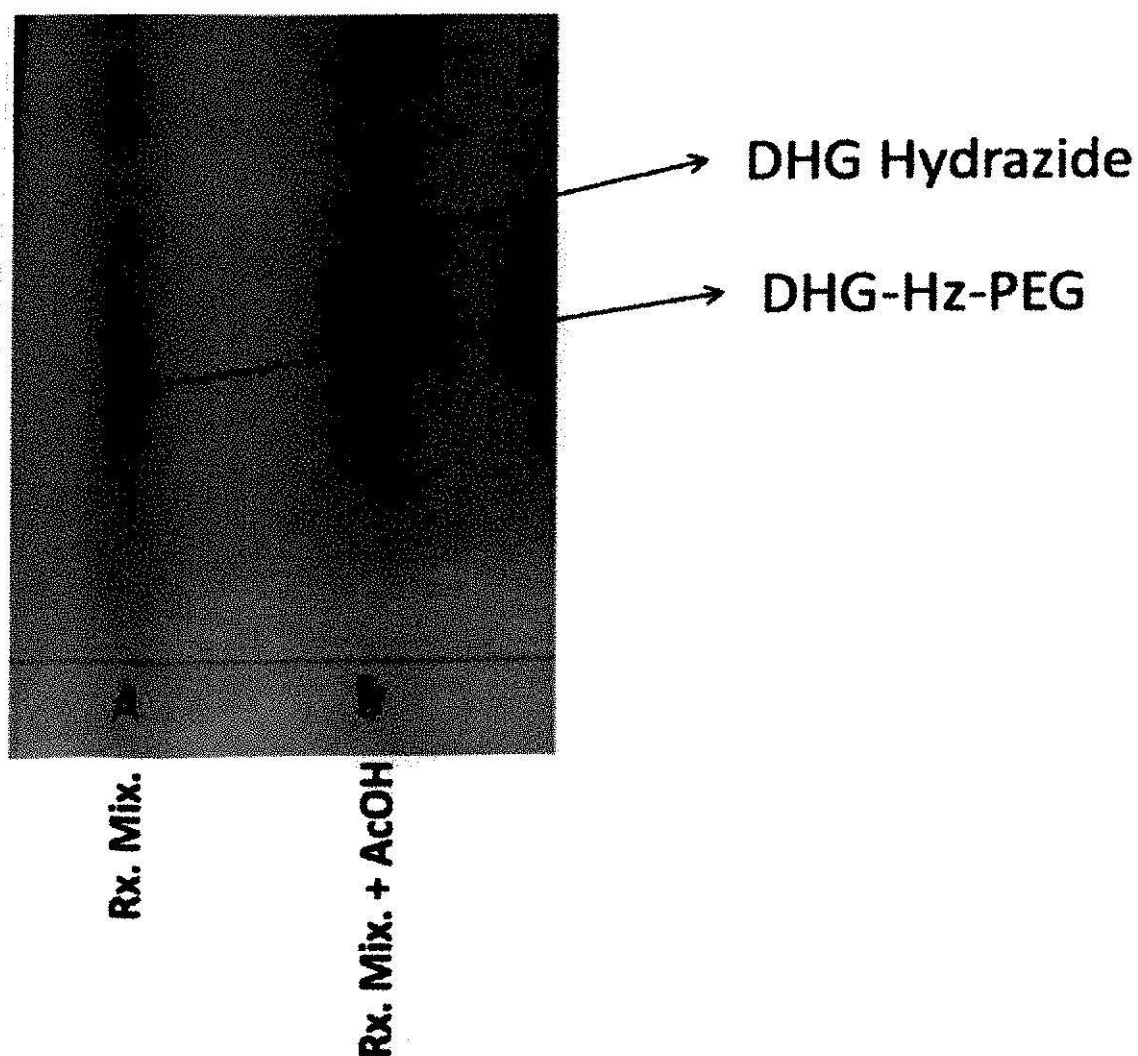


Fig. 2.16 Acidified hydrolysis of the reaction mixture shows the formation of DHG-hydrazide



### Separation of DHG-Hz-PEG

Separation of the conjugate DHG-Hz-PEG using HPLC did not show any peak with C4, C8 and C18 Columns. Neither did silica gel column show any conjugate eluting out of the column. Subsequently sepharose-crosslinked 4B gel column (1 cm x 23 cm, Length x Diameter) was used to purify the conjugate using pure water as eluent but did not show the conjugate eluting from the column at pH 7.4. However, at pH 10.5 (pH of water adjusted with 2 N NaOH) the conjugate started eluting out (Fig. 2.17). The elution time was 30-40 min.

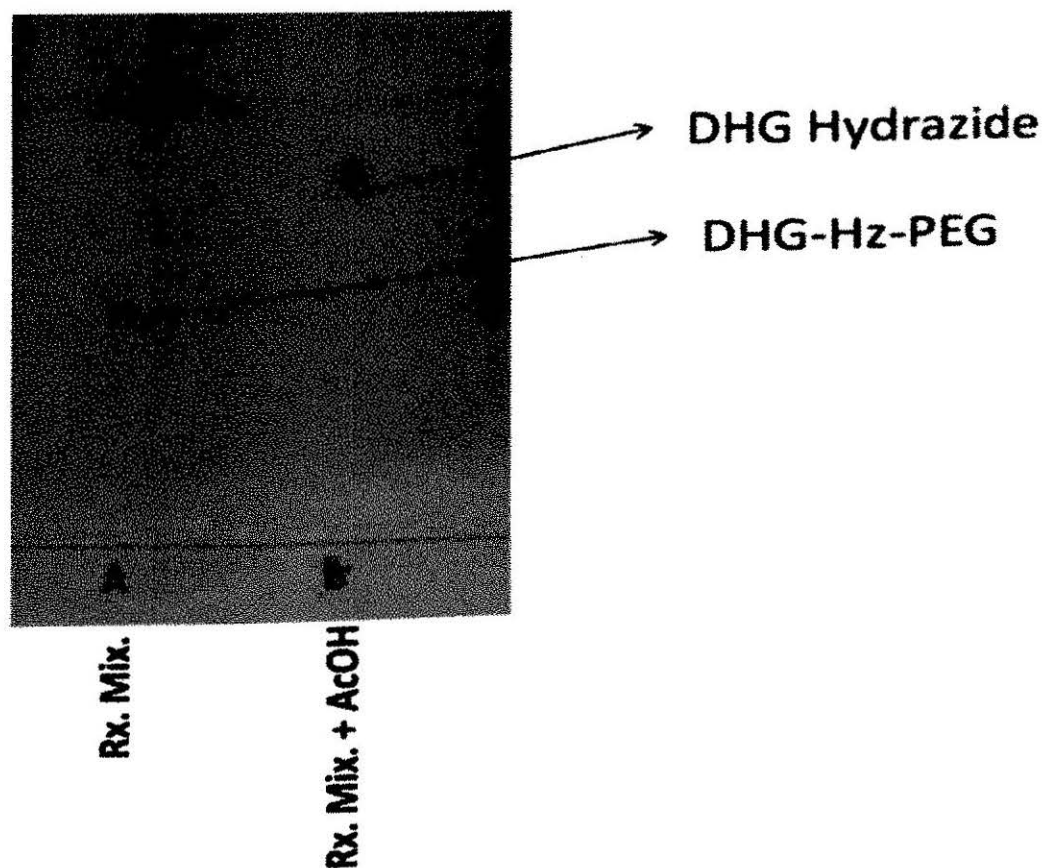


Fig. 2.17 TLC of the eluent showing the DHG-Hz-PEG eluting out of the column

The purification results of the DHG-Hz-PEG conjugate at different pH conditions using gel chromatography, indicate that the hydrazone-based lipid conjugate is highly unstable at physiological pH.

Torchilin et al (91) have previously synthesized a series of aliphatic and aromatic Aldehyde based hydrozone lipid conjugates. Their findings indicate that the half life of the aliphatic conjugates were less than 2 min. at pH 5.5 while the half life of the most stable aliphatic conjugate was no more than 2.5 h at pH 7.4. Inclusion of aromatic ring next to the hydrazone linker yielded very high stability where the half lives were more than 48 h and 72 h at pH 5.5 and 7.4, respectively for all the aromatic conjugates.

Our results show that the hydrazone-based lipid conjugates were highly unstable at pH 7.4 and therefore not suitable for liposome preparation and subsequent anticancer studies.

### **Chapter 3: Design, Preparation and Characteriation of pH-Sensitive Convertible Liposomes for Anticancer Drug Delivery**

#### **Introduction**

Advances in liposomal tumor targeting have received considerable attention for their potential advantages (102) (103) including: high drug to carrier ratio, ability to formulate lipophilic as well as hydrophilic drugs, targeting to tumor, long circulation half life (103), biocompatibility of the carrier and minimal toxicities of the constituent lipids. The advent of 'stealth liposomes' have resulted in increased blood circulation half life of the liposomes (35) and therefore increased accumulation in the perivascular environment by the 'Enhanced Permeation and Retention Effect'. However the PEG coating of the stealth liposome also reduces their interaction with tumor cells (see chapter I, Passive targeting) and their penetration in solid tumors (111).

To increase the cell-liposome interaction and intracellular uptake of the drug a broad spectrum of PEG-shedding strategies have been previously introduced (104). Of note, the strategies to shed the PEG coating from stealth liposomes include the incorporation of pH-sensitive linkers which can hydrolyze in the low-pH environment (see chapter II). However, lipids containing such pH-sensitive linkers show either poor stability (see chapter II, Separation of DHG-Hz-PEG) at physiological pH, or insufficient pH-

sensitivity to the mildly acidic pH in the tumor interstitium (see chapter II, Vinyl ether) (77) (79) (80). Furthermore, poor stability on shelf is another concern for such hydrolyzable liposomes (127). It is thus desirable to develop liposomes that are stable both on shelf and in blood circulation and yet can remove the PEG coating in response to lowered pH.

This project proposes a strategy to improve the shelf stability and intracellular delivery of drug by PEGylated liposomes. Instead of using lipids with an acid-labile linker we have developed imidazole-based lipids that can protonate at low-pH as seen in the tumor interstitium. The proposed convertible liposomes containing protonable imidazole lipids could convert from stealth to cationic liposomes in the tumoral interstitium (Fig. 3.1). The conversion to cationic liposome is based on protonation of imidazole lipids and clustering of PEG lipids on the liposome surface. The newly formed cationic liposome can then have greater interaction with the negatively charged cell membrane and extracellular matrix (123) (see chapter II). Because the liposome converts from stealth to cationic liposome we have given them the term 'Convertible Liposomes'.

The concept of design (Fig. 3.1) is based on the inherent property of the lipids to segregate into different phases based on electrostatics and vander waals force of interaction amongst them (124).

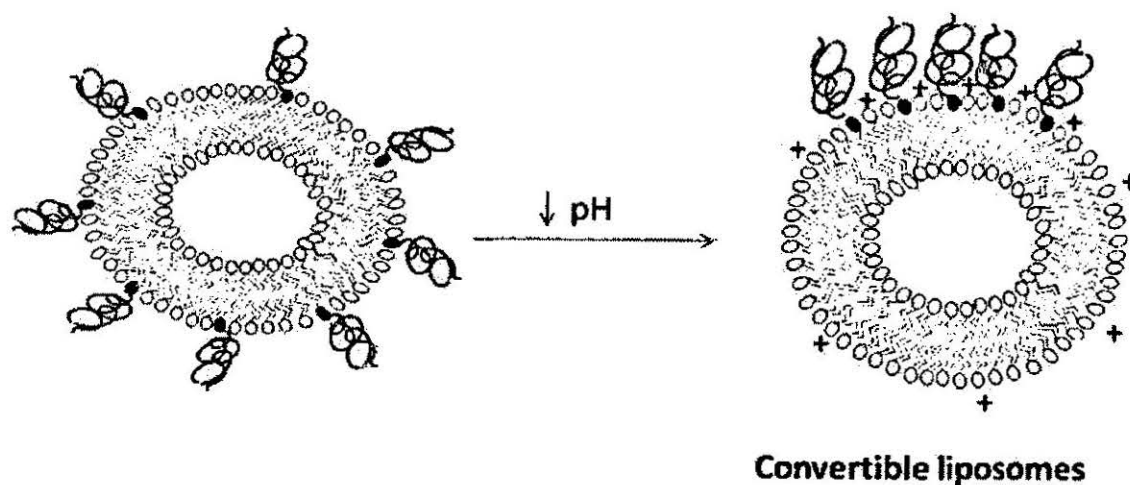


Fig. 3.1 Concept of design of convertible liposomes: protonation and clustering of PEG coating on liposome surface in response to lowered pH.

The convertible liposomal system essentially comprises of three different types of lipids (Fig. 3.3) 1) a negatively charged PEGylated lipid with two C16 hydrocarbon chains as the lipid tail (1,2-dipalmitoyl-*sn*-glycero-3-phosphoethanolamine-N-[methoxy(polyethylene glycol)-2000 (DPPE-PEG, shown by letter 'P' in Fig. 3.2), 2) an imidazole-based, protonable lipid with two C16 hydrocarbon chains as the lipid tail (shown by letter 'N' in Fig 3.2), and 3) a C18 chain lipid DSPC (1,2-distearoyl-*sn*-glycero-3-phosphocholine) that has no net charge. The molecular stimulus that triggers the phase separation of the lipids is the acidic pH of the tumoral interstitium. At acidic pH, protonable lipids will protonate and acquire positive charge on the surface. The protonated lipids are attracted to negatively charged PEGylated lipids due to the electrostatic interaction and vander waals force of interaction owing to the same carbon chain length (Fig. 3.3). This leads to the formation of PEG cluster on the membrane exposing excess positive charge on liposome surface. Such a formulation will allow for increased binding with cancer cells and higher uptake by the tumor cells.

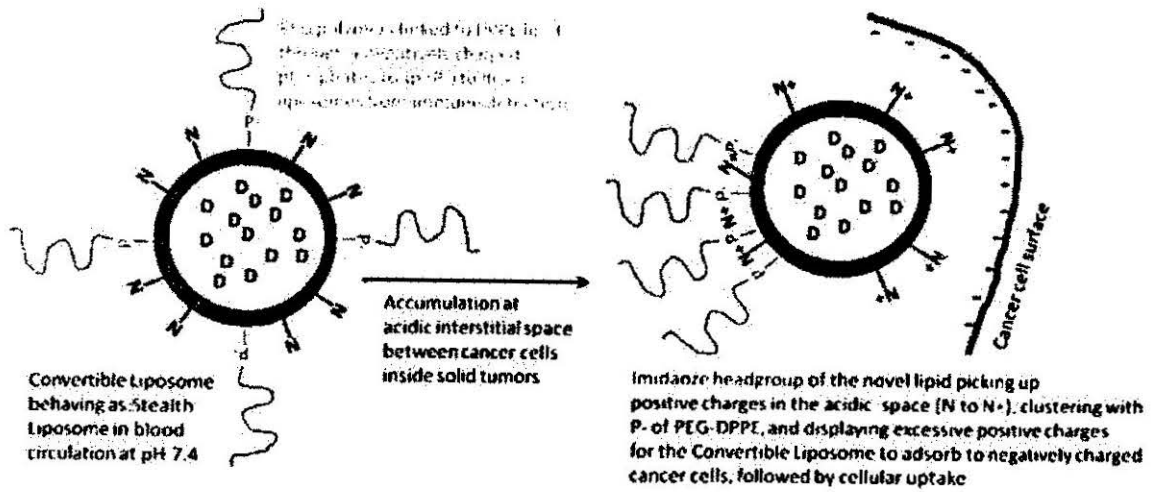


Fig. 3.2 Formation of lipid domains on the liposome surface at mildly acidic tumor microenvironment

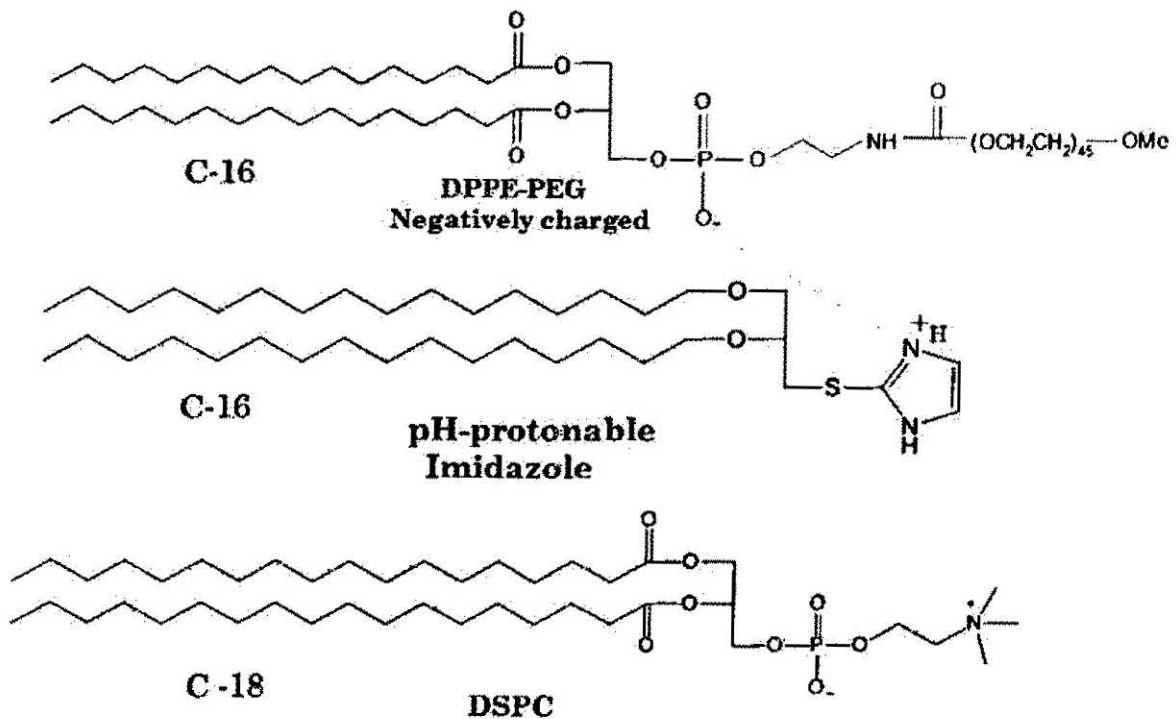


Fig. 3.3 Three types of lipids (DPPE-PEG, Imidazole lipid and DSPC) comprising the convertible liposome, Negatively charged DPPE-PEG and protonable Imidazole lipids interact at low pH

### **Tumor pH**

The trigger of the proposed convertible liposomal system is the pH of the solid tumor. The pH of the extracellular interstitium in solid tumor is between 6.0 to 7.0 (105) (106) (107) with the pH approaching close to 6.0 at the tumor core. The acidic pH in the tumor is due to the heterogeneous network of blood vessels in solid tumors which leaves parts of the tumor without sufficient oxygen supply (Fig. 3.4). The tumor cells in the hypoxic region are forced to undergo anaerobic glycolysis (108) (109) as a major metabolic pathway leading to the production of lactic acid and thence the acidic pH. Additionally, findings of Svastova et al suggested the role of carbonic anhydrase IX in the creation of acidic microenvironment in tumor (110).

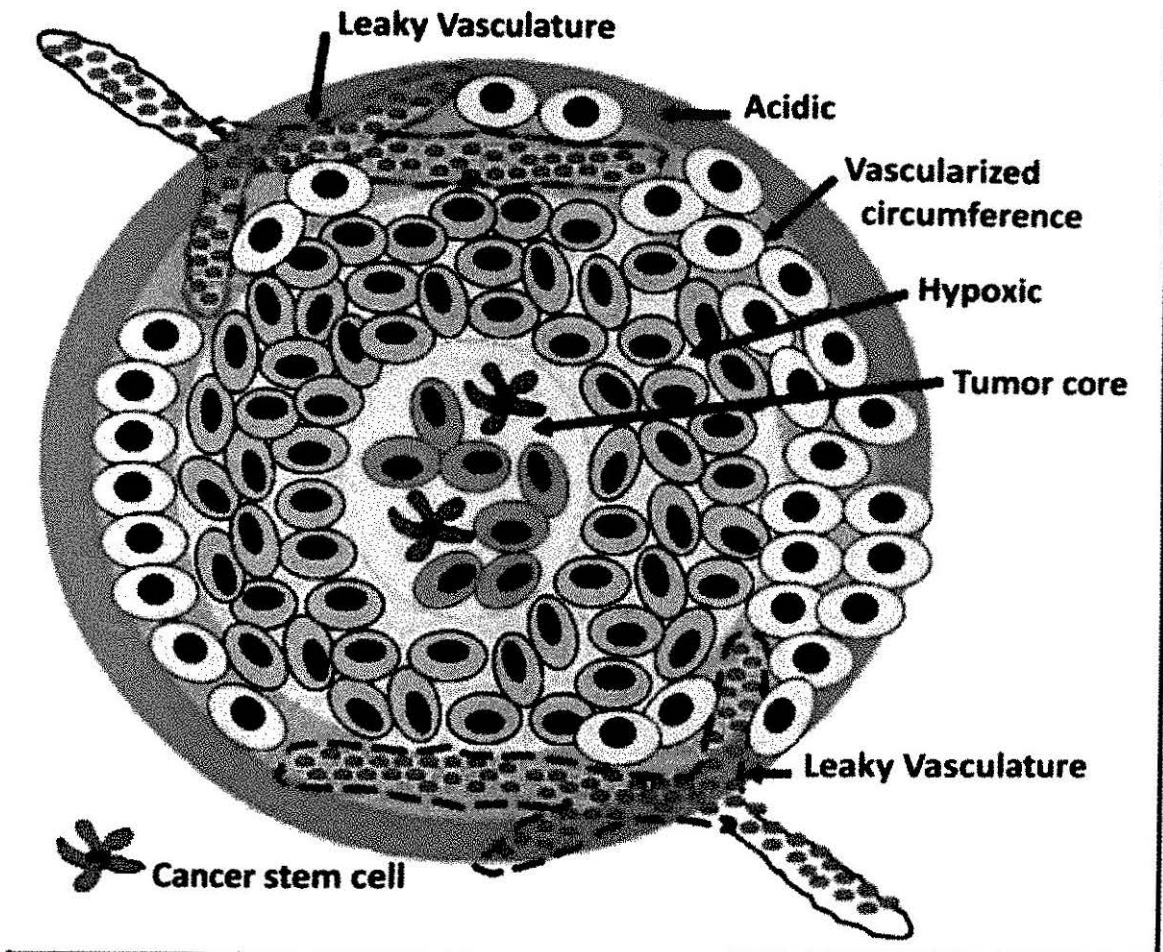


Fig. 3.4 Picture of solid tumor showing heterogeneous and leaky vasculature and hypoxic region (adapted with permission from (128)).

The convertible liposomal system has tunable surface topography (124) that starts as a stealth liposome and yet converts to a cationic liposome at the pH mimicking the tumor environment. The principal behind the formulation development is that the convertible liposome will remain masked by the Polyethylene Glycol (PEG) shell during the systemic circulation but the PEG shell will progressively de-shield as it encounters low-pH environment mimicking solid tumor and thereby exposing excess positive charges on the liposome surface acquired by protonation of imidazole lipids.



In this study, we have synthesized a series of imidazole based pH-titrable lipids with increasing pKa values (Fig. 3.5, estimated pKa values ranging from 5.36 to 6.75) and incorporated them into convertible liposomes to render liposomes with increasing pH-sensitivity. The formation of lipid domains and the potential of these liposomes to associate with and kill cancer cells at tumor-relevant pH is evaluated in B16F10 (mouse melanoma) and Hela (human cervical) cancer cells.

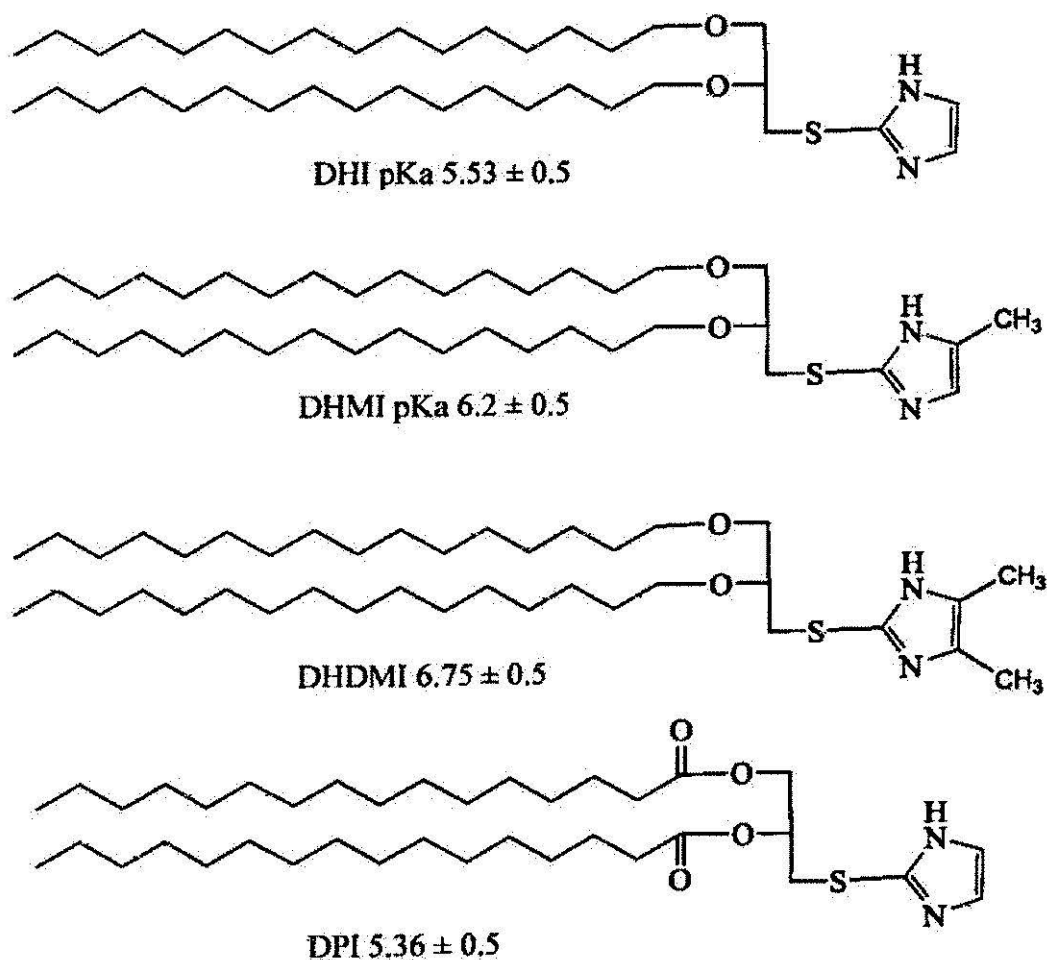


Fig. 3.5 Structure of pH-protonable imidazole lipids

## Materials and Methods

**3.1 Materials.** 1,2-Di-O-hexadecyl-*rac*-glycerol (DHG) was purchased from Bachem, Torrance, CA, *p*-Toluenesulfonyl chloride, Pyridine (anhydrous) from Fisher Scientific, 1,2-Dipalmitoyl-*sn*-glycerol from Chem-Impex International, Inc., Wood Dale, IL, 1,2-dioleoyl-*sn*-glycerol, 1,2-distearoyl-*sn*-glycero-3-phosphocholine (DSPC), 1,2-dipalmitoyl-*sn*-glycero-3-phosphoethanolamine-N-[methoxy(polyethylene glycol)-2000 (DPPE-PEG) from Avanti Polar Lipids, Inc., Alabaster, AL, 2-Mercaptoimidazole, Triethylamine from Sigma Aldrich, 4-Methyl-1H-imidazole-2-thiol and 4,5-Dimethyl-1H-imidazole-2-thiol from Oakwood Products, Inc., West Columbia, SC, Doxorubicin hydrochloride from Ontario Chemicals, ON, Canada. All organic solvents were purchased from Fisher Scientific, VWR or Sigma Aldrich.

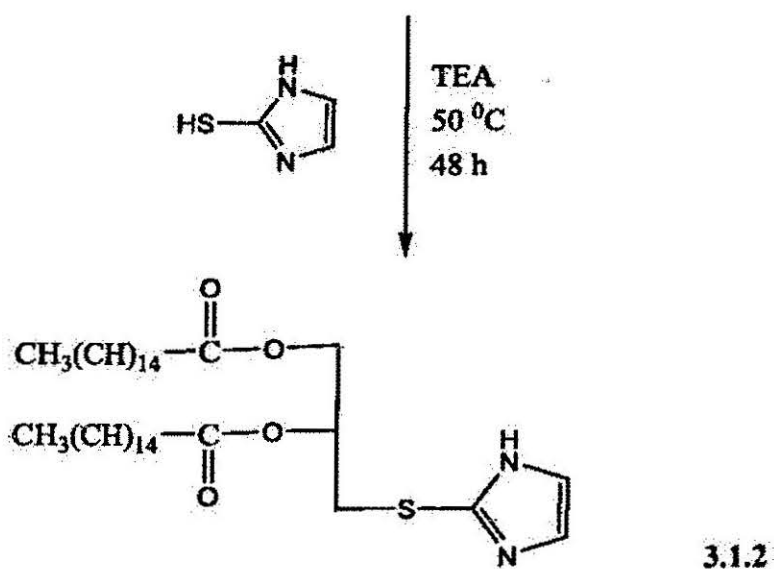
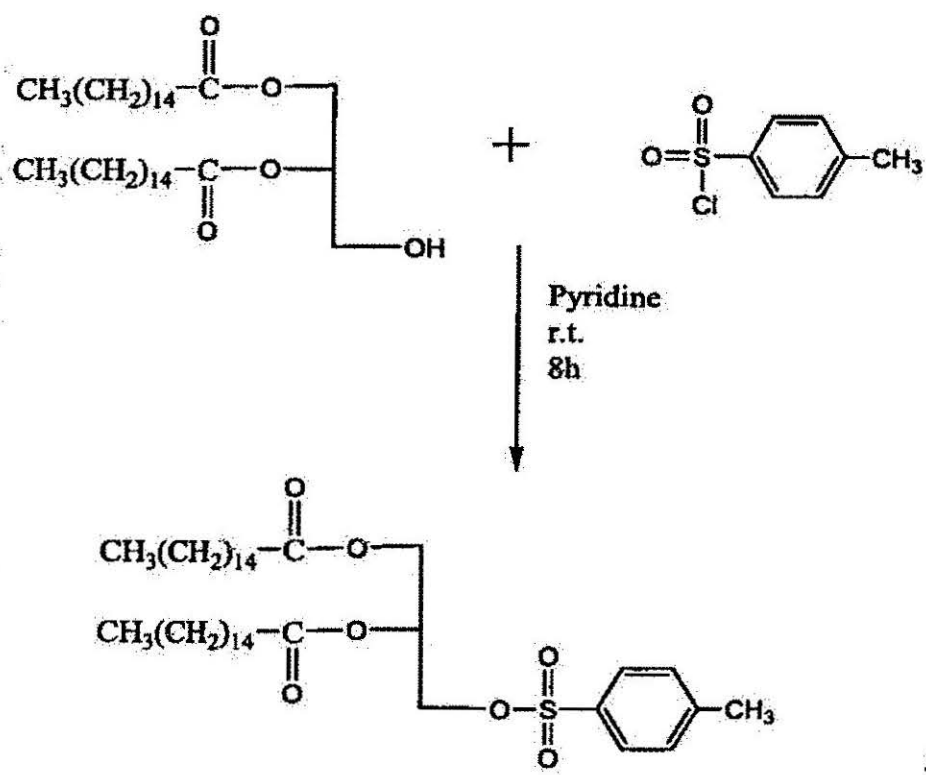
### 3.2 Synthesis of Ester lipid DPI

**3.2.1 Synthesis of *sn*-3-((phenylsulfonyl)oxy)propane-1,2-diyl dipalmitate (DPG Tosylate) (3.1.1, Scheme 3.1).** 1,2-Dipalmitoyl-*sn*-glycerol (DPG) (0.25 g, 0.44 mmol, 1 equiv), was dissolved in 20 mL of dichloromethane, followed by dropwise addition of pyridine (1.82 mL, 22 mmol, 50 equiv). *p*-Toluenesulfonyl chloride (0.17 g, 0.88 mmol, 2 equiv) was then added to the above solution. The reaction mixture was stirred under argon at room temperature for 8 h, and monitored by TLC developed with dichloromethane (Scheme 3.1). The reaction mixture was then washed three times with saturated sodium carbonate solution. The combined organic layers were dried over magnesium sulfate, filtered, concentrated in vacuum and separated by silica gel

chromatography with dichloromethane as mobile phase to yield the product. (Yield 56 %), DART (M+H)<sup>+</sup> 551.5

### 3.2.2 Synthesis of (*sn*)-3-((1*H*-imidazol-2-yl)thio)propane-1,2-diyl-dipalmitate (DPI)

(3.1.2, Scheme 3.1). 2-Mercaptoimidazole (0.1 g, 1.0 mmol, 5 equiv.) was dissolved in DMF and a small amount of Dichloromethane was added. Triethylamine (0.14 mL, 1.0 mmol, 5 equiv.) was added to the above solution followed by (*sn*)-3-((phenylsulfonyl)oxy)propane-1,2-diyl dipalmitate (0.15 g, 0.2 mmol, 1 equiv) and the reaction was allowed to run for 48 h at 55°C under argon. The solvent was evaporated and reaction mixture was re-dissolved in ethyl acetate and washed thrice with saturated sodium bicarbonate solution. The combined organic layers were dried over sodium carbonate, filtered, concentrated in vacuum and separated by silica gel chromatography with Ethyl acetate / Hexane = 3/7 as mobile phase to yield the product. (Yield 9 %), DART (M+H)<sup>+</sup> 651.5 (Fig. 3.6), <sup>1</sup>H-NMR (600 MHz, CDCl<sub>3</sub>) (Fig. 3.7): δ 0.87 (t, 6H, 2 CH<sub>3</sub>(CH<sub>2</sub>)<sub>15</sub>-), δ 1.15-1.35 (m, 52H, 2 -OOCCH<sub>2</sub>CH<sub>2</sub>(CH<sub>2</sub>)<sub>13</sub>CH<sub>3</sub>), δ 1.58 (t, 4H, 2 -OOCCH<sub>2</sub>CH<sub>2</sub>(CH<sub>2</sub>)<sub>13</sub>CH<sub>3</sub>), δ 2.3 (t, 4H, 2 -OOCCH<sub>2</sub>CH<sub>2</sub>(CH<sub>2</sub>)<sub>13</sub>CH<sub>3</sub>), δ 3.38, 3.66 (q, 2H, -H<sub>2</sub>CSCNH-), δ 4.2, 4.4 (q, 2H, CH<sub>3</sub>(CH<sub>2</sub>)<sub>14</sub>COOCH<sub>2</sub>-), δ 7.08 (d, 1H, H<sub>2</sub>CSC=NHC=CH-NH-), δ 8.04 (d, 1H, H<sub>2</sub>CSC=NHC=CH-NH-)



Scheme 3.1 Synthesis of DPI

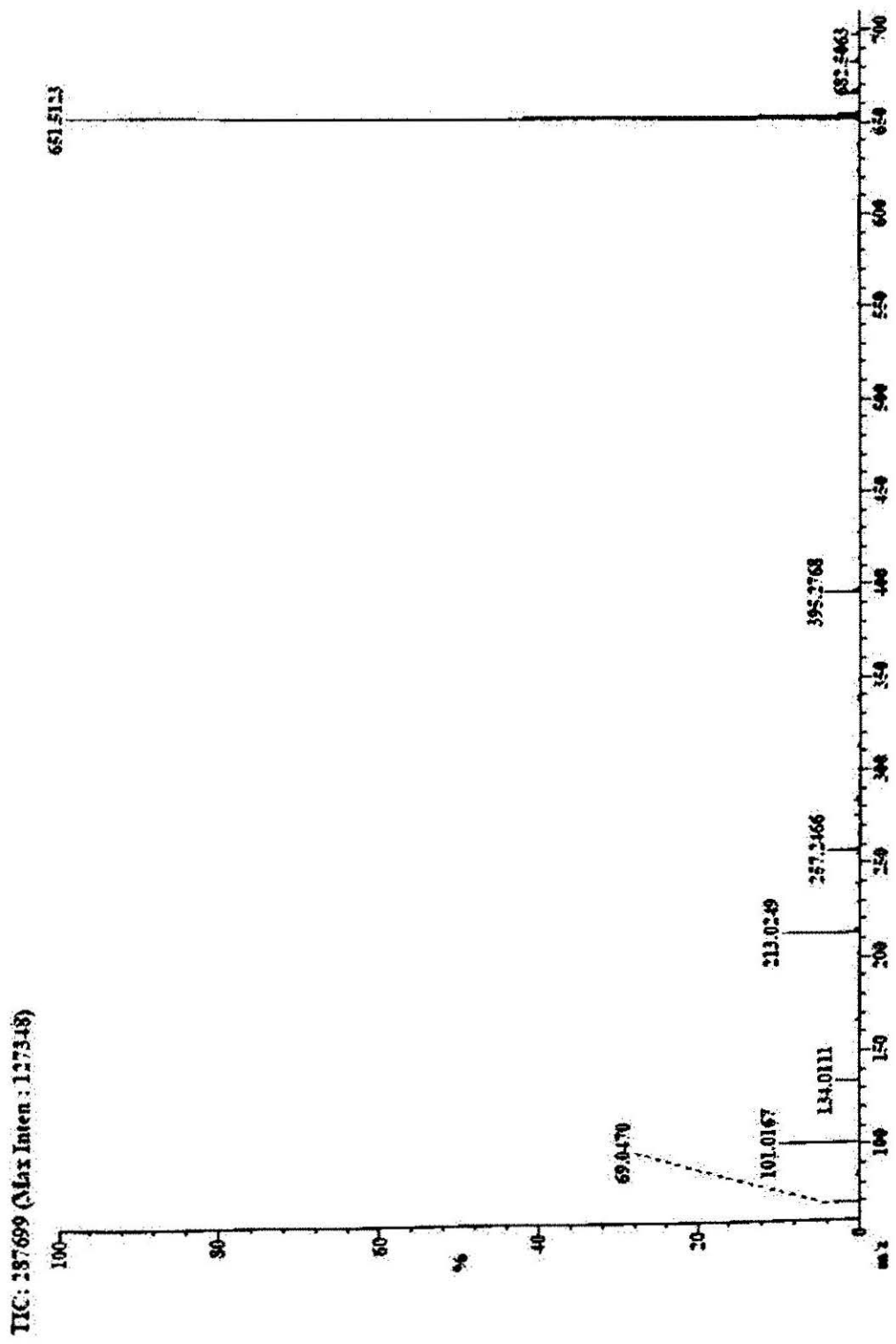


Fig. 3.6 DART mass spectral analysis of DPI

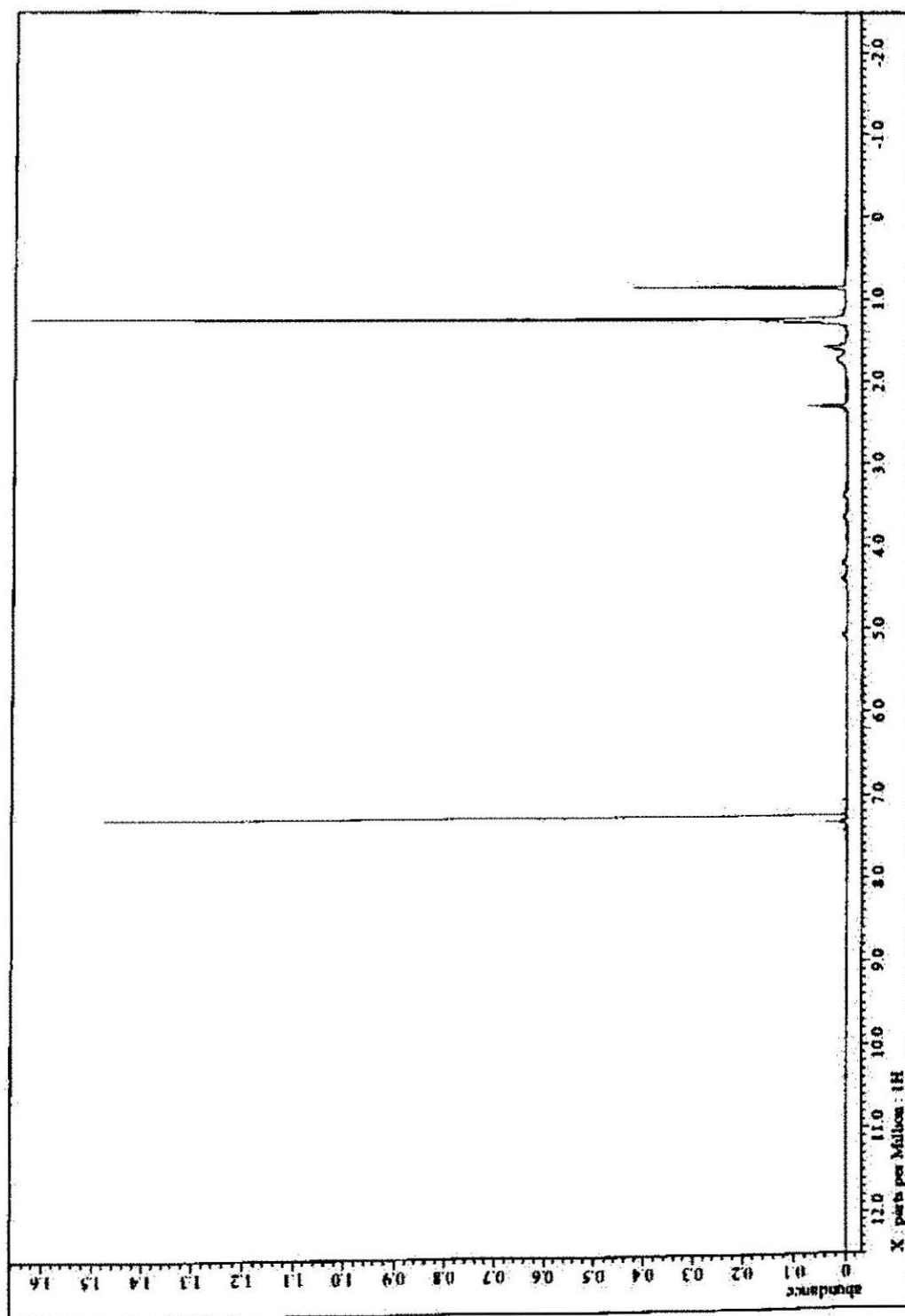


Fig. 3.7 NMR spectrum of DPI

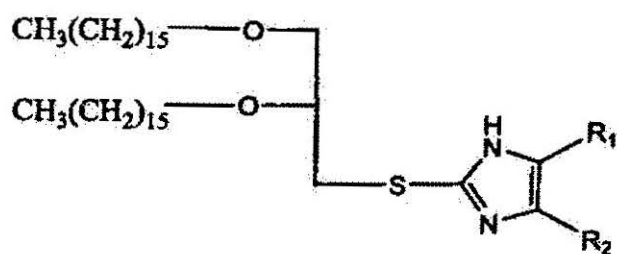
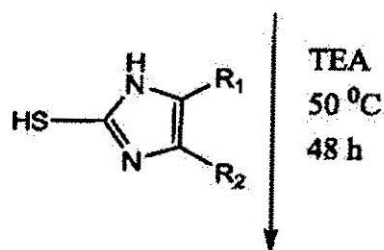
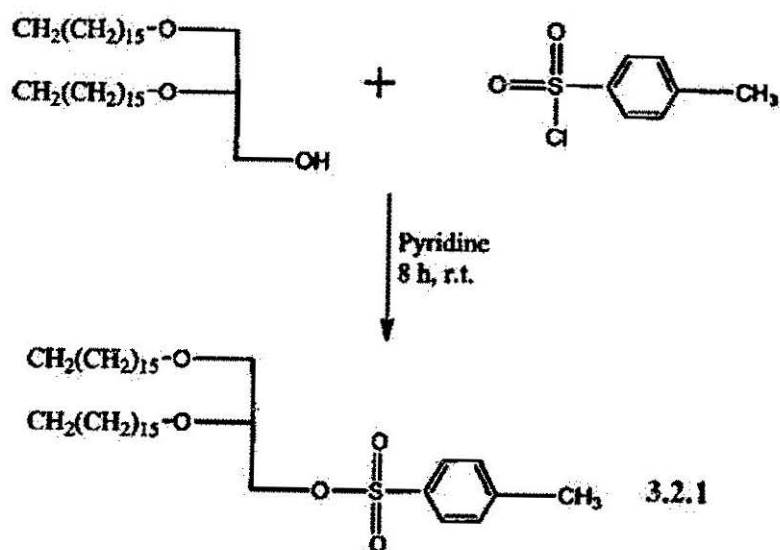
### 3.3 Synthesis of Ether lipids DHI, DHMI and DHDMI

**3.3.1 Synthesis of 1,2-Di-O-hexadecyl-*rac*-glyceryl tosylate (DHG Tosylate) (3.2.1, Scheme 3.2).** 1,2-Di-O-hexadecyl-*rac*-glycerol (DHG) (2.43 g, 4.5 mmol, 1 equiv), was dissolved in 20 mL of dichloromethane, followed by dropwise addition of pyridine (18.6 mL, 225 mmol, 50 equiv). *p*-Toluenesulfonyl chloride (1.71 g, 9.0 mmol, 2 equiv) was then added to the above solution (Scheme 3.2). The reaction mixture was stirred under argon at room temperature for 8 h, and monitored by TLC (silica gel 60 F254, EMD chemicals, Germany) developed with dichloromethane. The reaction mixture was then washed three times with saturated sodium carbonate solution. The combined organic layers were dried over magnesium sulfate, filtered, concentrated in vacuum and separated by silica gel chromatography with dichloromethane as mobile phase to yield the product. (Yield 65 %), DART (M+H)<sup>+</sup> 695.5, <sup>1</sup>H-NMR (600 MHz, CDCl<sub>3</sub>, δ ppm): 0.87 (t, 6H, 2 CH<sub>3</sub>(CH<sub>2</sub>)<sub>15</sub>-), 1.18-1.31 (m, 52H, 2 -OCH<sub>2</sub>CH<sub>2</sub>(CH<sub>2</sub>)<sub>13</sub>CH<sub>3</sub>), 1.46 (m, 4H, 2 -OCH<sub>2</sub>CH<sub>2</sub>(CH<sub>2</sub>)<sub>13</sub>CH<sub>3</sub>), 2.44 (s, 3H, -(C<sub>6</sub>H<sub>4</sub>)CH<sub>3</sub>), 3.31-3.62 (m, 5H, CH<sub>3</sub>(CH<sub>2</sub>)<sub>14</sub>CH<sub>2</sub>OCH<sub>2</sub>CHO-), δ 4.14 (m, 2H, -CH<sub>2</sub>SO<sub>2</sub>-), δ 7.33 (d, 2H, aromatic protons *ortho*- to -SO<sub>2</sub>-), and δ 7.78 (d, 2H, aromatic protons *ortho*- to CH<sub>3</sub>-)

**3.3.2 Synthesis of (*sn*)-2-((2,3-bis(hexadecyloxy)propyl)thio)-1H-imidazole (DHI) (3.2.2, Scheme 3.2).** 2-Mercaptoimidazole (0.66 g, 6.61 mmol, 5 equiv.) was dissolved in DMF and a small amount of Dichloromethane was added. Triethylamine (0.92 mL, 6.61 mmol, 5 equiv.) was added to the above solution followed by 1,2-Di-O-hexadecyl-*rac*-glyceryl tosylate (3.2.1) (0.92 g, 1.32 mmol, 1 equiv) and the reaction was allowed to run for 48 h at 55°C under argon (Scheme 3.2). The solvent was evaporated and reaction

mixture was re-dissolved in ethyl acetate and washed with saturated sodium bicarbonate solution (3x). The combined organic layers were dried over sodium carbonate, filtered, concentrated in vacuum and separated by silica gel chromatography with Ethyl acetate / Hexane = 3/7 as mobile phase. (Yield 26 %), DART (M+H)<sup>+</sup> 623.5 (Fig. 3.8), <sup>1</sup>H-NMR (600 MHz, CDCl<sub>3</sub>) (Fig. 3.9): δ 0.87 (t, 6H, 2 CH<sub>3</sub>(CH<sub>2</sub>)<sub>15</sub>-), δ 1.19-1.32 (m, 52H, 2 -OCH<sub>2</sub>CH<sub>2</sub>(CH<sub>2</sub>)<sub>13</sub>CH<sub>3</sub>), δ 1.55 (m, 4H, 2 -OCH<sub>2</sub>CH<sub>2</sub>(CH<sub>2</sub>)<sub>13</sub>CH<sub>3</sub>), δ 3.22, 3.65 (d,d 2H, -H<sub>2</sub>COCH<sub>2</sub>(CH<sub>2</sub>)<sub>14</sub>CH<sub>3</sub>), δ 3.38, 3.6 (d,d 2H, -H<sub>2</sub>CSCNH-), δ 3.44, 3.55 (m, 4H, 2 -H<sub>2</sub>COCH<sub>2</sub>(CH<sub>2</sub>)<sub>14</sub>CH<sub>3</sub>), δ 3.73 (m, 1H, CH<sub>3</sub>(CH<sub>2</sub>)<sub>15</sub>OCH-), δ 7.02 (d, 1H, H<sub>2</sub>CSC=NHC=CH-NH-), δ 7.21 (d, 1H, H<sub>2</sub>CSC=NHC=CH-NH-)





DHI  $\text{R}_1 = \text{H}, \text{R}_2 = \text{H}$  (3.2.2)

DHMI  $\text{R}_1 = \text{CH}_3, \text{R}_2 = \text{H}$  (3.2.3)

DHDMI  $\text{R}_1 = \text{CH}_3, \text{R}_2 = \text{CH}_3$  (3.2.4)

Scheme 3.2 Synthesis of DHI, DHMI and DHDMI

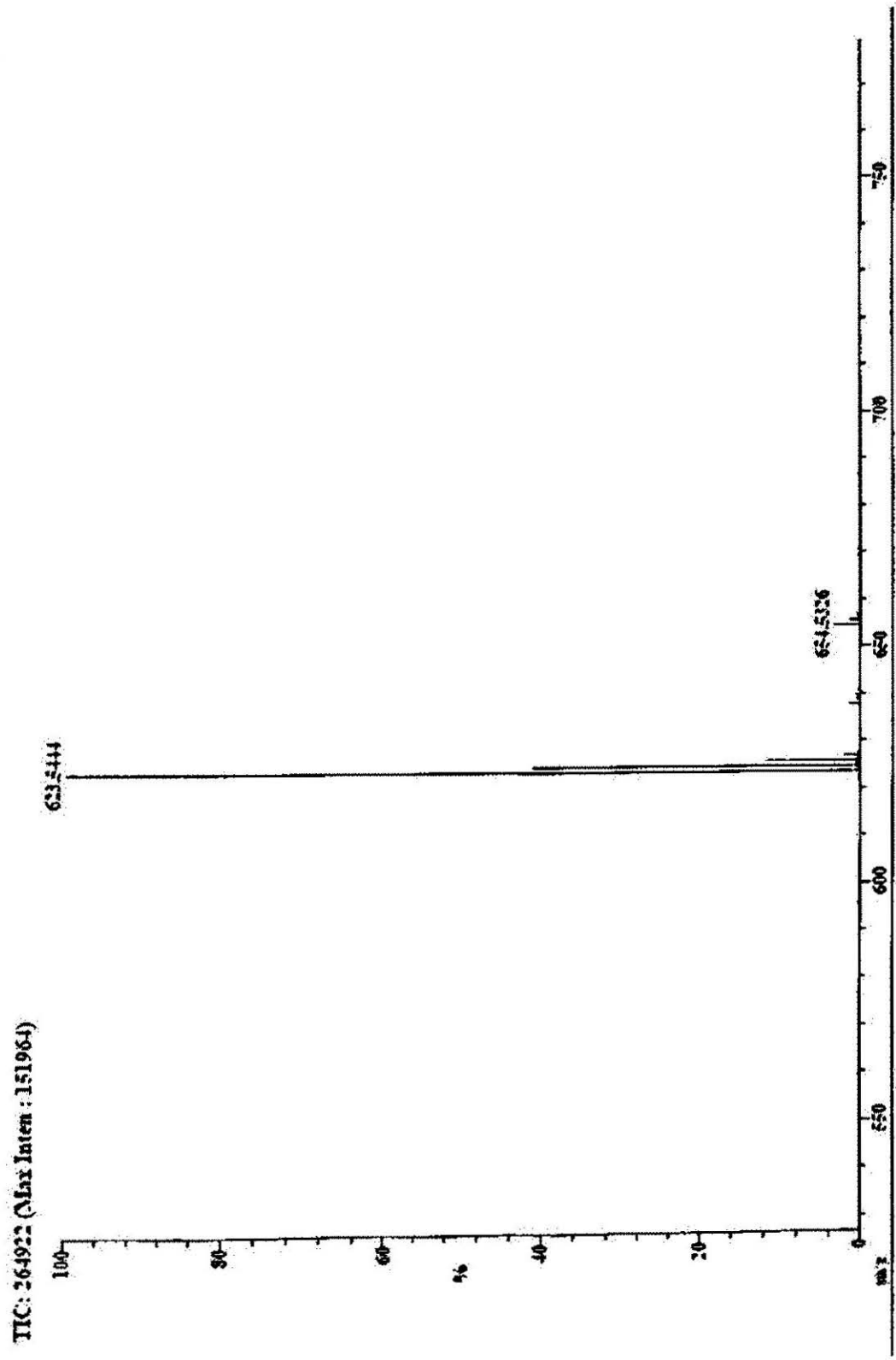


Fig. 3. 8 DART mass spectral analysis of DHI

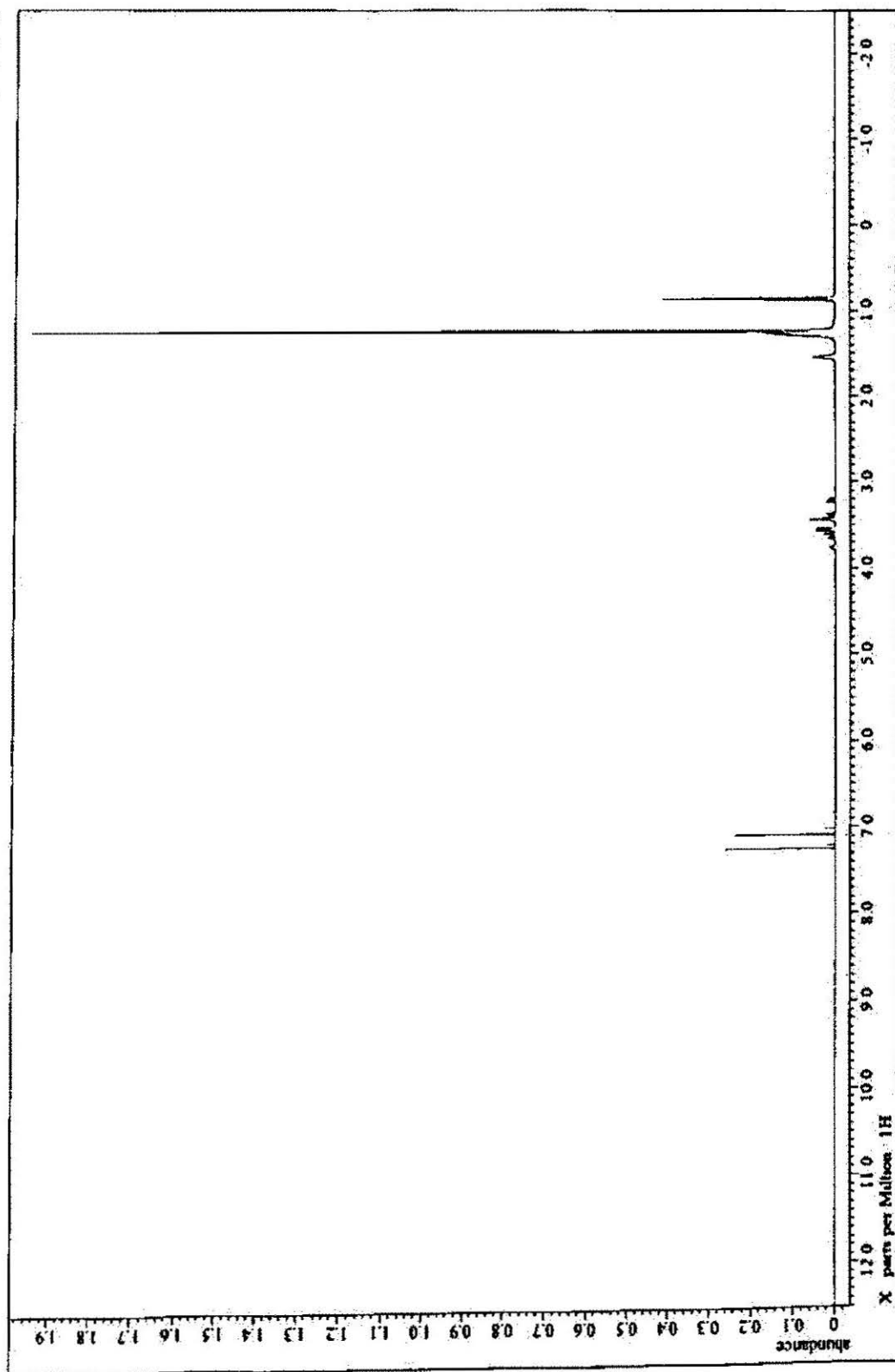


Fig. 3.9 NMR spectrum of DHI

**3.3.3 Synthesis of *sn*-2-((2,3-bis(hexadecyloxy)propylthio)-5-methyl-1H-imidazole (DHMI) (3.2.3, Scheme 3.2).** 4-Methyl-1H-imidazole-2-thiol (0.75 g, 6.61 mmol, 5 equiv.) was dissolved in DMF and a small amount of Dichloromethane was added. Triethylamine (0.92 mL, 6.61 mmol, 5 equiv.) was added to the above solution followed by 1,2-Di-O-hexadecyl-*rac*-glyceryl tosylate (3.2.1) (0.92 g, 1.32 mmol, 1 equiv) was then added to this solution and reaction was allowed to run for 48 h at 55°C under argon (Scheme 3.2). The washing and purification was the same as mentioned in 3.3.2. (Yield 22 %), DART (M+H)<sup>+</sup> 637.5 (Fig. 3.10), <sup>1</sup>H-NMR (600 MHz, CDCl<sub>3</sub>) (Fig. 3.11): δ 0.87 (t, 6H, 2 CH<sub>3</sub>(CH<sub>2</sub>)<sub>15</sub>-), δ 1.19-1.34 (m, 52H, 2 -OCH<sub>2</sub>CH<sub>2</sub>(CH<sub>2</sub>)<sub>13</sub>CH<sub>3</sub>), δ 1.53 (m, 4H, 2 -OCH<sub>2</sub>CH<sub>2</sub>(CH<sub>2</sub>)<sub>13</sub>CH<sub>3</sub>), δ 2.31 (s, 3H, -H<sub>2</sub>CSC=NHC=CH-CH<sub>3</sub>), δ 3.24, 3.66 (d,d, 2H, -H<sub>2</sub>COCH<sub>2</sub>(CH<sub>2</sub>)<sub>14</sub>CH<sub>3</sub>), δ 3.4, 3.6 (d,d 2H, -H<sub>2</sub>CSCNH-), δ 3.44, 3.55 (m, 4H, 2 -H<sub>2</sub>COCH<sub>2</sub>(CH<sub>2</sub>)<sub>14</sub>CH<sub>3</sub>), δ 3.73 (m, 1H, CH<sub>3</sub>(CH<sub>2</sub>)<sub>15</sub>OCH-), δ 6.81 (d, 1H, H<sub>2</sub>CSC=NHC=CH-NH-)

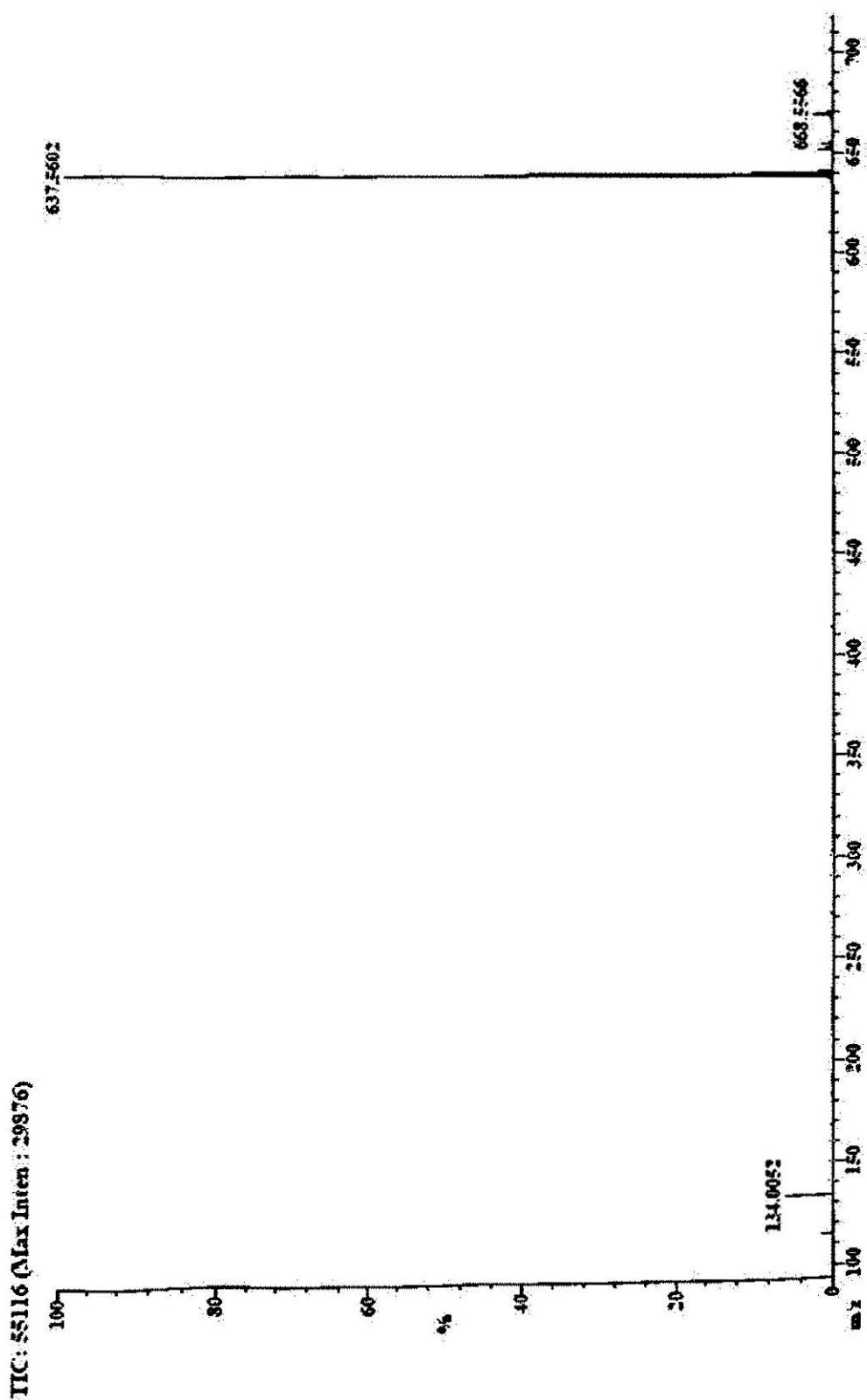


Fig. 3.10 DART mass spectral analysis of DHMI

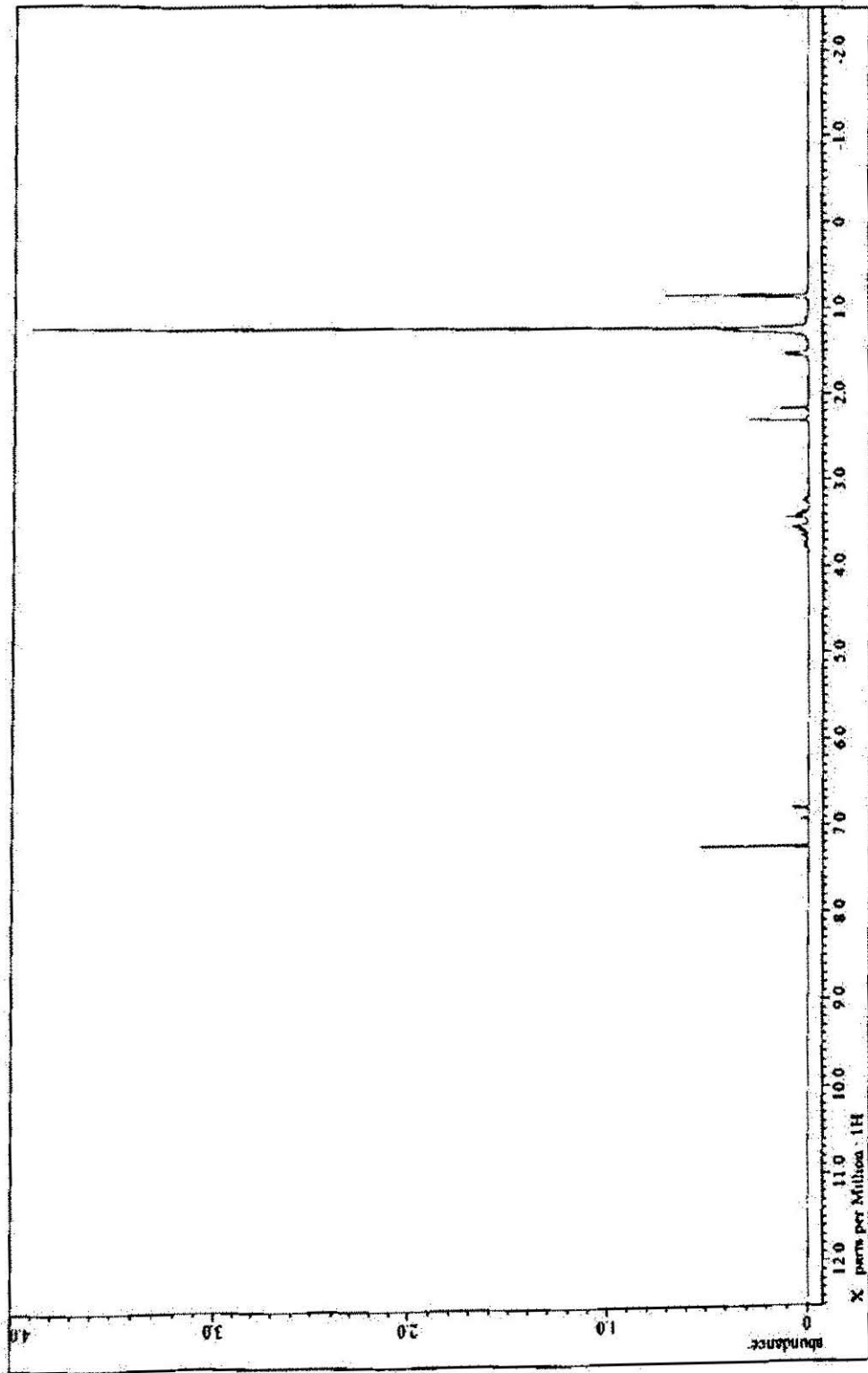


Fig. 3.11 NMR spectrum of DHMI

**3.3.4 Synthesis of *sn*-2-((2,3-bis(hexadecyloxy)propyl)thio)-4,5-methyl-1H-imidazole (DHDMI) (3.2.4, Scheme 3.2).** 4-Methyl-1H-imidazole-2-thiol (0.84 g, 6.61 mmol, 5 equiv.) was dissolved in DMF and a small amount of Dichloromethane was added. Triethylamine (0.92 mL, 6.61 mmol, 5 equiv.) was added to the above solution followed by 1,2-Di-O-hexadecyl-rac-glyceryl tosylate (3.2.1) (0.92 g, 1.32 mmol, 1 equiv) and reaction was allowed to run for 48 hrs at 55°C under argon (Scheme 3.2). The washing and purification was similar as mentioned in 3.3.2 (Yield 22 %), DART (M+H)<sup>+</sup> 651.5 (Fig. 3.12), <sup>1</sup>H-NMR (600 MHz, CDCl<sub>3</sub>) (Fig. 3.13): δ 0.87 (t, 6H, 2 CH<sub>3</sub>(CH<sub>2</sub>)<sub>15</sub>-), δ 1.19-1.34 (m, 52H, 2 -OCH<sub>2</sub>CH<sub>2</sub>(CH<sub>2</sub>)<sub>13</sub>CH<sub>3</sub>), δ 1.53 (m, 4H, 2 -OCH<sub>2</sub>CH<sub>2</sub>(CH<sub>2</sub>)<sub>13</sub>CH<sub>3</sub>), δ 2.11 (s, 3H, -H<sub>2</sub>CSC=NHC=CH-CH<sub>3</sub>), δ 2.17 (s, 3H, -H<sub>2</sub>CSC=NCCH<sub>3</sub>), δ 3.14, 3.65 (d,d 2H, -H<sub>2</sub>COCH<sub>2</sub>(CH<sub>2</sub>)<sub>14</sub>CH<sub>3</sub>), δ 3.29, 3.59 (d,d 2H, -H<sub>2</sub>CSCNH-), δ 3.42, 3.55 (m, 4H, 2 -H<sub>2</sub>COCH<sub>2</sub>(CH<sub>2</sub>)<sub>14</sub>CH<sub>3</sub>), δ 3.73 (m, 1H, CH<sub>3</sub>(CH<sub>2</sub>)<sub>15</sub>OCH-)

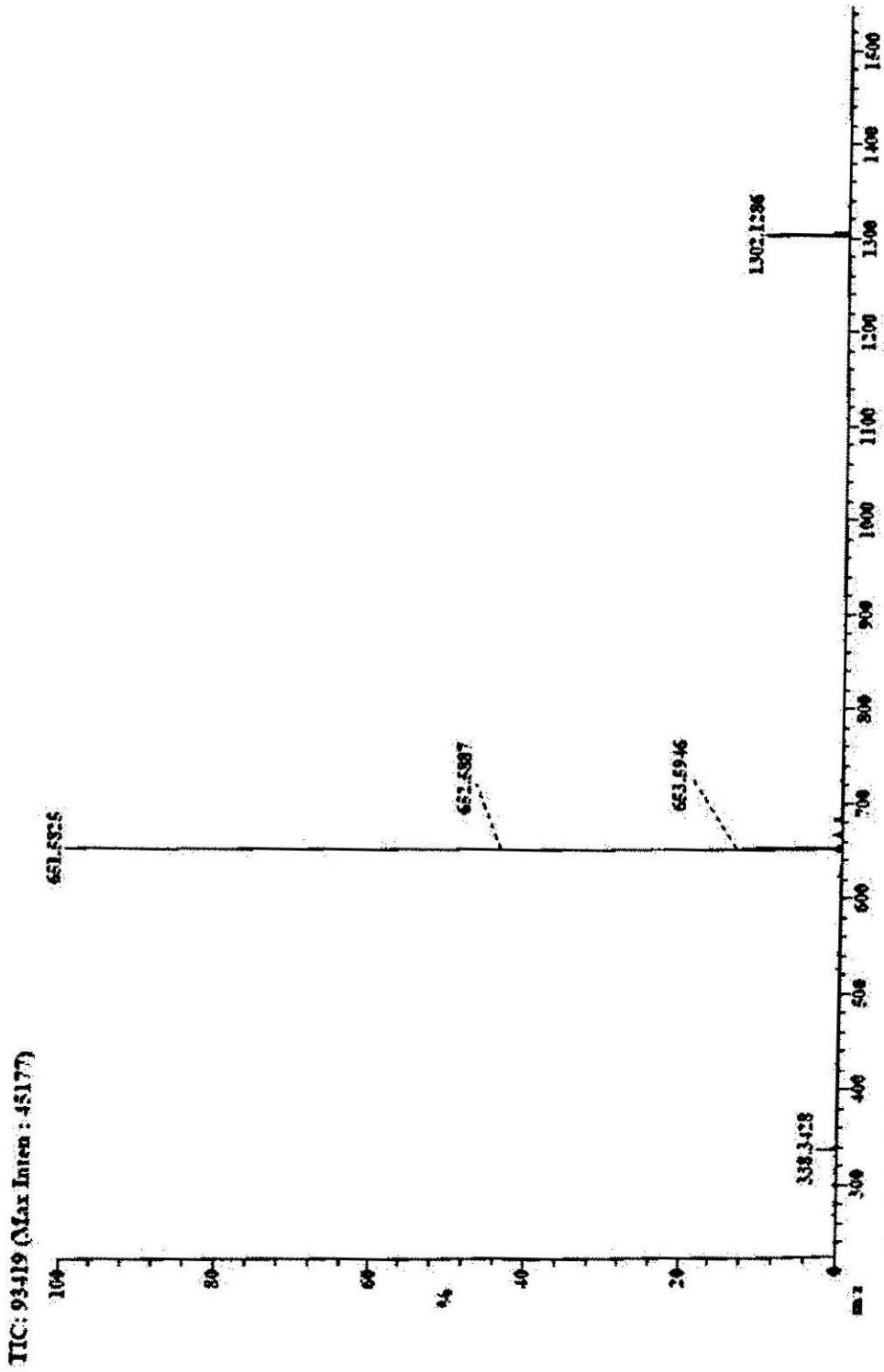


Fig. 3.12 DART mass spectral analysis of DHDMI



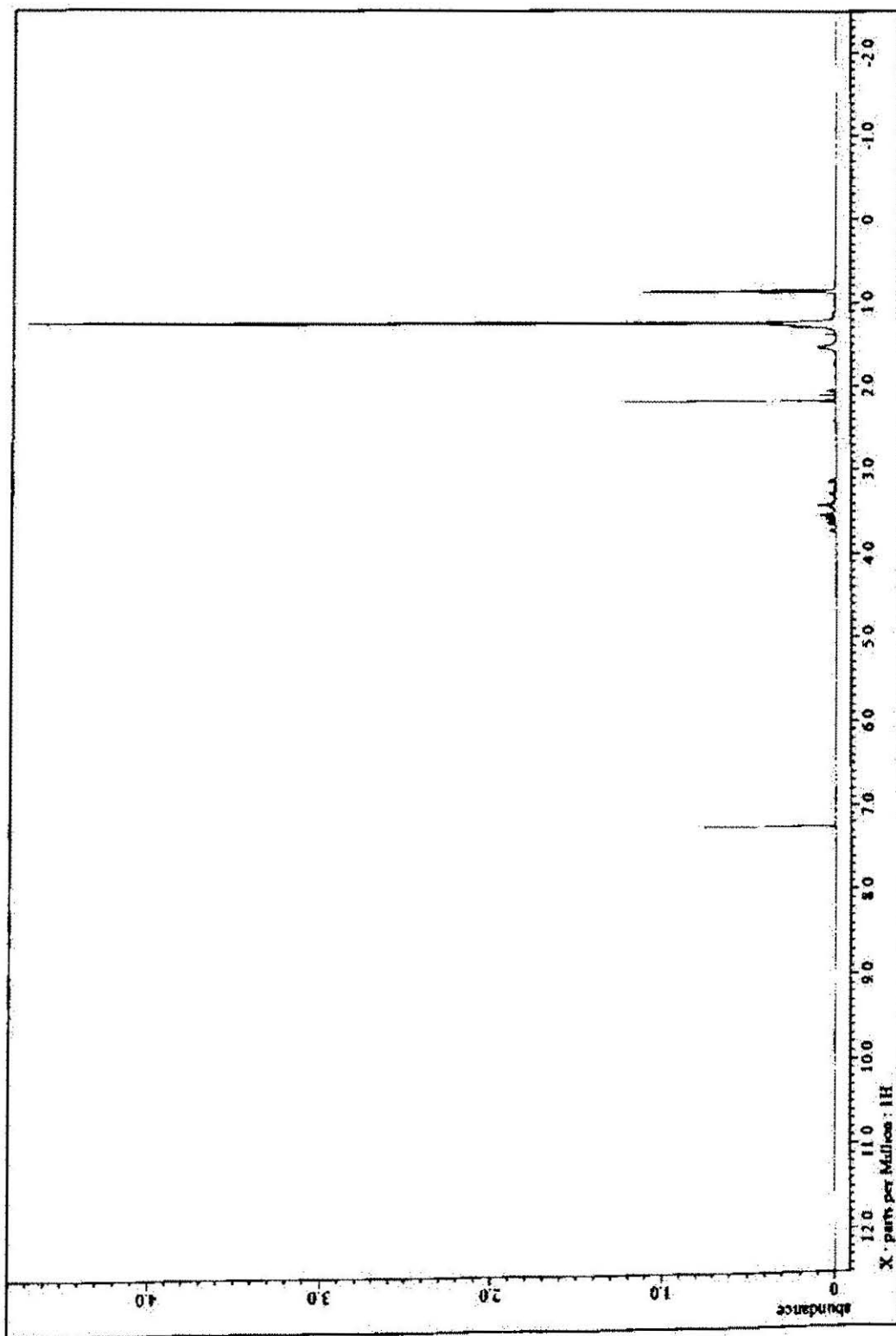


Fig. 3.13 NMR spectrum of DHDMI

**3.4 Calculation of pKa.** The pKa of the lipids (DHI, DHMI, DHDMI and DPI) was calculated using ACD/pKa DB software (Advanced Chemistry Developmet, Inc., Ontario, Canada) (126).

**3.5 Preparation of Liposomes.** Liposomes were prepared by lipid film hydration and extrusion (98). Chloroform solutions of appropriate lipids (Table 3.1) were mixed in a 25 mL round bottom flask. Chloroform was evaporated in a Buchi rotavapor and further dried in vaccum oven for 3 hours at room temperature to remove traces of the solvent. The lipid film was then hydrated with HEPES buffer (pH 7.4, 5 mM HEPES) with or without 140 mM NaCl using intermittent agitation to obtain a suspension of 7.5 mM total lipids. For pH dependent change of Zeta potential measurements, interaction between convertible and model liposomes and DSC experiments liposomes were prepared in 0 mM NaCl while for the cytotoxicity and doxorubicin uptake experiments, 140 mM NaCl was used to prepare liposomes. The liposome suspension was freeze-thawed (alternate immersion in dry ice/acetone and water bath at 40 °C) eleven times and extruded sequentially through 400 nm and 200 nm polycarbonate membranes (Nucleopore Corp., Pleasanton, CA) using a Mini-extruder (Avanti Polar Lipids Inc., Alabaster, AL) at 70° C to yield the liposome preparation. The particle diameter and  $\zeta$ -potential of the preparations were measured by photon correlation spectroscopy (Zetasizer ZS90, Malvern Instruments Ltd., UK).

The average liposome sizes for all the formulations studied ranged from 200-270 nm

### 3.6 Composition of \*Convertible, Control and Model liposomes

**Table 3.1** Lipid Composition of Convertible (I, II, III) and Control (IV) Liposomes

Liposome Preparation No.	Mol %				
	DHI	DHMI	DHDMI	DSPC	DPPE-PEG
I	25			70	5
II		25		70	5
III			25	70	5
IV				95	5

\*The ester based imidazole lipid (DPI) was not used for liposome preparation and subsequent experiments because of low yield and expensive precursor lipids.

Model liposomes (118) (119), that mimic the lipid composition of biomembranes were prepared with the lipid composition 50 mol % POPC, 20 mol % POPE, 5 mol % POPS, 10 mol % L- $\alpha$ -PI and 15 mol % cholesterol

**3.7 pH dependent change of Zeta potential.** The pH of an aliquot (1mL) of a liposome suspension (see section 3.5) was adjusted with acetic acid (5 mM, final pH confirmed by pH meter) immediately before taking zeta potential measurements. The zeta potentials were measured at 37 °C by electrophoresis mobility under applied voltage using Zetasizer ZS 90 (Malvern Instrument, Malvern, UK).

**3.8 Interaction between convertible and model liposomes.** Liposome suspensions of pH-sensitive liposomes I, II, III and IV (see section 3.5) were mixed with equal volume of model liposome (see section 3.5) and pH was adjusted with acetic acid (5 mM, final pH confirmed by pH meter). The liposome mixture was incubated for one hour at 37 °C and average sizes were measured at 37°C by dynamic light scattering using Zetasizer ZS 90 (Malvern Instrument, Malvern, UK).

**3.9 Differential Scanning Calorimetry of liposome formulations I and IV.** A VP-DSC Instrument (MicroCal, LLC, Northampton, MA) was used for the differential scanning calorimetry (DSC) studies. DSC scans were performed on vesicle suspensions of 0.5 mL sample volume containing 2.5 mM total lipid at pH values 7.4 and 6.0. The thermograms of vesicle suspensions were acquired from 35°C to 70°C at a scan rate of 5°C/h. The excess heat capacity curves of samples were normalized by subtraction of the thermograms of the buffer acquired simultaneously under identical conditions.

### **3.10 Loading of doxorubicin (DOX) in liposomes**

**3.10.1 Doxorubicin loading by ammonium sulfate gradient.** Earlier in the study, the remote loading of doxorubicin into liposomes were driven by a transmembrane ammonium sulfate gradient according to reference (99) (100) with minor modification. Briefly, chloroform solutions of appropriate lipids (Table 3.1) were mixed in a round bottom flask. Chloroform was evaporated in a Buchi rotavapor and further dried in vacuum oven for 3 hours at room temperature to remove traces of the solvent. Each lipid film was hydrated with 250 mM ammonium sulfate solution in water and agitated intermittently to form a liposome suspension. The pH of the ammonium sulfate solution

was adjusted to 7.0 with ammonium hydroxide solution. The resultant liposome suspension was freeze/thawed (dry ice/acetone, water bath at 40 °C) eleven times and extruded sequentially through a 400 nm and a 200 nm polycarbonate membrane (Nucleopore Corp., Pleasanton, CA) using a Mini-extruder (Avanti Polar Lipids Inc., Alabaster, AL) at 70 °C to yield the liposome preparation. To establish the transmembrane ammonium sulfate gradient, the extruded liposomes were separated from unencapsulated ammonium sulfate by a Sephadex G-25 column (Sigma, St. Louis, MO) equilibrated with isotonic HEPES buffered saline (5 mM HEPES, 140 mM NaCl, pH 7.4). One volume of 0.75 mg/mL DOX in the same isotonic HEPES buffered saline was added into 2 volumes of liposome suspension (lipid concentration = 7.5 mM) and incubated for 1.5 h at 70 °C. The liposome preparations were then passed through Sephadex G-200 column eluted with isotonic HEPES buffered saline to separate the liposomal-DOX from unencapsulated DOX.

**3.10.2 Doxorubicin loading by manganese sulfate gradient.** Later in this study, the loading of doxorubicin was driven by a transmembrane manganese sulfate gradient (101) with minor modification. Lipids film was prepared as mentioned earlier (see section 3.5). Each lipid film was hydrated with 300 mM Manganese sulfate solution prepared in HEPES buffer (pH 7.4, 5 mM HEPES, 140 mM NaCl) and agitated intermittently to get the liposomal suspension. The resultant liposome suspension was freeze/thawed (dry ice/acetone, water bath at 40 °C) eleven times and extruded sequentially through a 400 nm and a 200 nm polycarbonate membrane (Nucleopore Corp., Pleasanton, CA) using a Mini-extruder (Avanti Polar Lipids Inc., Alabaster, AL) at 70° C to yield the liposome preparation. To establish the transmembrane manganese sulfate gradient, the extruded

liposomes were separated from unencapsulated ammonium sulfate by a Sephadex G-25 column (Sigma, St. Louis, MO) equilibrated with isotonic HEPES buffered saline (5 mM HEPES, 140 mM NaCl, pH 7.4). 1 volume of 0.75 mg/mL DOX in the same isotonic HEPES buffered saline was added into 2 volumes of liposome suspension (lipid concentration = 7.5 mM) and incubated for 1.5 h at 70°C. The liposome preparations were then passed through Sephadex G-200 column eluted with isotonic HEPES buffered saline to separate the liposomal-DOX from unencapsulated DOX.

**3.11 Determination of DOX concentration and encapsulation efficiency.** An aliquot of a DOX-loaded liposome formulation was lysed with 90% isopropanol containing 0.075 M HCl (125) followed by quantification of the released DOX by Spectrofluorometer (Shimadzu, rf 5301 pc, Ex. = 484 nm, Em. = 587 nm). The DOX in the corresponding liposome formulation before purification was quantified in parallel. The Encapsulation Efficiency (EE) of the liposome formulation was then calculated using the formula:

$$EE = \frac{\text{DOX in purified liposome formulation}}{\text{DOX in liposome formulation before purification}} \times 100\%$$

DOX encapsulation by  $\text{MnSO}_4$  yielded an EE 40-45 % for all the liposome formulations while the encapsulation by  $(\text{NH}_4)_2\text{SO}_4$  yielded an EE  $\approx$  12 %

**3.12 Doxorubicin retention studies.** Retention of DOX in liposomal formulation I was determined by equilibrium microdialysis using rapid equilibrium dialysis device (Thermo Scientific, inserts with membrane, MWCO = 8000 Da) according to manufacturer's recommendations. The pH of liposome formulation of DOX (see section 3.10.2) was

adjusted with MES buffer (pH 5.93, 50mM, 145mM NaCl). Precisely, 40, 100 and 500  $\mu$ L of the MES buffer was added to 1mL of liposome suspension to adjust the pH to 6.97, 6.5 and 6.05 respectively. 100  $\mu$ L of liposome suspension was added to the sample chamber while 300  $\mu$ L of buffer was added to the buffer chamber. The percent DOX retained in liposomes at different time points was calculated using the following equation.

$$\% \text{ DOX retained} = 100 \times \left\{ 1 - \frac{(V_b + V_s)(C_b)}{C_d V_d} \right\}$$

Where,  $V_b$  = Volume of buffer chamber,  $V_s$  = Volume of sample chamber,  $C_b$  = concentration of DOX in buffer chamber,  $C_d$  = initial liposomal DOX concentration added to sample chamber,  $V_d$  = initial volume of sample chamber

**3.13 Cell culture conditions.** The B16-F10 (murine melanoma) cells and Hela (human cervical cancer) cells were purchased from American Type Culture Collection (Rockville, MD). B16-F10 cells were maintained in DMEM media supplemented with 10% fetal bovine serum, 1% Glutamine and 1% penicillin-streptomycin. Hela cells were maintained in EMEM media supplemented with 10% fetal bovine serum, 1% Glutamine and 1% penicillin-streptomycin. Cells were cultured with complete medium at 37°C in a humidified atmosphere of 5% CO<sub>2</sub> in air. Cell concentrations were determined with a cell coulter counter.

**3.14 MTS cytotoxicity assay on B16F10 and Hela cells.** B16-F10 cells (~ 20,000 cells/well) and Hela cells (~ 80,000 cells/well) were seeded on 96-well plates and grown overnight in complete medium. The cells were then washed with PBS and treated with

100  $\mu\text{L}$  of either complete or serum free media containing free DOX, Liposomal DOX at a dosage of 0.1, 1.0, 10.0  $\mu\text{g}$  DOX per mL and empty liposome formulation I.

The pH of the media (10 mL) was adjusted with glacial acetic acid (Table 3.2) and final pH was confirmed with pH meter.

**Table 3.2** Adjustment of pH of the media with glacial acetic acid

Media (10 mL)	Glacial Acetic Acid ( $\mu\text{L}$ )		
	pH 7.0	pH 6.5	pH 6.0
DMEM (Serum Free)	6.5	13	20
DMEM (Complete Media)	7	17	20
EMEM (Serum Free)	0.5	2	5
EMEM (Complete Media)	0.5	3	6

Each test was performed in quadruplet. Cells were incubated for 3 h and 12 h at 37°C and 5% CO<sub>2</sub>. After incubation for 3 and 12 hours respectively, the medium was removed, and the cells were washed three times with 100  $\mu\text{L}$  PBS buffer and supplemented with 100  $\mu\text{L}$ /well of the complete medium and 20  $\mu\text{L}$ /well of MTS-based CellTiter 96® AQueous One Solution Cell Proliferation Assay Reagent (Promega Corp., WI, USA) and incubated at 37°C for 2 h. The absorbance at 570 nm was measured using a microplate reader (Berthold Tristar, LB 941).



The cells that are not treated by any formulations were grown at pH's 7.4, 7.0, 6.5 and 6.0 and their viabilities were determined by MTS assay to rule out significant cytotoxicity caused by the change of pH in the media.

**3.15 Quantitation of cellular uptake of doxorubicin with flow cytometry.** B16-F10 cells (~ 600,000 cells/well) were seeded on 6-well plates and grown overnight in complete medium. The cells were then washed with PBS and treated with 2 mL of serum free media containing either free DOX or DOX loaded liposome formulation II at a dosage of 10 µg DOX per mL. The pH of the media was adjusted with glacial acetic acid (Table 3.2). Cells were incubated for 4 h at 37°C and 5% CO<sub>2</sub>. After incubation cells were detached with detachin (Genlantis, San Diego, CA), centrifuged and resuspended in PBS before taking measurement in FL2-H channel in FACScan (Becton Dickinson, San Jose, CA, USA).

## Results and Discussion

**3.16 Design of imadazole-based lipids.** We have chosen imidazole head group in our lipid design due it's unique properties. The N3 position of imidazole moiety is basic and protonates at mildly acidic conditions (130). Additionally, addition of methyl group at the C4 and C5 position of the imidazole moiety gives the flexibility to tune the pKa of the molecule to a higher value (Table 3.3). When incorporated into liposomes, the protonation of imidazole at low pH provides positive charges to these lipids which interacts with negatively charged PEGylated lipid (DPPE-PEG). To further aid this interaction, we have chosen C16 chains as lipid tails for the imidazole lipid which renders

additional force of attraction (Vander Waals) with the C16 chain DPPE-PEG owing to same chain length.

**3.17 Synthesis of imidazole-based, pH-titratable lipids.** The synthesis of both ester and ether based lipids were carried out to yield a series of pH titratable lipids. The synthesis was based on first the tosyl activation of the commercially available lipid (DHG) or (DPG) with para toluene sulfonyl chloride and then substitution of the tosyl group with the imidazole moiety using mercaptoimidazole compounds (112) (113). Tosylate is a good leaving group and therefore was exploited for the conjugation of lipid with the imidazole compounds. The high temperature conditions were maintained and DMF was added to the reaction mixture because of the limited solubility of mercaptoimidazole in dichloromethane. The reaction time was optimized for best yield and at the same time fewer side products.

**3.18 Lipid pKa calculation.** The pKa of the lipids (DHI, DHMDI, DHDMI and DPI) were determined by ACD/pKa software. Calculation was used rather than the experimental methods for pKa determination as these lipids assemble in aqueous media and therefore it's hard to trace each molecule. Additionally pKa of a lipid molecule is sensitive to its liposomal environment. We calculated this, but later did the zeta potential measurements of liposomes composed of these lipids was measured at different pH conditions to monitor the protonation process which is more relevant to the function of these lipids. The imidazole-based lipids showed estimated pKa ranging from 5.36 to 6.75 (Table 3.3).

**Table 3.3** Calculated pKa of Imidazole based Lipids.

Lipid	pKa
DHI	5.53 ± 0.5
DHMI	6.2 ± 0.5
DHDMI	6.75 ± 0.5
DPI	5.36 ± 0.5

**3.19 Zeta potential measurements.** The ability of the imidazole lipids to protonate at mild acidic conditions when incorporated in liposomes has been previously demonstrated (116), moreover their efficiency as carriers for gene transfer has also been examined at acidic pH (114) (117).

The convertible liposomes (I, II, III) prepared and tested herein, show increase in their zeta potential with increasing pKa of the corresponding imidazole lipids. The liposome formulation I shows an increase in average zeta potential value from -5.43 mV at pH 7.4 to 2.72 mV at pH 6.0 while formulation II shows zeta potential increase from -2.5 mV to 5.04 mV (Fig. 3.14 (a), (b)). The liposome formulation III starts at -0.93 mV and reaches 12.99 mV value at pH 6.0. The zeta potential change of the control liposome IV did not show significant change in the zeta potential values from pH 7.4 to pH 6.0. The increase in zeta potential values of the pH tunable liposomes is indicative of the protonation of the imidazole lipids, moreover the increase in zeta potential values is consistent with the fact that liposomes with higher calculated pKa of the imidazole lipid show high initial and

final zeta potential values, suggesting the protonation of more number of the imidazole lipids with increasing pKa of the lipids.

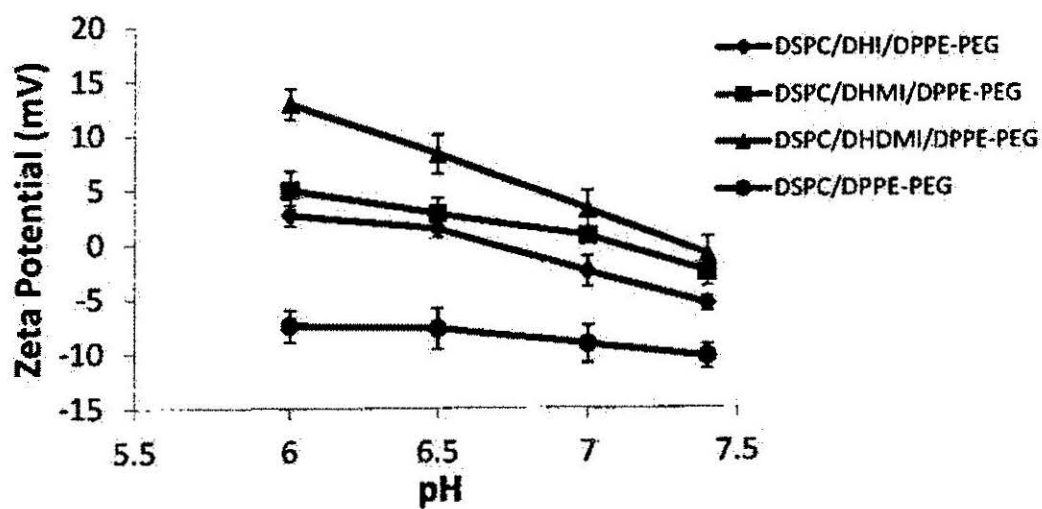


Fig. 3.14 (a) Change of zeta potential values of liposome formulations (I-IV) with pH

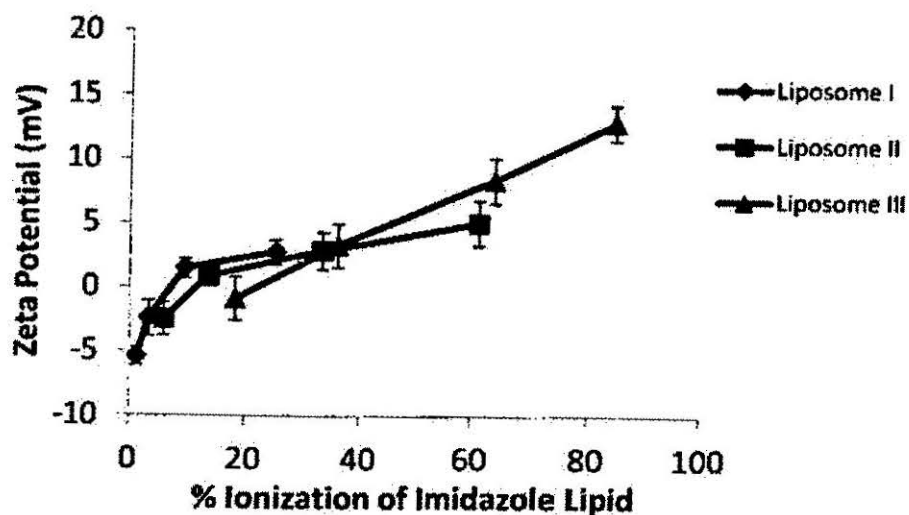


Fig. 3.14 (b) Change of zeta potential values of liposome formulations (I-IV) with percent (%) Ionization of imidazole lipid incorporated in convertible liposomes. \*Percent Ionization was calculated by Henderson-Hasselbalch equation using estimated average pKa values of imidazole lipids.

**3.20 Phase separation of liposome into lipid domains (DSC characterization).** The liposomes prepared with saturated lipids of carbon chain lengths differing by only two carbon atoms or less show ideal mixing of lipids (120) (121). The DSC thermogram of liposome I (Fig. 3.15) show one broad melting peak at pH 7.4 between 56 °C to 65 °C indicating homogenous mixing of the C16 and C18 chain lipids. At pH 6.0 the formulation I shows the emergence of a second broad peak at 52° C suggesting the formation of the domain rich in DSPC lipids ( $T_m = 55\text{ }^\circ\text{C}$ ) doped with the C 16 chain imidazole lipids. The formation of the DSPC domain on the liposome is due to the interaction of newly protonated imidazole lipids and negatively charged PEGylated lipids which squeezes out the DSPC lipids, thus forming a two phase system.

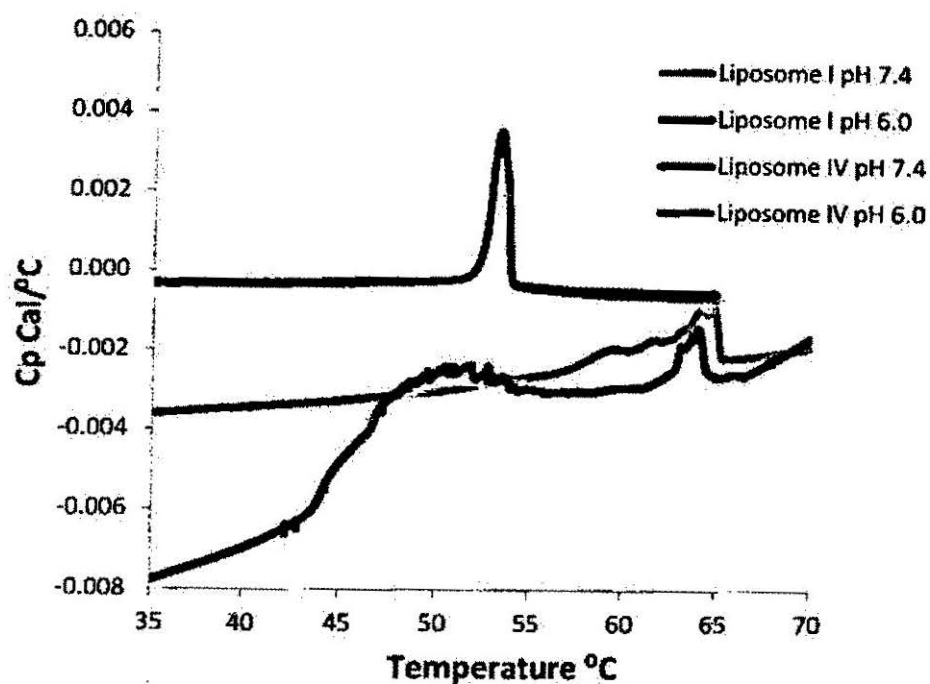


Fig. 3.15 DSC thermogram of control liposome IV and convertible liposome formulation I

The DSC thermogram of the control liposome IV (Fig. 3.15) show one melting peak suggesting the homogenous mixing of lipids at both pH 7.4 and 6.0 and therefore a one phase system.

**3.21 Interaction of convertible liposomes with model liposomes mimicking cell membrane.** To evaluate whether the increase in the zeta potential values in fact translates into interaction with negatively charge cell membrane, we prepared model liposome (118) (119) carrying 15 mol % of negatively charged lipids to mimic the charge of the cell membrane (85) (88). The convertible liposomes were mixed with equal volume of equimolar model liposomes and their sizes were measured at different pH conditions.

The increase in the average size of the model liposome upon mixing with the pH convertible liposomes is consistent with the increase in the pKa values of the imidazole lipids and the corresponding increase in zeta potential of the respective liposomes (Fig. 3.16). Liposome formulation III shows approx. three times increase in average size values at pH 6.0 ( $\approx 2770$  nm) compared to average sizes at pH 7.4. Similarly formulations I and II show increase in average sizes 3.5- to 4- times the values at pH 7.4. The average sizes of the liposomes of the control liposome on the other hand showed no significant change in the average sizes of the liposomal mixture at both the pH conditions.

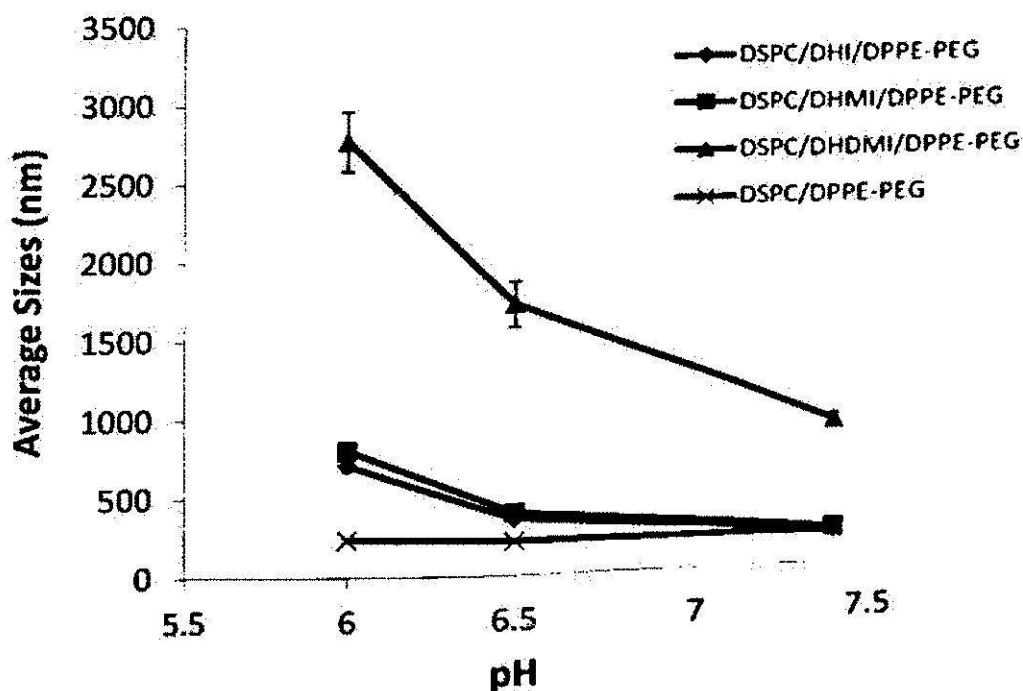


Fig. 3.16 Change of average sizes of equimolar mixture of model liposome and either I, II, III or IV with pH

**3.22 Doxorubicin loading in liposomes.** Doxorubicin has been conventionally loaded in liposomes using an ammonium sulfate gradient wherein the concentration of ammonium sulfate is higher in the liposome than the extraliposomal medium. The pH inside the liposome is maintained at 4-5 pH units while the extraliposomal pH is at pH 7.4. The remote loading of DOX occurs when the unprotonated DOX molecule diffuses from the extraliposomal space and gets charged at the low pH environment inside the liposome and forms a sulfate salt from the sulfate of the ammonium sulfate solution (Fig. 3.17). The DOX-sulfate salt is then precipitated in the low pH environment. The limitation with this approach is the requirement to form the liposomes at low pH environments which is a challenging task for pH sensitive liposomes.

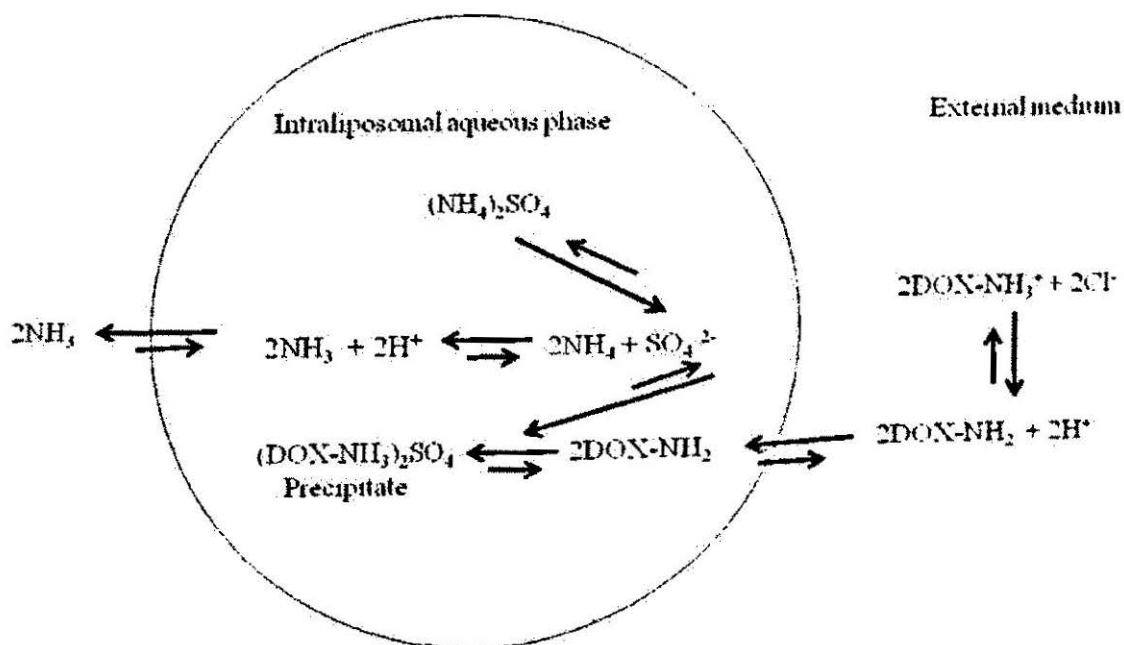


Fig. 3.17 Loading of DOX into liposomes by ammonium sulfate gradient



For our study, we first attempted a modification in this procedure where we adjusted the  $(\text{NH}_4)_2\text{SO}_4$  solution to pH 7.0 instead of pH 4-5 and then proceeded with lipid hydration, extrusion, purification and remote loading of DOX. However, such modification resulted in poor DOX encapsulation ( $\approx 12\%$ ) and poor DOX retention where only 40% of the DOX remained inside the liposome after 50 h of incubation at pH 7.4 at  $37^\circ\text{C}$  (Fig. 3.18)

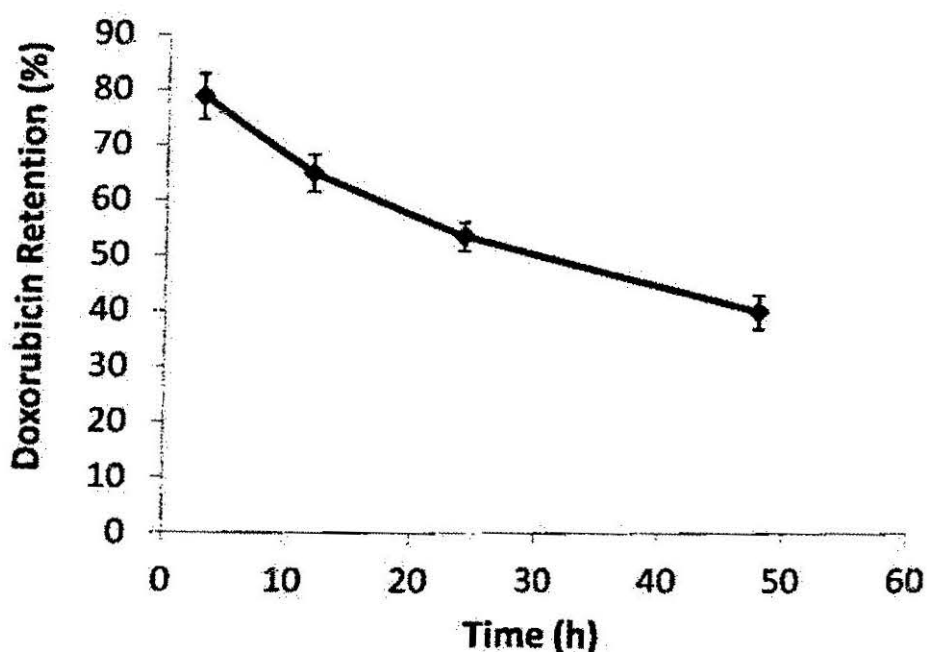


Fig. 3.18 DOX retention in convertible liposome formulation I at pH 7.4 prepared by ammonium sulfate gradient method

To circumvent this problem we prepared the liposome in manganese sulfate solution maintained at pH 7.4 (101). The manganese is known to complex with DOX molecules and therefore increase the retention of the drug in liposome (101). The retention of DOX

with this method was at around 64 % at pH 7.4 and 56 % at pH 6.0 after 48 h of incubation at 37 ° C (Fig. 3.19)

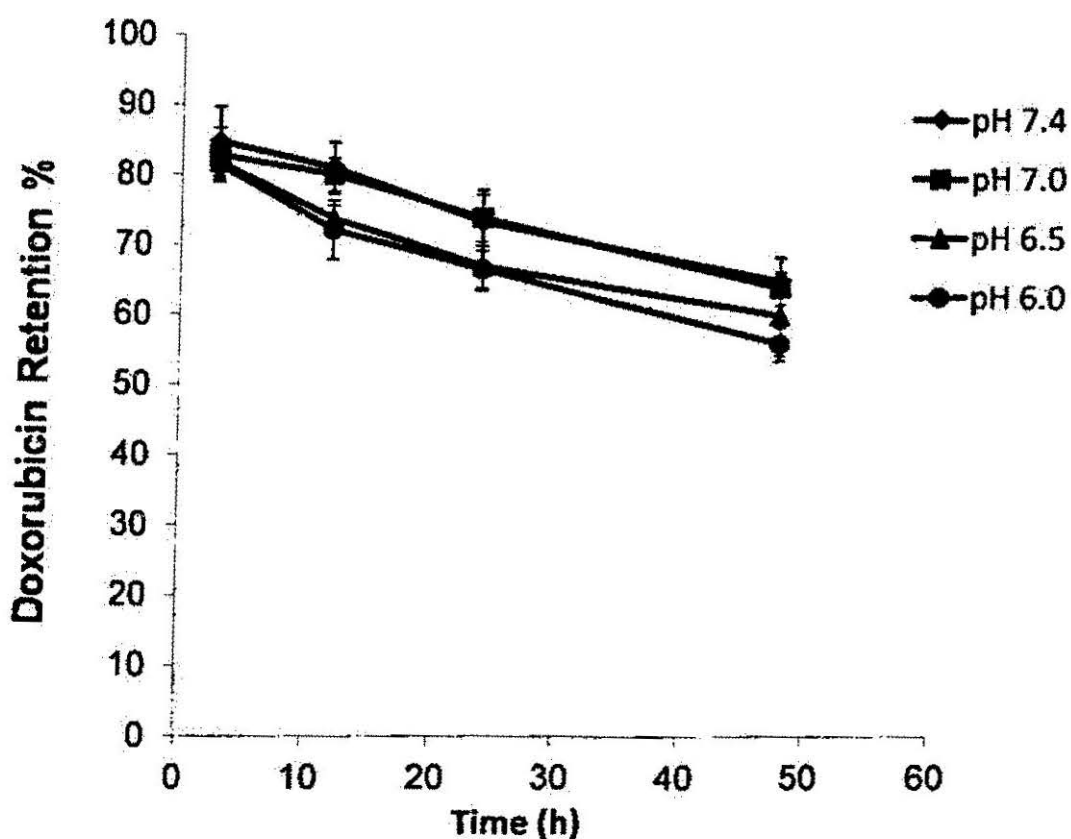


Fig. 3.19 DOX retention in liposome formulation I prepared by manganese sulfate method

**3.23 Cytotoxicity of convertible liposomal formulations of DOX.** B16F10 and Hela cells were treated with all the liposomal formulations (I-IV) and free DOX. The free DOX was studied as positive control while liposome IV was taken as a negative control. All the formulations show dose dependent cytotoxicity in both cell lines. The pH tunable

liposomes show increased cytotoxicity as the pH is lowered from 7.4 to 6.0 at 10  $\mu\text{g/mL}$  DOX concentration both in complete media and serum free media. In B16F10 cells, the average cell viability values for formulations I, II and III were  $\approx 71\%$ ,  $75\%$  and  $50\%$  respectively at pH 7.4 while the averages values were  $\approx 59\%$ ,  $57\%$  and  $41\%$  at pH 6.0 in serum free media at 10  $\mu\text{g/mL}$  DOX concentration after 3 hrs of incubation (Fig. 3.20). After 12 hr of incubation the average cell viability values were  $\approx 57\%$ ,  $54\%$  and  $42\%$  at pH 7.4 and  $\approx 46\%$ ,  $43\%$  and  $31\%$  at pH 6.0 respectively for liposomes I, II, and III (Fig. 3.21, 3.28). The control liposome IV did not show any significant difference between the cell viabilities at pH 7.4 and 6.0 after 3 and 12 hrs of incubation (Fig. 3.20, 3.21). Free DOX was the positive control and showed highest toxicities with cell viability at  $\approx 25\%$  after 12 hours of incubation at both pH values (Fig. 3.21, 3.28). The cytotoxicities were diminished for all formulations in complete media. After 3 hrs of incubation although there was a clear trend in the decreasing cell viabilities as the pH decreased from 7.4 to 6.0, the values were not significantly different (Fig. 3.22). However after 12 hours of incubation the cytotoxicity values for formulations I, II, and III became significantly different with liposome III showing highest cytotoxicity at  $\approx 61\%$  and  $\approx 52\%$  cell viability at pH 7.4 and 6.0 respectively (Fig. 3.23).

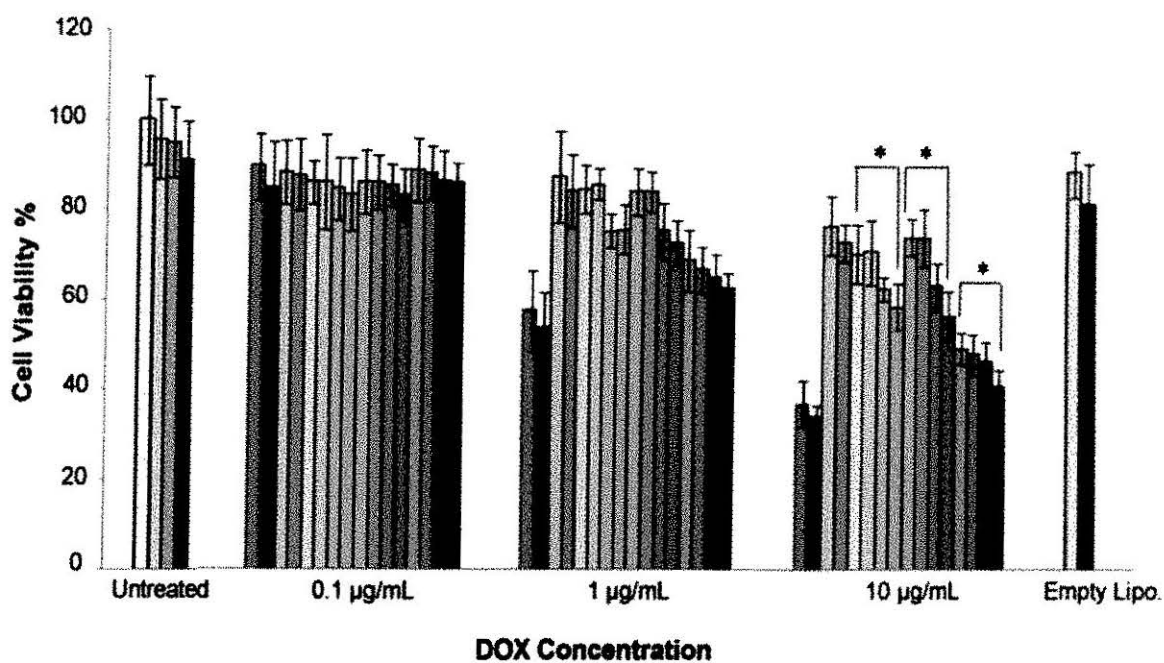
For HeLa cells, the cell viabilities were  $\approx 67\%$ ,  $65\%$  and  $53\%$  at pH 7.4 and  $\approx 55\%$ ,  $53\%$  and  $43\%$  at pH 6.0 respectively for formulations I, II and III after 3 hrs of incubation in serum free media (Fig. 3.24). After 12 hrs of incubation with the convertible liposome formulations I, II and III the cell viability values were  $\approx 63\%$ ,  $58\%$  and  $38\%$  at pH 7.4 and  $\approx 50\%$ ,  $46\%$  and  $28\%$  at pH 6.0 (Fig. 3.25, 3.29). Free DOX showed highest toxicity with  $\approx 22\%$  at both pH 7.4 and 6.0 (Fig. 3.25, 3.29). The observations for

cytotoxicities in complete media were similar as observed in B16F10 cells where cell viabilities did not show any significant difference at pH 7.4 and 6.0 for formulations I, II and III (Fig. 3.26). However cell viability difference at pH 7.4 and 6.0 did become significant after 12 hours of incubation (Fig. 3.27) with liposome III showing highest cytotoxicity at 59 % and 51 % at pH 7.4 and 6.0 respectively.

For both the cell lines the increase in toxicity was greater after 12 hours of incubation compared to the 3 hr of incubation which indicates the high uptake of drug by the cells at longer times. Additionally, the difference in the cytotoxicity of the control liposome IV remained insignificant at pH 7.4 and 6.0 at all DOX concentrations suggesting its lack of interaction with the negatively charged cell surface.

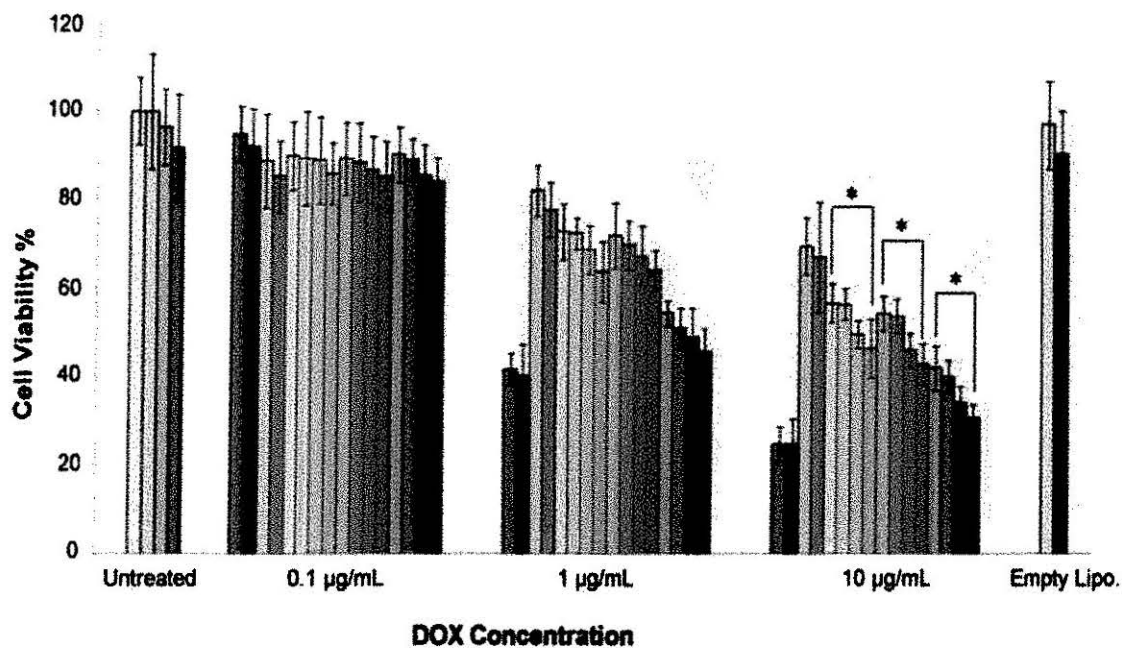
Furthermore, at both incubation times, the cytotoxicity was greater for formulation III which is consistent with the liposome binding assay with model liposome, suggesting more interaction of liposome with higher percentage of positive charges at low pH with the negatively charged cell surface and hence higher uptake and greater toxicity.

Also, the cytotoxicity of empty liposome I remained insignificant for all the experiments indicating inherent insignificant cytotoxicity of the imidazole lipids.



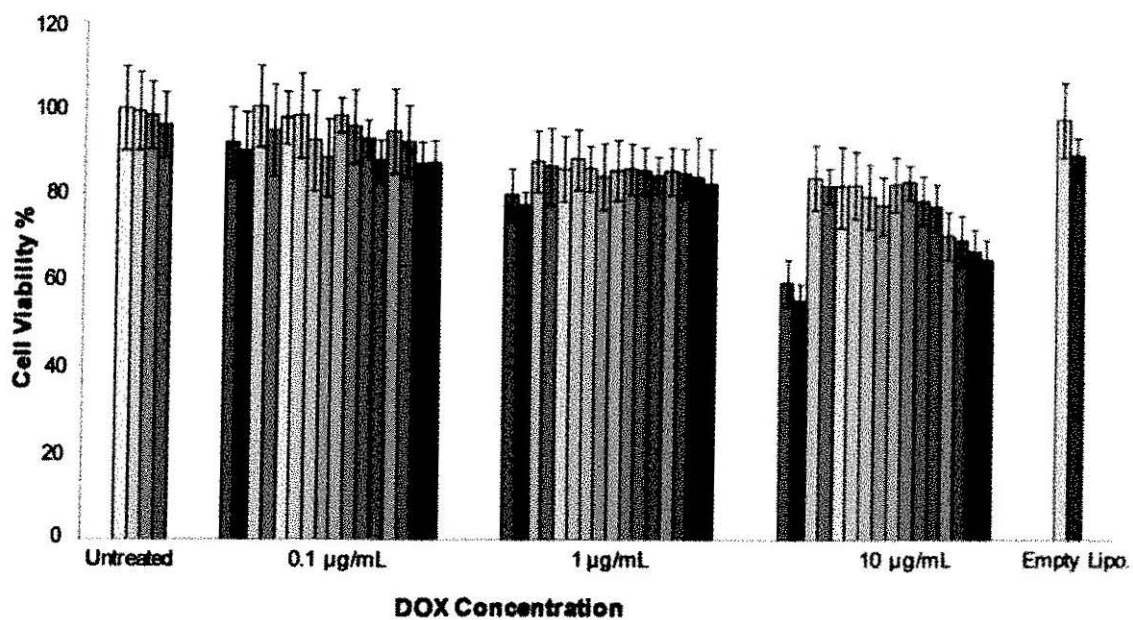
pH	Untreated Cells	Free Doxorubicin	Liposome IV	Liposome I	Liposome II	Liposome III
7.4	Lightest	Dark	Light	Light	Light	Light
7.0	Lightest	Medium	Light	Light	Light	Light
6.5	Lightest	Medium	Light	Light	Light	Light
6.0	Lightest	Dark	Light	Light	Light	Light

Fig. 3.20 Cytotoxicity of free DOX, liposome formulations of DOX and empty liposome (formulation I without DOX) against B16-F10 murine melanoma cells in serum-free medium after three hours of incubation. Mean and SD of cell viability (%) are presented (n = 4) (\* p < 0.05, student t-test)



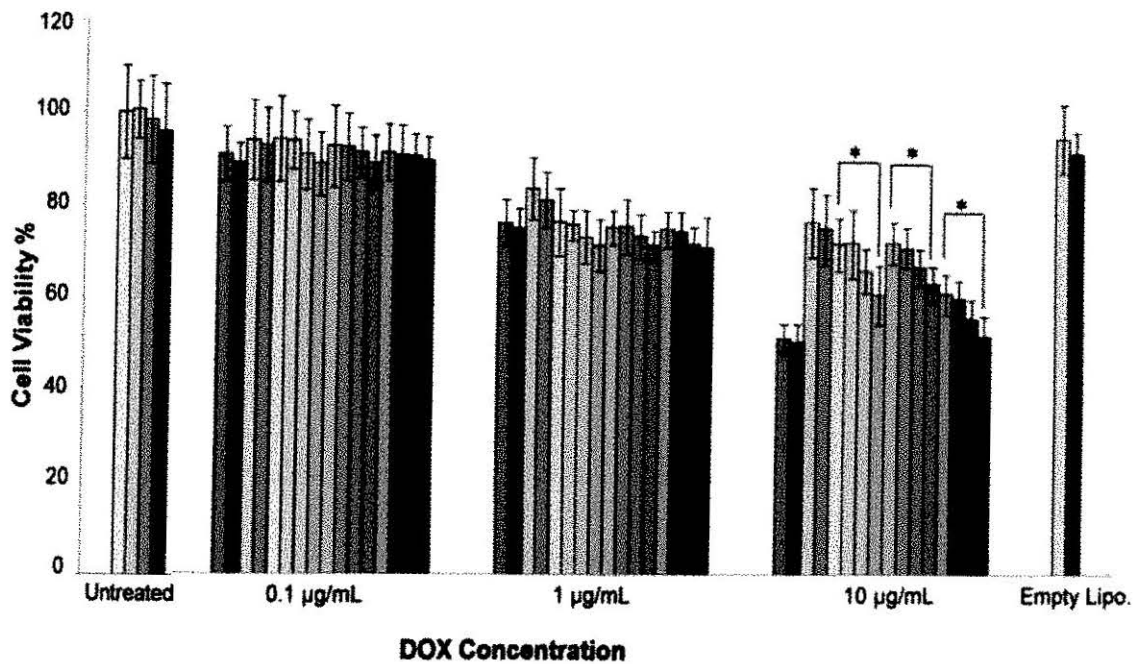
pH	Untreated Cells	Free Doxorubicin	Liposome IV	Liposome I	Liposome II	Liposome III
7.4						
7.0		---	---			
6.5		---	---			
6.0						

Fig. 3.21 Cytotoxicity of free DOX, liposome formulations of DOX and empty liposome (formulation I without DOX) against B16-F10 murine melanoma cells in serum-free medium after twelve hours of incubation. Mean and SD of cell viability (%) are presented (n = 4) (\* p < 0.05, student t-test)



pH	Untreated Cells	Free Doxorubicin	Liposome IV	Liposome I	Liposome II	Liposome III
7.4						
7.0		---	---			
6.5		---	---			
6.0						

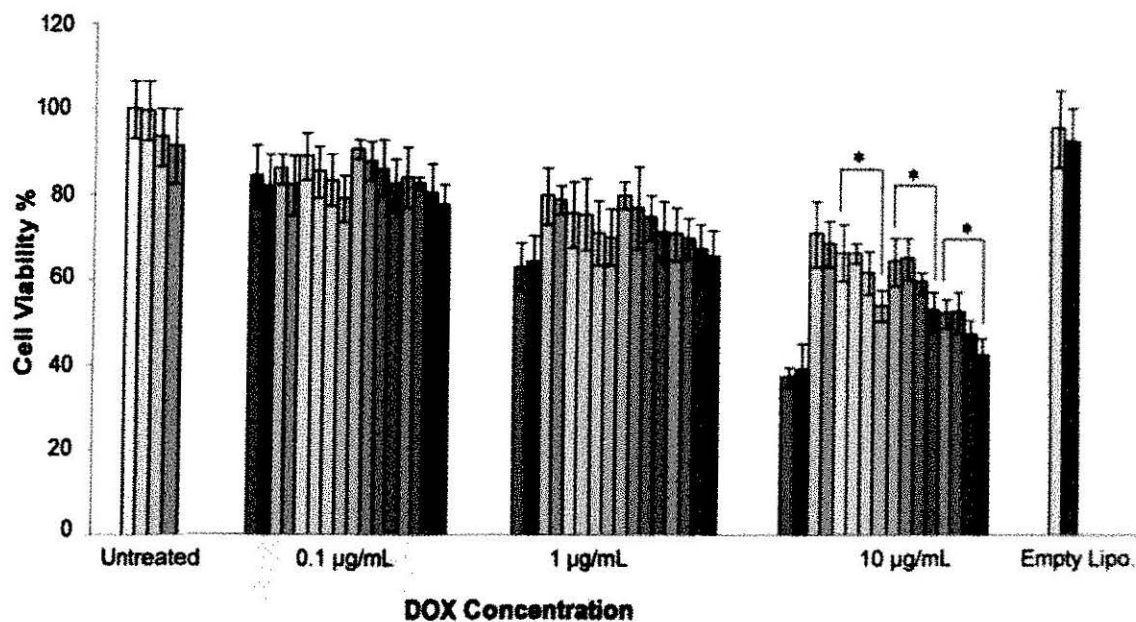
Figure 3.22 Cytotoxicity of free DOX, liposome formulations of DOX and empty liposome (formulation I without DOX) against B16-F10 murine melanoma cells in complete medium after three hours of incubation. Mean and SD of cell viability (%) are presented (n = 4)



pH	Untreated Cells	Free Doxorubicin	Liposome IV	Liposome I	Liposome II	Liposome III
7.4						
7.0		—	—			
6.5		—	—			
6.0						

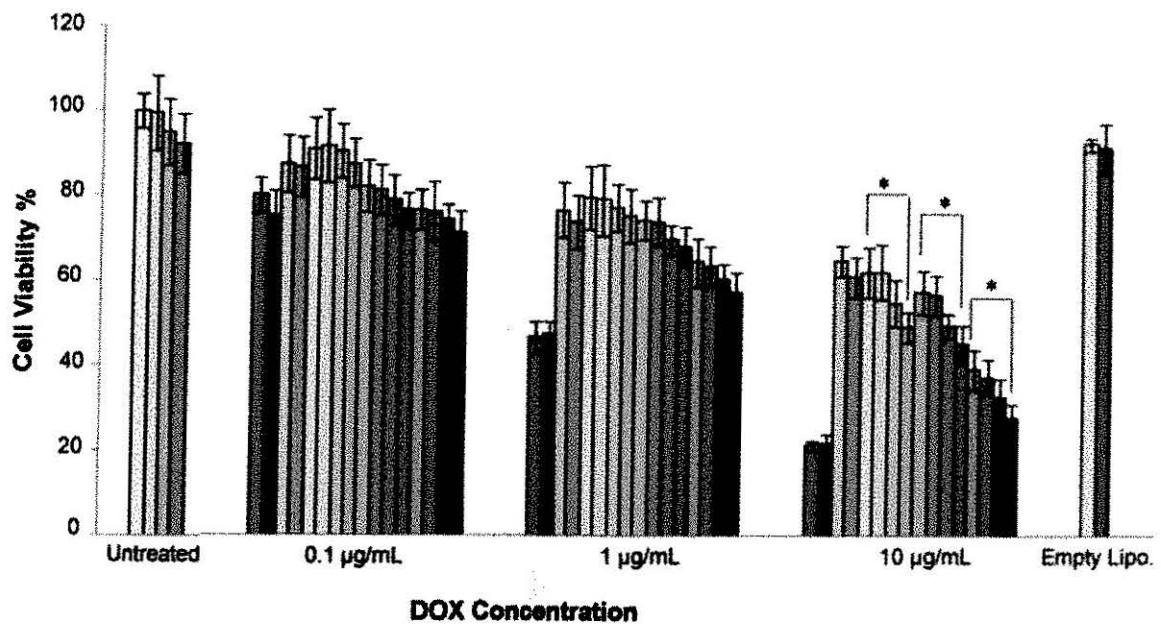
Fig. 3.23 Cytotoxicity of free DOX, liposome formulations of DOX and empty liposome (formulation I without DOX) against B16-F10 murine melanoma cells in complete medium after twelve hours of incubation. Mean and SD of cell viability (%) are presented (n = 4) (\* p < 0.05, student t-test)





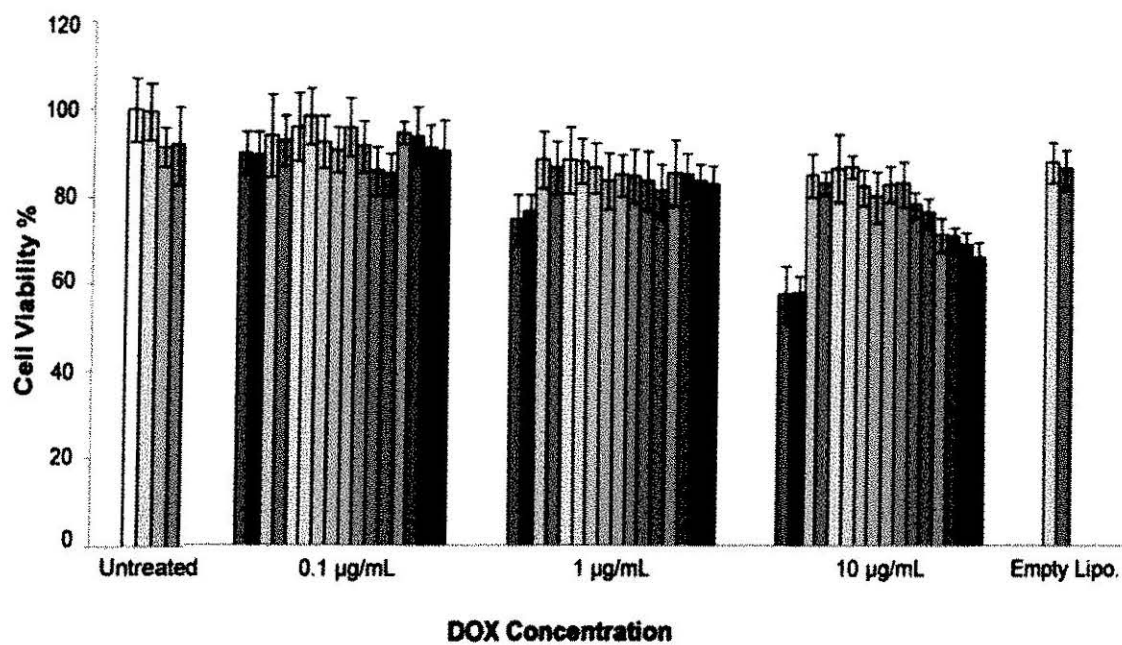
pH	Untreated Cells	Free Doxorubicin	Liposome IV	Liposome I	Liposome II	Liposome III
7.4						
7.0		—	—			
6.5		—	—			
6.0						

Fig. 3.24 Cytotoxicity of free DOX, liposome formulations of DOX and empty liposome (formulation I without DOX) against Hela cells in serum-free medium after three hours of incubation. Mean and SD of cell viability (%) are presented ( $n = 4$ ) (\*  $p < 0.05$ , student t-test)



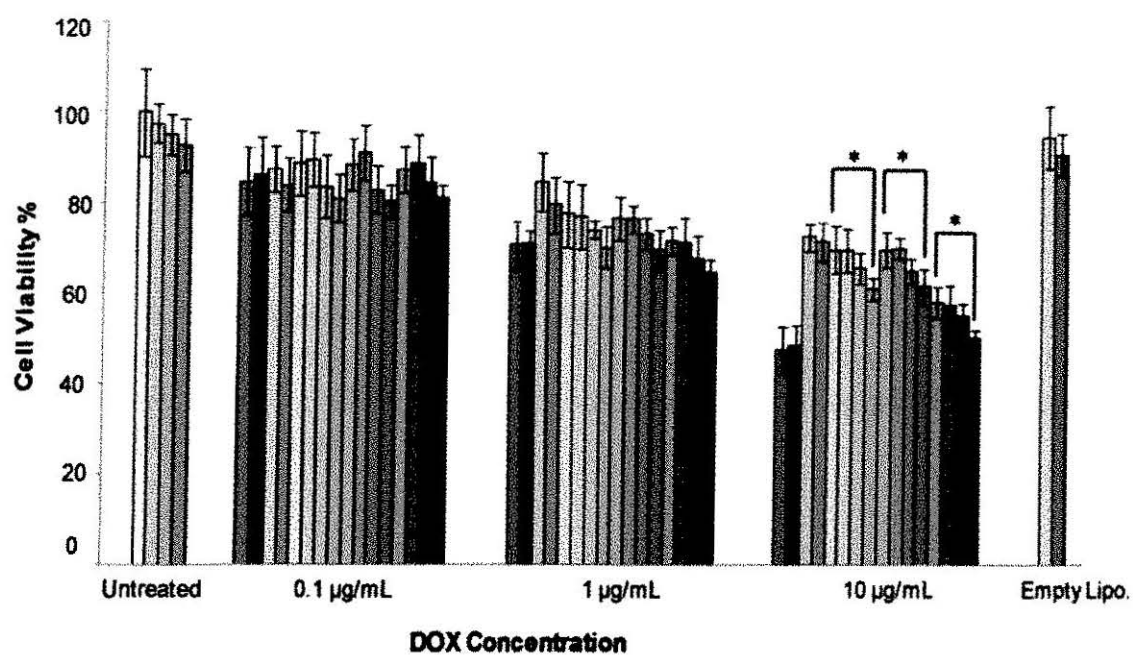
pH	Untreated Cells	Free Doxorubicin	Liposome IV	Liposome I	Liposome II	Liposome III
7.4						
7.0		---	---			
6.5		---	---			
6.0						

Fig. 3.25 Cytotoxicity of free DOX, liposome formulations of DOX and empty liposome (formulation I without DOX) against Hela cells in serum-free medium after twelve hours of incubation. Mean and SD of cell viability (%) are presented (n = 4) (\* p < 0.05, student t-test)



pH	Untreated Cells	Free Doxorubicin	Liposome IV	Liposome I	Liposome II	Liposome III
7.4						
7.0		—	—			
6.5		—	—			
6.0						

Fig. 3.26 Cytotoxicity of free DOX, liposome formulations of DOX and empty liposome (formulation I without DOX) against Hela cells in complete medium after three hours of incubation. Mean and SD of cell viability (%) are presented (n = 4)



pH	Untreated Cells	Free Doxorubicin	Liposome IV	Liposome I	Liposome II	Liposome III
7.4	High Viability	Low Viability	High Viability	High Viability	High Viability	High Viability
7.0	High Viability	Low Viability	High Viability	High Viability	High Viability	High Viability
6.5	High Viability	Low Viability	High Viability	High Viability	High Viability	High Viability
6.0	High Viability	Low Viability	High Viability	High Viability	High Viability	High Viability

Fig. 3.27 Cytotoxicity of free DOX, liposome formulations of DOX and empty liposome (formulation I without DOX) against Hela cells in complete medium after twelve hours of incubation. Mean and SD of cell viability (%) are presented (n = 4) (\* p < 0.05, student t-test)

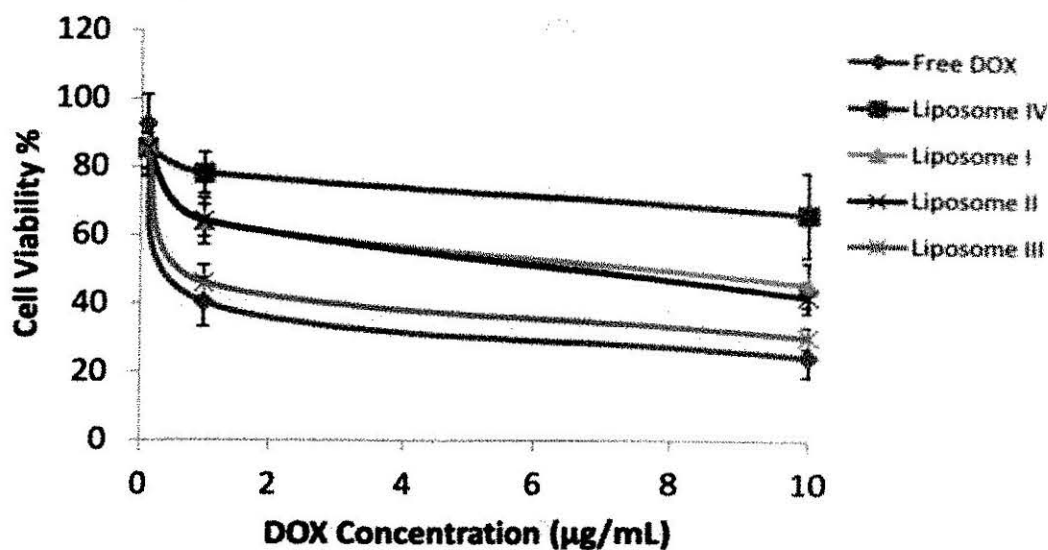


Fig. 3.28 Cytotoxicity of free DOX and liposome formulations of DOX against DOX concentrations (0.1, 1, 10 µg/mL) in B16F10 cells at pH 6.0 in serum free media after 12 hours of incubation. \*Average values of percent cell viability were taken.

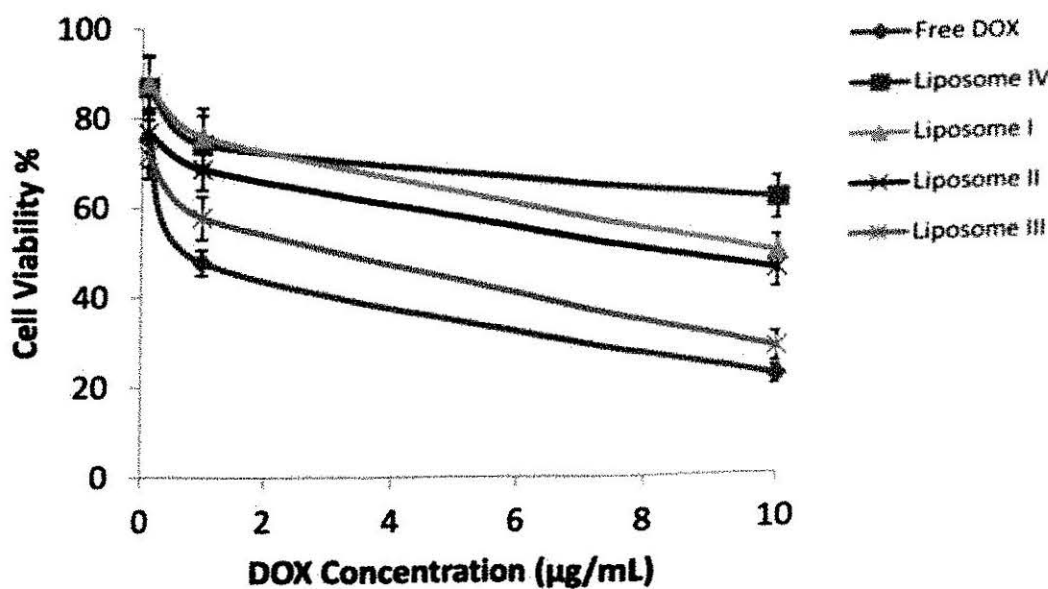


Fig. 3.29 Cytotoxicity of free DOX and liposome formulations of DOX against DOX concentrations (0.1, 1, 10 µg/mL) in Hela cells at pH 6.0 in serum free media after 12 hours of incubation. \*Average values of percent cell viability were taken.

**3.24 Cellular uptake of free DOX and liposomal DOX.** Based on the cytotoxicity results of the previous section, the uptake of pH-convertible formulation II and control liposome by B16F10 cells was characterized by flow cytometric analysis of the fluorescence of the cargo drug doxorubicin. Free DOX was employed as the positive control. A detachin solution (Genlantis, San Diego, CA) was used to detach cells as the detachin is much milder than the trypsin for detachment and centrifugation of cells. The time of incubation of the formulations with the cells is critical as high time points result in the high cell kill and which results in poor analysis of the DOX uptake by cells. On the other hand a very short time may not result in sufficient formulation uptake by the cells. After optimization, 4 hours of incubation was elected for the uptake studies.

The flow cytometry data (Fig 3.30, 3.31) indicate that the change in mean fluorescent intensity of cells incubated by control liposome was not significant between pH 7.4 and pH 6.0. In contrast, the average fluorescence values for liposome II show an increase of 57 % at pH 6.0 compared to pH 7.4. This clearly indicates higher DOX uptake by cells at lowered pH owing to the increased interaction between the cells and the newly turned cationic liposome II.

It is also interesting to note that the uptake of free DOX in fact decreased at lowered pH, which might be due to higher proportion of charged DOX molecules at low pH with doxorubicin being a weakly basic drug. However, this small decrease did not translate to lower cytotoxicity of free DOX at pH 6.0

Our strategy to formulate doxorubicin in pH tunable liposomes insulates doxorubicin from the low pH microenvironment and yet exploits the acidic microenvironment for the

increase in the surface charge of the liposomes and subsequent greater interaction with cancer cells.

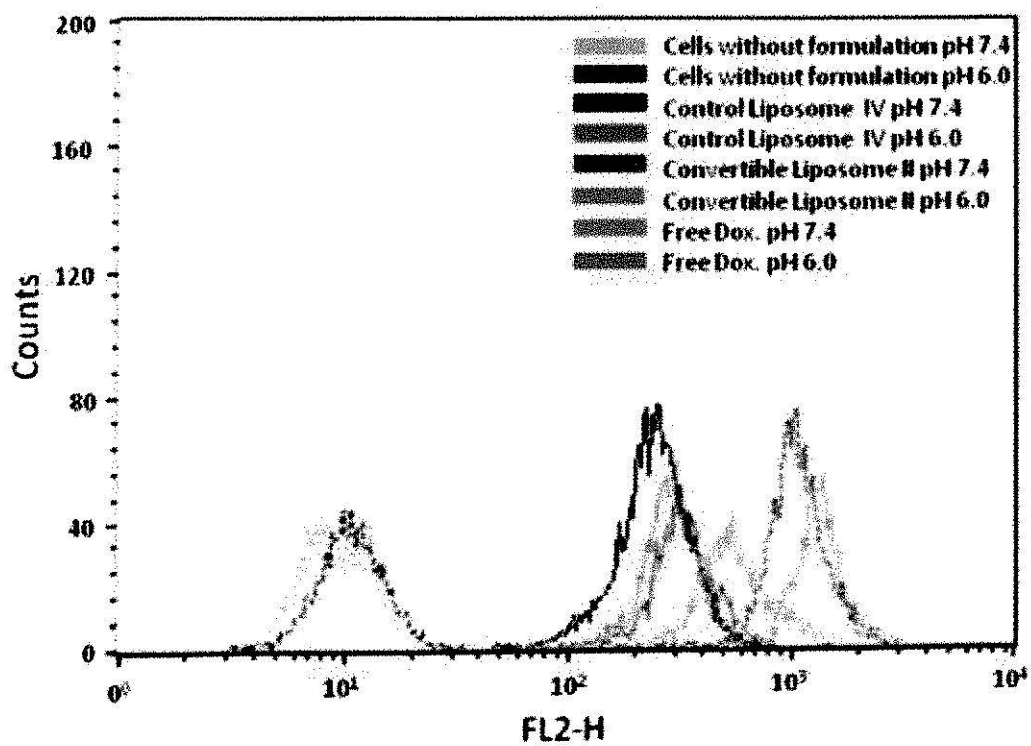


Fig. 3.30 Flow Cytometry of DOX uptake by B16F10 cells

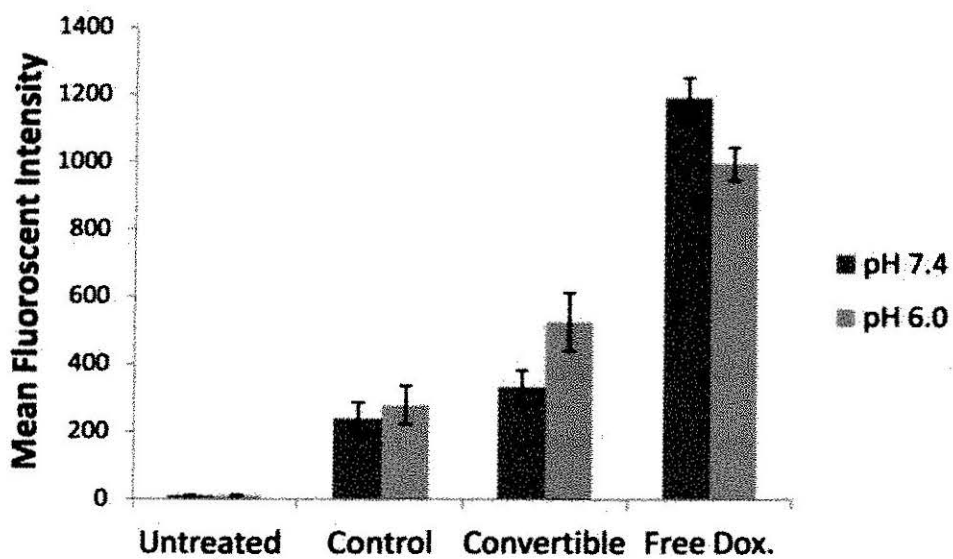


Fig. 3.31 Mean fluorescent intensity of B16F10 cells treated with free DOX or liposomal DOX by flow cytometry.



#### Chapter 4: Summary and Conclusion

Liposomal drug delivery system that can encapsulate and deliver anticancer agents was developed in our studies. An ideal anticancer delivery system has primarily four requirements: (1) selectivity to cancer (2) efficient delivery of anticancer agent inside the cancer cells (3) stability of the liposome formulation (4) high blood circulation half life. To achieve these goals, two strategies were employed.

Firstly, a pH-sensitive liposome was envisaged by incorporating a pH-sensitive PEGylated lipid that can hydrolyze at low pH tumor environment. The hydrolysis at mildly acidic tumor conditions was envisioned to be exploited by placing a hydrozone linker between the PEG head group and hydrocarbon chains of the PEGylated lipid. The shedding of PEG coating would expose positive charges and would result in greater tumor interaction. The synthesis of the hydrozone-based pH-sensitive lipid revealed that the lipid hydrolyzes even at a neutral pH and was not highly stable at physiological pH. Therefore, such approach would not be a good choice for developing a pharmaceutically viable drug delivery system.

To achieve the aforementioned goals, we changed the strategy to designing a pH-convertible liposome with more stable imidazole-based lipids. The design principal works on the basis of acquisition of positive charges by protonation of the imidazole moiety rather than hydrolysis. Such protonation strategy renders better formulation than

previously reported acid-labile liposomes owing to its better stability on shelf. Additionally, the PEG coating on the surface of the convertible liposomes is also clustered upon exposure to mildly acidic pH as seen in tumor interstitium due to electrostatic and vander waal interaction between the protonated imidazole lipids and the negatively charged PEGylated lipid.

We have used doxorubicin as the liposome cargo to study the cytotoxicity and cellular uptake of these liposomes. DOX acts both as an anticancer agent encapsulated in the liposome and also as a fluorescent marker of intracellular uptake of this liposomal system using flow cytometry. The encapsulation and retention of our model drug doxorubicin was enhanced by using a previously reported manganese sulfate remote loading approach (101).

Our cytotoxic studies indicate the increase of cytotoxicity at pH 6.0 in all the pH-convertible liposomes compared to pH 7.4 in two cancer cell lines (B16 F10 and Hela). Furthermore, the formulation (II) show significantly higher uptake in the B16F10 cells at lower pH. The anticancer cytotoxicities of the pH-convertible liposomes are better than the control PEGylated liposomes which were reported to have minimum interaction with the cancer cells and rely mostly on the slow release of drug from the formulation, which can be suboptimal to efficiently kill the cancer cells. The slow release of doxorubicin and many other anticancer drugs for a sustained period can induce the previously mentioned 'multi-drug resistance' and thereby further reducing the efficacy of the formulation.

Our studies supports the approach of exploiting the lower pH in tumoral interstitium by careful choice of lipids in the design of liposomes that interact more strongly with cancer

cells in response to lowered pH. Another potential advantage of this liposomal delivery system would be its lower cost because its lipid components are either inexpensive or can be conveniently synthesized.

It is interesting to note that while increasing the pKa of the imidazole lipid does increase the cytotoxic effect of the formulation, it also increases the interaction of these systems with negatively charged model liposomes at the physiological pH. It remains to be explored whether the increase in pKa of the imidazole lipid in the liposomal formulation would cause higher interaction with components of blood in circulation.

It is also important to note that the proposed liposome formulation will find limitation in patients with conditions of metabolic acidosis which may arise due to dysfunction of liver (lactic acidosis), kidney or lung (hypoventilation). The resultant decrease in blood pH under such clinical situations may trigger premature display of positive charges by the liposomes and subsequently their excessive clearance from the blood by RES.

### References

1. Cancer facts and figures 2013, American cancer society, Atlanta, 2013.
2. <http://www.cancer.gov/cancertopics/cancerlibrary/what-is-cancer>
3. <http://globocan.iarc.fr/factsheets/populations/factsheet.asp?uno=900>
4. Cancer statistics 2009, American cancer society, Atlanta, 2009.
5. William E. Luttrell, Warren W. Jederberg, Kenneth R. Still. *Toxicology Principles for the Industrial Hygienist*, AIHA, 2008
6. <http://www.iarc.fr/en/publications/pdfs-online/epi/cancerepi/CancerEpi-1.pdf>
7. Gisele M. Hodges, Charles Rowlatt. *Developmental Biology and Cancer*, CRC Press, 1994
8. Geoffrey M. Cooper. *Elements of Human Cancer*, Jones & Bartlett Learning, 1992
9. Allen TM, Ligand-Targeted Therapeutics In Anticancer Therapy, *Nature Reviews Cancer*, 2002, 2, (10), 750-63
10. Chatelut, Etienne; Delord, Jean-Pierre; Canal, Pierre., *Investigational New Drugs* 2003, 21, (2), 141-148
11. Yao, Xin; Panichpisal, Kessarín; Kurtzman, Neil; Nugent, Kenneth, *The American Journal of the Medical Sciences*, 2007, 334, (2), 115-124
12. Pfeffer, Brad; Tziros, Constantine; Katz J, Richard, Current concepts of anthracycline cardiotoxicity: pathogenesis, diagnosis and prevention, *British Journal of Cardiology*, 2009, 16, (2), 85-89.

13. Hockel, Michael; Vaupel, Peter, Tumor Hypoxia: Definitions and Current Clinical, Biologic, and Molecular Aspects, *Journal of the National Cancer Institute*, 2001, 93, (4), 266-276.
14. Partridge, Ann H.; J. Burstein, Harold; Winer, Eric P. Side Effects of Chemotherapy and Combined Chemohormonal Therapy in Women With Early-Stage Breast Cancer, *Journal of the National Cancer Institute Monographs*, 2001, (30), 135-42 .
15. Singh, P.; Singh, A., Ocular adverse effects of anti-cancer chemotherapy and targeted therapy, *Journal of Cancer Therapeutics and Research*, 2012.
16. Fabbrocini, G.; Cameli, N.; Romano, MC; Mariano, M.; Panariello, L.; Bianca, D.; Monfrecola, G., Chemotherapy and skin reactions, *Journal of Experimental & Clinical Cancer Research*, 2012, 31, (50), 1-6.
17. Bentzen SM., Preventing or reducing late side effects of radiation therapy: radiobiology meets molecular pathology, *Nature Reviews Cancer*, 2006, 6, (9), 702-713.
18. Kim, WY; Oh, SH; Woo, JK; Hong, WK; Lee, HY., Targeting heat shock protein 90 overrides the resistance of lung cancer cells by blocking radiation-induced stabilization of hypoxia-inducible factor-1alpha, *Cancer Research*, 2009, 69, (4), 1624-32.
19. <http://www.cancer.gov/cancertopics/factsheet/Therapy/biological>
20. <http://training.seer.cancer.gov/treatment/biotherapy/sideeffects.html>
21. Hoag, JB; Azizi, A; Doherty, TJ; Lu, J; Willis, RE; Lund, ME., Association of cetuximab with adverse pulmonary events in cancer patients: a comprehensive review, *Journal of Experimental & Clinical Cancer Research*, 2009, 28,(113).
22. Hanson, ED; Hurley, BF; Intervening on the side effects of hormone-dependent cancer treatment: the role of strength training, *Journal of aging research*, 2011, 903291
23. Kumar, RJ.; Barqawi, Al; Crawford, David E.; Adverse Events Associated With Hormonal Therapy for Prostate Cancer, *Reviews in Urology*, 2005, 7, (5), S37-S43

24. <http://www.cancer.org/cancer/breastcancer/detailedguide/breast-cancer-treating-hormone-therapy>
25. Bosslet K, Straub R, Blumrich M, Czech J, Gerken M, Sperker B, Kroemer HK, Gesson JP, Koch M, Monneret C., Elucidation of the mechanism enabling tumor selective prodrug monotherapy, *Cancer research*, 1998, 58, (6), 1195-201
26. R. Srinivasan, *Nanotechnology for Cancer Therapy*, Cyber Tech Publications, 2008
27. Gottesman, M. M.; Fojo, T.; Bates, S. E., Multidrug resistance in cancer: Role of ATP-dependent transporters, *Nature Reviews Cancer*, 2002, 2, (1), 48-58
28. Peer, D; Karp, JM; Hong, S; Farokhzad, OC; Margalit, R; Langer R, Nanocarriers as an emerging platform for cancer therapy, *Nature Nanotechnology*, 2007, 2, (12), 751-760
29. Allen TM, Ligand-Targeted Therapeutics In Anticancer Therapy, *Nature Reviews Cancer*, 2002, 2, (10), 750-63.
30. Adams, GP; Schier, R; McCall, AM; Simmons, HH; Horak, EM; Alpaugh, RK; Marks, JD; Weiner, LM; High affinity restricts the localization and tumor penetration of single-chain fv antibody molecules, *Cancer Research*, 2001, 61, (12), 4750-4755.
31. Tolcher, Anthony W.; Sugarman, Steven; Gelmon, Karen A.; Cohen, Roger; Saleh, Mansoor; Isaacs, Claudine; Young, Leslie; Healey, Diane; Onetto, Nicole; Slichenmyer, William, Randomized Phase II Study of BR96-Doxorubicin Conjugate in Patients With Metastatic Breast Cancer, *Journal of Clinical Oncology*, 1999, 17, (2), 478-484
32. Napier, MP; Sharma, SK; Springer, CJ; Bagshawe, KD; Green, AJ; Martin, J; Stribbling, SM; Cushen, N; O'Malley, D; Begent, RH, Antibody-directed enzyme prodrug therapy: efficacy and mechanism of action in colorectal carcinoma, *Clinical Cancer Research*, 2000, 6, (3), 765-772
33. Hovorka, O; St'astný, M; Etrych, T; Subr, V; Strohalm, J; Ulbrich, K; Říhová, B. Differences in the intracellular fate of free and polymer-bound doxorubicin, *Journal of Controlled Release*, 2002, 80, (1-3), 101-117

34. Satchi, R; Connors, TA; Duncan, R, PDEPT: polymer-directed enzyme prodrug therapy, *British Journal of Cancer* (2001) 85(7), 1070–1076
35. Immordino, Maria Laura; Dosio, Franco; Cattel, Luigi, Stealth liposomes: review of the basic science, rationale, and clinical applications, existing and potential, *International Journal of Nanomedicine*, 2006, 1,(3) 297–315
36. Scherphof, G. L.; Dijkstra, J.; Spanjer, H. H.; Derksen, J. T. P.; Roerdink, F. H., Uptake and intracellular processing of targeted and nontargeted liposomes by rat Kupffer cells in vivo and in vitro, *Annals of the New York Academy of Sciences*, 1985, 446, 368–84.
37. Philippot, Jean R.; Schube, Francis. *Liposomes As Tools in Basic Research and Industry*, CRC Press, 1994, 181
38. Chonn, A; Cullis, PR; Devine, DV, The role of surface charge in the activation of the classical and alternative pathways of complement by liposomes, *Journal of Immunology*, 1991, 146, (12), 4234–41
39. Philippot, Jean R.; Schube, Francis. *Liposomes As Tools in Basic Research and Industry*, CRC Press, 1994, 181
40. Cullis, PR; Chonn, A; Semple, SC, Interactions of liposomes and lipid-based carrier systems with blood proteins: Relation to clearance behaviour in vivo, *Advanced Drug Delivery Reviews*, 1998 32, (1-2), 3–17
41. Senior, J; Trimble, K.R.; Maskiewicz, R., Interaction of positively-charged liposomes with blood: Implications for their application in vivo, *Biochimica et Biophysica Acta*, 1991, 1070, (1), 173–179.
42. Oku, N.; Tokudome, Y.; Namba, Y.; Saito, N.; Endo, M.; Hasegawa, Y.; Kawai, M.; Tsukada, H.; Okada, S., Effect of serum protein binding on real-time trafficking of liposomes with different charges analyzed by positron emission tomography, *Biochimica et Biophysica Acta*, 1996, 1280, (1), 149–154
43. Hong, RL; Huang, CJ; Tseng, YL; Pang, VF; Chen, ST; Liu, JJ; Chang, FH, Direct comparison of liposomal doxorubicin with or without polyethylene glycol coating in C-26 tumor-bearing mice: is surface coating with polyethylene glycol beneficial?, *Clinical Cancer Research*, 1999, 5, (1), 3645–3652

44. Parr, MJ; Masin, D; Cullis, PR; Bally, MB, Accumulation of Liposomal Lipid and Encapsulated Doxorubicin in Murine Lewis Lung Carcinoma: The Lack of Beneficial Effects by Coating Liposomes with Poly(ethylene glycol), *The Journal of Pharmacology and Experimental Therapeutics*, 1997, 280, (3), 1319-1327.
45. Daleke, D. L.; Hong, K.; Papahadjopoulos, D., Endocytosis of liposomes by macrophages: binding, acidification and leakage of liposomes monitored by a new fluorescence assay, *Biochimica et Biophysica Acta*, 1990, 1024, (2), 352-366
46. Du, H; Chandaroy, P; Hui, SW., Grafted poly-(ethylene glycol) on lipid surfaces inhibits protein adsorption and cell adhesion, *Biochimica et Biophysica Acta*, 1997, 1326, (2), 236-248
47. Huang, SL; MacDonald, RC., Acoustically active liposomes for drug encapsulation and ultrasound-triggered release, *Biochimica et Biophysica Acta*, 2004, 1665, (1-2), 134 - 141.
48. Rapoport N., Combined cancer therapy by micellar-encapsulated drug and ultrasound, *International Journal of Pharmaceutics*, 2004, 277, (1-2), 155-162
49. Leung, SJ; Romanowski, M., Light-Activated Content Release from Liposomes *Theranostics*, 2012, 2(10), 1020-1036
50. Pidgeon, C; Hunt, CA., Light sensitive liposomes, *Photochemistry and Photobiology*, 1983, 37, (5), 491 - 494.
51. Ohya, Y; Okuyama, Y; Fukunaga, A; Ouchi, T., Photo-sensitive lipid membrane perturbation by a single chain lipid having terminal spiropyran group, *Supramolecular Science*, 1998, 5, (1-2), 21-29.
52. Anderson, VC; Thompson, DH., Triggered release of hydrophilic agents from plasmalogen liposomes using visible light or acid, *Biochimica et Biophysica Acta*, 1992, 1109, (1), 33-42.
53. Wan, Y; Angleson, JK; Kutateladze, AG., Liposomes from novel photolabile phospholipids: Light-induced unloading of small molecules as monitored by PFG NMR, *Journal of American Chemical Society*, 2002, 124, (20), 5610-5611.
54. Li, Z; Wan, Y; Kutateladze, AG., Dithiane-based photolabile amphiphiles: toward photolabile liposomes, *Langmuir*, 2003, 19, (16), 6381-6391.



55. Zhang, ZY; Smith, BD., Synthesis and characterization of NVOC-DOPE, a caged photoactivatable derivative of dioleoylphosphatidylethanolamine. *Bioconjugate Chemistry*, 1999; 10, (6), 1150-1152.
56. O'Brien, DF; Armitage, B; Benedicto, A; Bennett, DE; Lamparski, HG; Lee, YS; Srisiri, W; Sisson, TM., Polymerization of preformed self-organized assemblies *Accounts of Chemical Research*, 1998, 31, (12), 861-868.
57. Gerasimov, OV; Boomer, JA; Qualls, MM; Thompson, DH., Cytosolic drug delivery using pH- and light-sensitive liposomes, *Advanced Drug Delivery Reviews*, 1998, 38, (3), 317-338
58. Yatvin, M.B; Weinstein, J.N; Dennis, W.H; Blumenthal, R., Design of liposomes for enhanced local release of drugs by hyperthermia, 1978, *Science* 202, (4374) 1290-1293
59. Ta, T; Porter, TM., Thermosensitive liposomes for localized delivery and triggered release of chemotherapy; *Journal of controlled release*, 2013, 169, (1-2), 112-125
60. Borchman, D; Yappert, M C., Lipids and the ocular lens, *The Journal of Lipid Research*, 2010, 51, (9), 2473-2488
61. Gaber, M.H; Hong, K.; Huang, S.K.; Papahadjopoulos, D., Thermosensitive sterically stabilized liposomes: formulation and in vitro studies on mechanism of doxorubicin release by bovine serum and human plasma, *Pharmaceutical research*, 1995, 12 (10), 1407-1416
62. Meshorer, A.; Prionas, S.D.; Fajardo, L.F.; Meyer, J.L.; Hahn, G.M.; Martinez, A.A., The effects of hyperthermia on normal mesenchymal tissues: application of a histologic grading system, *Archives of Pathology and Laboratory Medicine*, 1983, 107, (6), 328-334
63. Anyarambhatla, G.R.; Needham, D., Enhancement of the phase transition permeability of DPPC liposomes by incorporation of MPPC: a new temperature-sensitive liposome for use with mild hyperthermia, *Journal of Liposome Research*, 1999, 9, (4), 491-506
64. Needham, D.; Anyarambhatla, G.; Kong, G.; Dewhirst, M.W., A new temperature sensitive liposome for use with mild hyperthermia: characterization and testing in a human tumor xenograft model, *Cancer Research*, 2000, 60, (5), 1197-1201

65. Banno, B.; Ickenstein, L.M.; Chiu, G.N.; Bally, M.B.; Thewalt, J.; Brief, E.; Wasan, E.K., The functional roles of poly(ethylene glycol)-lipid and lysolipid in the drug retention and release from lysolipid-containing thermosensitive liposomes in vitro and in vivo, *Journal of Pharmaceutical sciences*, 2010, 99, (5) 2295–2308
66. Sandstrom, M.C.; Ickenstein, L.M.; Mayer, L.D.; Edwards, K., Effects of lipid segregation and lysolipid dissociation on drug release from thermosensitive liposomes, *Journal of Controlled Release*, 2005, 107, (1), 131–142
67. Hauck, M.L.; LaRue, S.M.; Petros, W.P.; Poulson, J.M.; Yu, D.; Spasojevic, I.; Pruitt, A.F.; Klein, A.; Case, B.; Thrall, D.E.; Needham, D.; Dewhirst, M.W., Phase I trial of doxorubicin-containing low temperature sensitive liposomes in spontaneous canine tumors, *Clinical Cancer Research*, 2006, 12, (13), 4004–4010.
68. Amstad, E.; Köhlbrecher, J.; Müller, E.; Schweizer, T.; Textor, M.; Reimhult, E.; Triggered release from liposomes through magnetic actuation of iron oxide nanoparticle containing membranes, *Nano Letters*, 2011, 11, (4), 1664–1670
69. Babincová, M.; Cicmanec, P.; Altanerová, V.; Altaner, C.; Babinec, P., AC-magnetic field controlled drug release from magnetoliposomes: design of a method for site-specific chemotherapy, *Bioelectrochemistry*, 2002, 55, (1-2), 17–19
70. Nobuto, H.; Sugita, T.; Kubo, T.; Shimose, S.; Yasunaga, Y.; Murakami, T.; Ochi M., Evaluation of systemic chemotherapy with magnetic liposomal doxorubicin and a dipole external electromagnet, *International journal of Cancer*, 2004, 109, (4), 627–635
71. Kubo, T.; Sugita, T.; Shimose, S.; Nitta, Y.; Ikuta, Y.; Murakami, T., Targeted systemic chemotherapy using magnetic liposomes with incorporated adriamycin for osteosarcoma in hamsters, *International Journal of Oncology*, 2001, 18, (1), 121–125
72. Babincová, M.; Altanerová, V.; Lampert, M.; Altaner, C.; Machová, E.; Srámka, M.; Babinec, P., Site-specific in vivo targeting of magnetoliposomes using externally applied magnetic field, *Z. Naturforsch C.*, 2000, 55, (3-4), 278–281
73. Jain, S.; Mishra, V.; Singh, P.; Dubey, P.K.; Saraf, D.K.; Vyas, S.P., RGD-anchored magnetic liposomes for monocytes/neutrophils-mediated brain targeting, *International Journal of Pharmaceutics*, 2003, 261, (1-2) 43–55

74. Matsunaga, T.; Higashi, Y.; Tsujimura, N., Drug delivery by magnetoliposomes containing bacterial magnetic particles. *Cell Engineering*, 1997, 2, 7-11
75. Saiyed, ZM.; Telang, SD.; Ramchand, CN., Application of magnetic techniques in the field of drug discovery and biomedicine, *BioMagnetic Research and Technology*, 2003, 1, (1), 2
76. Cordes, E. H.; Bull, H.G., Mechanism and catalysis for hydrolysis of acetals, ketals, and ortho esters. *Chemical Reviews*, 1974, 74, (5), 581-603
77. Song, Jie; Hollingsworth, R. I., Synthesis, Conformational Analysis, and Phase Characterization of a Versatile Self-Assembling Monoglucosyl Diacylglycerol Analog, *Journal of American Chemical Society*, 1999, 121, (9), 1851-1861
78. Asokan, A.; Cho, MJ.; Cytosolic delivery of macromolecules. 3. Synthesis and characterization of acid-sensitive bis-detergents, *Bioconjugate Chemistry*, 2004, 15, (6), 1166-1173
79. Shin, J.; Shum, P.; Thompson, DH., Acid-triggered release via dePEGylation of DOPE liposomes containing acid-labile vinyl ether PEG-lipids, *Journal of Controlled Release*, 2003, 91, (1-2), 187-200
80. Rui, Y., Wang, S., Low, P.S., and Thompson, D.H., Dipalmitoylcholine-folate liposomes: an efficient vehicle for intracellular drug delivery, *J Am Chem Soc* 1998, 120, (44), 11213-11218
81. Chen, H.; Zhang, H.; McCallum, CM.; Szoka, FC.; Guo, X., Unsaturated cationic ortho esters for endosome permeation in gene delivery, *Journal of Medicinal Chemistry*, 2007, 50, (18), 4269-4278
82. Bergstrand N, Arfvidsson MC, Kim JM, Thompson DH, Edwards K., Interactions between pH-sensitive liposomes and model membranes, *Biophysical Chemistry*, 2003, 104, (1), 361-379
83. Guo, X.; Szoka, FC Jr., Steric stabilization of fusogenic liposomes by a low-pH sensitive PEG--diortho ester--lipid conjugate, *Bioconjugate Chemistry*, 2001, 12, (2), 291-300
84. Masson, C.; Garinot, M.; Mignet, N.; Wetzler, B.; Mailhe, P.; Scherman, D.; Bessodes, M., pH-sensitive PEG lipids containing orthoester linkers: new

- potential tools for nonviral gene delivery, *Journal of Controlled Release*, 2004, 99, (3), 423 – 434
85. Vance, JE.; Steenbergen, R., Metabolism and functions of phosphatidylserine, *Progress in Lipid Research*, 2005, 44, (4), 207–234
86. Mounkes, LC.; Zhong, W.; Cipres-Palacin, G.; Heath, TD.; Debs, RJ., Proteoglycans mediate cationic liposome-DNA complex-based gene delivery in vitro and in vivo, *The Journal of Biological Chemistry*, 1998, 273, (40), 26164–26170
87. Mislick, KA.; Baldeschwieler, JD., Evidence for the role of proteoglycans in cation-mediated gene transfer, *Proceedings of the National Academy of Sciences*, 1996, 93, (22), 12349–12354
88. Szachowicz-Petelska, B.; Dobrzyńska, I.; Figaszewski, Z.; Sulkowski, S., Changes in physico-chemical properties of human large intestine tumour cells membrane, *Molecular and Cellular Biochemistry*, 2002, 238, (1-2), 41–47
89. Szakács, G.; Paterson, JK.; Ludwig, JA.; Booth-Genthe, C.; Gottesman MM., Targeting multidrug resistance in cancer, *Nature Reviews Drug Discovery*, 2006, 5, (3), 219–234
90. Immordino, ML.; Dosio, F.; Cattel, L., Stealth liposomes: review of the basic science, rationale, and clinical applications, existing and potential, *International Journal of Nanomedicine*, 2006, 1, (3), 297–315
91. Kale, AA.; Torchilin, VP., Design, synthesis, and characterization of pH-sensitive PEG-PE conjugates for stimuli-sensitive pharmaceutical nanocarriers: the effect of substitutes at the hydrazone linkage on the pH stability of PEG-PE conjugates, *Bioconjugate Chemistry*, 2007, 18, (2), 363–370
92. The Association of British Pharmaceutical Industry, London, UK
93. <http://nanosmartpharma.com/Technology-Pipeline.aspx>
94. <http://www.healthdigest.org/topics/category/3369-doxil-drug-and-prescription-information-side-effects-use-and-dosage>

95. Aissaoui A., Martin B.; Kan E.; Oudrhiri N.; Hauchecorne M.; Vigneron, JP.; Lehn, JM.; and Lehn P., Novel Cationic Lipids Incorporating an Acid-Sensitive Acylhydrazone Linker: Synthesis and Transfection Properties; *Journal of Medicinal Chemistry*, 2004, 47, (21), 5210-5223
96. Marik, J.; Tartis, MS.; Zhang, H.; Fung, JY.; Kheirulomoom, A.; Sutcliffe, JL.; Ferrara, KW., Long-circulating liposomes radiolabeled with [<sup>18</sup>F]fluorodipalmitin ([<sup>18</sup>F]FDP), *Nuclear Medicine and Biology*, 2007, 34, (2), 165-171
97. Stamatova, SD.; Stawinski, J., A Simple and Efficient Method for Direct Acylation of Acetals with Long Alkyl-Chain Carboxylic Acid Anhydrides, *Tetrahedron*, 56, (49), 9679-9703
98. Torchilin, V.; Weissig, V., *Liposomes: A Practical Approach* 2003, 4-7, Oxford University Press
99. Haran, G.; Cohen, R.; Bar, L. K.; Barenholz, Y., Transmembrane ammonium sulfate gradients in liposomes produce efficient and stable entrapment of amphipathic weak bases. *Biochimica et Biophysica Acta* 1993, 1151, (2), 201-15
100. Bolotin, E. M.; Cohen, R.; Bar, L.K.; Emanuel, N.; Ninio, S.; Lasic, D.D.; Barenholz, Y., Ammonium sulfate gradients for efficient and stable remote loading of amphipathic weak bases into liposomes and ligandoliposomes. *Journal of Liposome Research*, 1994, 4, (1), 455-479
101. Cheung, BC.; Sun, TH.; Leenhouts, JM.; Cullis, PR., Loading of doxorubicin into liposomes by forming Mn<sup>2+</sup>-drug complexes, *Biochimica et Biophysica acta*, 1998, 1414, (1-2), 205-216
102. Huwyler, J.; Drewe, J.; Krähenbühl, S., Tumor targeting using liposomal antineoplastic drugs, *International Journal of Nanomedicine*, 2008, 3, (1), 21-29
103. Gabizon, AA., Stealth Liposomes and Tumor Targeting: One Step Further in the Quest for the Magic Bullet, *Clinical Cancer Research*, 2001, 7, (2), 223-225
104. Romberg, B.; Hennink, WE.; Storm, G., Sheddable Coatings for Long-Circulating Nanoparticles, *Pharmaceutical Research*, 2008, 25, (1), 55-71

105. Danhier, F.; Feronb, O.; Préat, V., To exploit the tumor microenvironment: Passive and active tumor targeting of nanocarriers for anti-cancer drug delivery, *Journal of Controlled Release*, 2010, 148, (2), 135-146
106. Iessi, E.; Marino, ML.; Lozupone, F.; Fais, S.; Milito, AD.; Tumor acidity and malignancy: novel aspects in the design of anti-tumor therapy, *Cancer Therapy*, 2008, 6, 55-66
107. Vaupel, P.; Kallinowski, F.; Okunieff, P., Blood flow, oxygen and nutrient supply, and metabolic microenvironment of human tumors: a review. *Cancer Research*, 1989, 49, (23), 6449-65
108. Tannock, IF.; Rotin, D., Acid pH in Tumors and Its Potential for Therapeutic Exploitation, *Cancer Research*, 1989, 49, (16), 4373-4384
109. Song, CW.; Griffin, R.; Park, HJ., Influence of Tumor pH on Therapeutic Response, *Cancer Drug Discovery and Development*, 2006, 21-42
110. Svastová, E.; Hulíková, A.; Rafajová, M.; Zát'ovicová, M.; Gibadulinová, A.; Casini, A.; Cecchi, A.; Scozzafava, A.; Supuran, CT.; Pastorek, J.; Pastoreková, S., Hypoxia activates the capacity of tumor-associated carbonic anhydrase IX to acidify extracellular pH, *FEBS Letters*, 2004, 577, (3), 439-45
111. Needham, D.; Dewhirst, MW., The development and testing of a new temperature-sensitive drug delivery system for the treatment of solid tumors, *Advanced Drug Delivery Reviews*, 2001, 53, (3), 285-305
112. Demakova, MY.; Sudarikov, DV.; Rubtsova, SA.; Slepukhin, PA.; Kuchin, AV, Synthesis of neomenthylsulfanylimidazoles, *Chemistry of Natural Compounds*, 2012, 47, (6), 899-902
113. Demakova, MY.; Sudarikov, DV.; Rubtsova, SA.; Frolova, LL.; Popov, AV.; Slepukhin, PA.; Kuchin, AV., Synthesis and Asymmetric Oxidation of (Caranylsulfanyl)-1H-imidazoles, *Helvetica Chimica Acta*, 2012, 95(6), 940-950
114. Singh, RS.; Gonçalves, C.; Sandrin, P.; Pichon, C.; Midoux, P.; Chaudhuri, A., On the Gene Delivery Efficacies of pH-Sensitive Cationic Lipids via Endosomal Protonation: A Chemical Biology Investigation, *Chemistry and Biology*, 2004, 11, (5), 713-723

115. Ravi, MNK.; Bakowsky, U.; Lehr, CM., Preparation and characterization of cationic PLGA nanospheres as DNA carriers, *Biomaterials*, 2004, 25, (10), 1771-1777
116. Budker, V.; Gurevich, V.; Hagstrom, JE.; Bortzov, F.; Wolff, JA., pH-sensitive, cationic liposomes: a new synthetic virus-like vector, *Nature Biotechnology*, 1996, 14, (6), 760-764
117. Gao, H.; Hui, KM., Synthesis of a novel series of cationic lipids that can act as efficient gene delivery vehicles through systematic heterocyclic substitution of cholesterol derivatives, *Gene Therapy*, 2001, 8, (11), 855-863
118. Chen, H.; Zhang, H.; McCallum, CM.; Szoka, FC.; Guo, X., Unsaturated Cationic Ortho Esters for Endosome Permeation in Gene Delivery, *Journal of Medicinal Chemistry*, 2007, 50, (18), 4269-4278
119. Bergstrand, N.; Arfvidsson, MC.; Kim, JM.; Thompson, DH.; Edwards, K., Interactions between pH-sensitive liposomes and model membranes. *Biophysical Chemistry*, 2003, 104, (1), 361-379
120. Mabrey, S.; Sturtevant, JM., Investigation of phase transitions of lipids and lipid mixtures by high sensitivity differential scanning calorimetry, *Proceedings of the national Academy of Sciences of the USA*, 1976, 73, (11), 3862-3866
121. Wolf, DE., Lipid domains: The parable of the blind men and the elephant, *Commun. Molec. and Cell. Biophys*, 1992, 8, 83-95.
122. Cheung, BC.; Sun, TH.; Leenhouts, JM.; Cullis, PR., Loading of doxorubicin into liposomes by forming  $Mn^{2+}$ -drug complexes, *Biochimica et Biophysica acta*, 1998, 1414, (1-2), 205-216
123. Miller, CR.; Bondurant, B.; McLean, SD.; McGovern, KA., Liposome-Cell Interactions in Vitro: Effect of Liposome Surface Charge on the Binding and Endocytosis of Conventional and Sterically Stabilized Liposomes, *Biochemistry*, 1998, 37, (37), 12875-12883
124. Karve, S.; Alaouie, A.; Zhou, Y.; Rotolo, J.; Sofou, S., The use of pH-triggered leaky heterogeneities on rigid lipid bilayers to improve intracellular trafficking and therapeutic potential of targeted liposomal immunochemotherapy, *Biomaterials*, 2009, 30, (30), 6055-6064

125. Amselem, S.; Gabizon, A.; Barenholz, Y., Optimization and upscaling of doxorubicin-containing liposomes for clinical use. *Journal of Pharmaceutical Sciences*, 1990, 79, (12), 1045–1052
126. Zimmer, A.; Aziz, SA.; Gilbert, M.; Werner, D.; Noe, CR., Synthesis of cholesterol modified cationic lipids for liposomal drug delivery of antisense oligonucleotides, *European journal of pharmaceutics and biopharmaceutics*, 1999, 47, (2), 175- 178
127. Guo, X.; MacKay, JA; Szoka, Jr, FC.; Mechanism of pH-Triggered Collapse of Phosphatidylethanolamine Liposomes Stabilized by an Ortho Ester Polyethyleneglycol Lipid, *Biophysical Journal*, 2003, 84, (3), 1784–1795
128. <http://www.bme.umich.edu/labs/centlab/research/overview.php>
129. Koyama, TM.; Stevens, CR.; Borda, EJ.; Grobe, KJ.; Cleary, DA., Characterizing the Gel to Liquid Crystal Transition in Lipid-Bilayer Model Systems, *The Chemical Educator*, 5, (3), S1430-4171(99) 01273-1
130. Bhatnagar, A.; Sharma, PK.; Kumar, N., A Review on “Imidazoles”: Their Chemistry and Pharmacological Potentials, *International Journal of PharmTech Research*, 2011, 3, (1), 268-282